Title	Novel luminescent oxygen sensor systems for smart food packaging
Author(s)	Kelly, Caroline Ann
Publication date	2017
Original citation	Kelly, C. A. 2017. Novel luminescent oxygen sensor systems for smart food packaging. PhD Thesis, University College Cork.
Type of publication	Doctoral thesis
Rights	**© 2017, Caroline Ann Kelly.** http://creativecommons.org/licenses/by-nc-nd/3.0/ ![CC BY NC ND]
Embargo information	No embargo required
Item downloaded from	http://hdl.handle.net/10468/3685

NOVEL LUMINESCENT OXYGEN SENSOR SYSTEMS FOR SMART FOOD PACKAGING

A THESIS SUBMITTED TO THE NATIONAL UNIVERSITY OF IRELAND, CORK IN FULFILMENT OF THE REQUIREMENTS FOR THE DEGREE OF

DOCTOR OF PHILOSOPHY

BY

CAROLINE ANN KELLY

SCHOOL OF BIOCHEMISTRY AND CELL BIOLOGY

UNIVERSITY COLLEGE CORK

JANUARY 2017

SUPERVISOR: PROF. DMITRI PAPKOVSKY

CO-SUPERVISOR: PROF. JOE KERRY

HEAD OF SCHOOL: PROF. DAVE SHEEHAN

Contents

Declaration of Originality

This thesis is entirely the result of the author's original work, except where clearly attributed otherwise. The thesis has been composed by the author and has not previously been submitted partly or wholly for examination that has led to the award of a degree.

I hereby declare that this is all my own work with full and proper accreditation in relevant parts.

Signed: Caroline Ann Kelly

_____

Date:

Acknowledgements

Abstract

For industrial applications, solid-state O_2 sensors based on the quenching of photoluminescence, should be accurate, robust, easy-to-use in a calibration-free manner. These sensors generally consist of an O_2 sensitive luminescent dye in a polymer matrix. The properties of this matrix such as dye compatibility, O_2 permeability, mechanical strength and chemical resistance have a significant influence on the sensors final operating parameters.

Although used in many applications, the existing solid-state sensing materials and manufacturing processes remain complex, rigid and expensive for large scale fabrication while incurring a substantial extra cost. Currently, as few sensors fit these ideals, there is a need for new sensor materials, fabrication techniques and integration technologies.

We created and evaluated five new solid-state O_2 sensitive materials: four based on microporous polypropylene fabric materials and one on polyphenylene sulphide films. The onus was on simplifying composition of sensors and ergo reduction in material consumption and manufacturing cost. The sensors exhibited lifetime signals and working characteristics suitable for use in food packaging. When tested in food simulants and in direct contact with food, the sensor based on ungrafted polypropylene membrane fabricated by the swelling method, outperformed the other sensors. This sensor is cheaper than commercial sensors, is easily incorporated into current packaging materials by means of heat-sealing or lamination and has a storage shelf-life of at least 12 months when stored in normal atmospheric conditions.

Proof-of-concept tests, using commercial sensors, were carried out for industry customers. Sensors were used to track oxygen levels in meat packaging and also to select optimum packaging for a beverage product.

List of abbreviations

AA	ascorbic acid
BODIPY	boron-dipyrromethene
BPW	buffered peptone water
CCD	charge-coupled device
CFU	colony forming unit
DHA	L-dehydroascorbic acid
DIC	digital image correlation
EFSA	European Food Safety Authority
EtAc	ethyl acetate
EtOH	ethanol
EVOH	ethylene vinyl alcohol
FDA	Food and Drug Administration
FLIM	fluorescence-lifetime imaging microscopy
GC	gas chromatography
H	hydrogen
h	hour(s)
HDPE	high-density polyethylene
Hz	Hertz
HPLC	high performance liquid chromatography
Ir^{2+}	iridium (II) complex
K_{SV}	stern-volmer constant
LAE	N^{α}-Lauroyl-L-arginine ester monohydrochloride
LDPE	low-density polyethylene
LED	light-emitting diode
MA	modified atmosphere
MAP	modified atmosphere packaging
min	minute(s)
NIR	near infrared
OTR	oxygen transmission rate
PAH	polyaromatic hydrocarbon
PALE	physically active liquid environment
Pd(II)	palladium (II) complex
PE	polyethylene
PET	polyethylene terephthalate
PFPP	pentafluorophenyl propyl
PLA	polylactic acid
PLIM	phosphorescence-lifetime imaging microscopy
PMMA	poly(methyl methacrylate)
PP	polypropylene
PPS	polyphenylene sulphide
PS	polystyrene

PSu	polysulfone
Pt(II)	platinum (II) complex
PtBP	Platinum(II) benzoporphyrin
PtOEP	Pt(II) octaethylporphyrin
PtOEPK	Pt(II) octaethylporphyrinketone
PtTFPP	Pt(II)-tetrakis(pentafluorophenyl) porphyrin
PtTPTBPF	platinum(II) meso-tetra(4-fluorophenyl)tetrabenzoporphyrin
PVC	poly(vinyl chloride)
RFID	radio frequency identification tag
RH	relative humidity
RSD	relative standard deviation
Ru(dpp)	ruthenium(II)-tris(diphenyl-phenanthroline)
Ru(II)	ruthenium(II) complex
S.D./STD	standard deviation
STP	standard temperature and pressure
T	temperature
TBP	tributyl phosphate
TFEM	trifluoroethylmethacrylate
THF	tetrahydrofuran
TTI	time-temperature indicator
TVC	total viable count
UV	ultraviolet
VSC	volatile sulphur compound

1 Chapter 1: Literature Review - The use of phosphorescent solid-state O_2 sensors as a means to monitor product quality in food packaging.

1.1 Smart packaging

The traditional function of food packaging has been to extend shelf-life, maintain quality and safety and to protect the food product from physical damage or contamination. There has been increased attention to intelligent and active packaging technologies as a means to increase the above attributes. More effort has also been made to reduce food wastage, use more environmentally friendly materials and to limit the amount of packaging through the use of new packaging approaches.

Active packaging methods are used to increase shelf-life and prolong food quality. Active packaging concepts include freezing, chilling, acidifying, vacuum and modified atmosphere packing, scavengers, moisture absorbers, antimicrobial and antioxidant releasing components [1]. While active packaging is efficient, intelligent packaging is required to monitor in-pack conditions. Intelligent (or smart) packaging contains additional elements which enables the key quality attributes of food products to be monitored from the point of packaging in the factory to when it reaches the consumer's fork[1-2]. Intelligent packaging senses, records and informs on deterioration of the food package or food product, and alert any issues with production or transport [3]. Examples of existing intelligent packaging systems include those with sensors or indicators which can measure physical, chemical and biological parameters of the package[4]. A sensor detects or responds to the presence of a specific analyte or physical property and reports the presence by means of an indicator or electronic transmission. Indicators, in particular, report the presence or absence of an

analyte through a characteristic change, such as colour or fluorescence. Indicator systems (such as the time-temperature indicators) are usually irreversible/end-point, while sensors provide reversible, real-time response to an analyte.

One of the most widely used active packaging concepts is MAP which acts as a barrier against contaminants and reduces the potential of microorganisms to spoil food. In MAP packaging, food products are enclosed in gas impermeable containers and flushed with set gas mixture compositions before sealing.

While MAP systems are relatively efficient and reliable, failures can occur due to many factors; such as incorrect gas composition, oxygen (O_2) ingress due to poor barrier materials, flushing or storage condition, damage occurring during handling and transport. Conventional MAP systems provide no real time data of the conditions within the packaging, and detection of MAP quality is carried out using relatively expensive and destructive techniques. For instance, headspace analysis by GC, and O_2/CO_2 gas analysers such as Dansensor[TM] [5] which often need a skilled operator and consume the analyte being measured.

Initial quality monitoring involved the use of time-temperature indicators (TTI) to provide temperature tracing of a food product over time[6]. These sensors can be based on enzymatic reactions[7], polymerisation reactions[8] or temperature dependent diffusion[9] and display irreversible visual readouts of temperatures to which the product has been exposed. Since then, TTI indicators have been combined with other sensor technology such as radio frequency identification tags (RFIDs) as a means of contactless product tracing via radio waves [10].

As additional sensing technologies were developed, freshness indicators became popular. These sensors produce a response (e.g. colour changes) due to chemical

interactions between the indicator material and analyte within the package [11]. In particular, detection of metabolites such as H_2S[12], amine-based compounds [13], ethanol [14] and lactic acid [15] which can be attributed to microbial action within the product, have been connected to product freshness and quality. The above sensors can be used to correlate food quality to any points in the food chain where the quality is put at risk.

As well as monitoring the food product itself, it is necessary to monitor the packaging which protects the food from outside interference. Integrity indicators which use dyes that change colour on oxidation, denote when packages have been punctured or ruptured. One of the most commonly used sensors based on this principle is the Ageless Eye[TM] produced by the Mitsubishi company [16]. The material turns from colourless (methylene blue in reduced form when $[O_2] < 0.1$ %) to blue when oxidised by O_2 concentrations greater than 0.5 %. It has the advantages of being irreversible and easily incorporated into food packaging by printing or spin-coating. However, due to the heightened sensitivity to trace levels of O_2 and irreversible nature, false readouts can occur. In addition, careful storage of the indicators in inert conditions is necessary before incorporation into the packages.

Residual O_2 is an important parameter of both food quality and also of package integrity. Even trace levels of O_2 can cause major disruption in food quality through lipid oxidation, encouragement of microbial growth, loss of taste, fast ripening and browning through enzyme catalysed reactions or oxidisation of vitamin C in some beverages.

As a result, the development of luminescence based solid-state sensors has come to the fore. These sensors utilise the principle of quenching of luminescence

lifetime/intensity of dye molecules embedded in a polymeric support, by collision with O_2 molecules. These sensors are advantageous over conventional systems as they provide quick, quantitative, contactless and non-destructive readouts of O_2 content and can be modified or adapted to fit a multitude of purposes[17]. In addition, the sensors can be made inexpensive, disposable, calibration free (or batch calibrated) and can be used on a large scale to mass monitor the quality of packages on the manufacturing line in real time. This is an improvement on electrochemical techniques such as Clark's electrode[18], where packages must be taken at random off the production line and are destroyed during the testing process. Additionally, there are issues with the method's sensitivity to gas flow rate, stirring rate, operational temperature and poisoning by other gases[19]

1.2   Quenched-luminescence sensing of O_2

Luminescent O_2 sensors utilise the quenching by molecular oxygen of electronically excited triplet state molecules [20]. (Fig. 1.1)
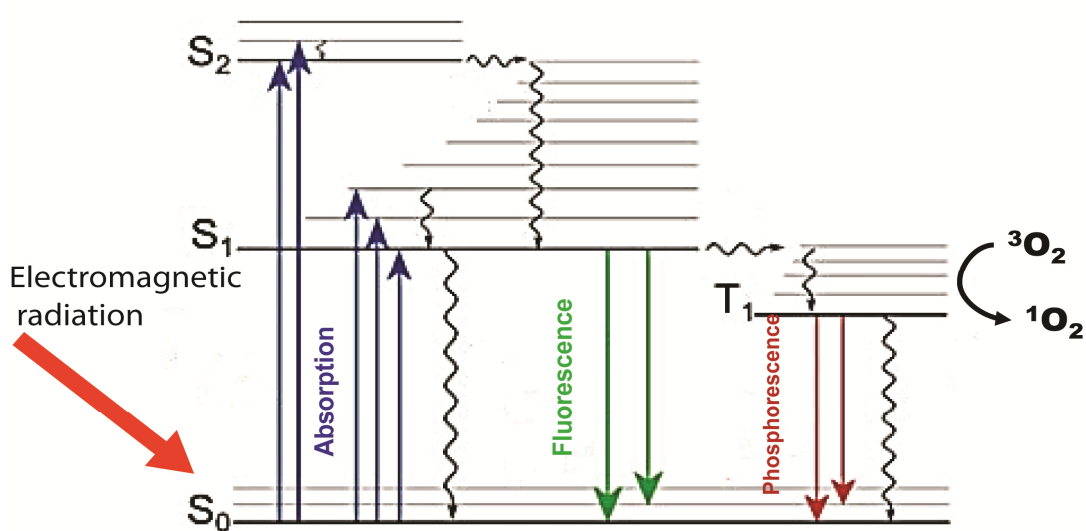
Fig. 1.1 Diagram showing different photophysical processes occurring within O_2-sensitive luminescent dyes when excited by electromagnetic radiation. Molecular oxygen interacts with long-liver triplet states and quenches them and phosphorescence emission.

For phosphorescence to occur, the dye must have high triplet state yield upon light excitation and low deactivation by non-radiative pathways.

At this point, the triplet state dye molecules can be deactivated through collisions with O_2 molecules which decrease the intensity and lifetime of the phosphorescence in a concentration dependent way.

The main detection formats for quantifying O_2 concentration/partial pressure are based on the intensity (I) or lifetime (τ) measurements. The relationships are described by the Stern-Volmer equation (Eq. 1) [20] :

$$\frac{I_0}{I} = \frac{\tau_0}{\tau} = 1 + k_q \tau_0 [O_2] = 1 + K_{SV}[O_2] \qquad \text{(Eq. 1)}$$

Where I_0 and I are luminescent intensities of the dye; in the absence and presence of O_2 respectively. τ_0 and τ are the corresponding lifetime values; k_q is the quenching constant.

Stern-Volmer plots reflect the relationship between the sensor luminescence parameters and the O_2 concentration[21]. (Fig. 1.2).
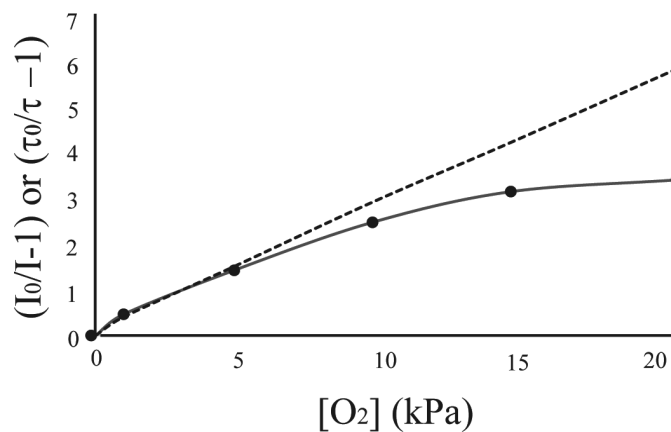
Fig. 1.2 Schematic representation of a Stern-Volmer plot for Intensity or lifetime showing the ideal linear plot (broken line) and the more common curved plot (solid line).

The plot is linear when the dye dispersion within the sensor is homogeneous [22]. For heterogeneous polymeric sensor materials, the Stern-Volmer plots deviate from the linearity. Such cases are often better described by the two-site model [23]:

$$\frac{I_0}{I} = \frac{\tau_0}{\tau} = \frac{f_1}{1 + K_{SV}^1 [O_2]} + \frac{f_2}{1 + K_{SV}^2 [O_2]} \qquad \text{(Eq. 2)}$$

Where I and I_0 are the luminescence intensities of the dye; in the presence and in the absence of O_2 respectively, and τ and τ_0 are the corresponding lifetimes. f_1 and f_2 represent the fractions of total emission arising from each component and $f_1 + f_2 = 1$. K_{SV}^1 and K_{SV}^2 are the Stern-Volmer constants corresponding to each component. Although, designed primarily for intensity quenching, equation 2 can be used to analyse lifetime quenching in non-linear systems[23-24]. O_2 concentration is quantified as a function of lifetime and the Stern-Volmer constant of the particular sensor (K_{SV}) (Eq. 3).

$$[O_2] = \frac{\dfrac{\tau_0}{\tau} - 1}{K_{SV}} \qquad \text{(Eq. 3)}$$

Intensity-based systems are used in some O_2 sensors, but they can be influenced by factors such as position of the sensor, fluctuation of light-source intensity, changes in path light, degradation of dye molecules within the sensor, detector drift and instrument to instrument variability. This can lead to unstable calibrations and measurement errors. To combat this, ratiometric intensity methods can be used in which intensities are read at two different wavelengths, where one is O_2-sensitive and the other is insensitive[25]. The ratio generally gives more stable and reliable readouts. However, it usually requires two dyes in a sensor (one-dye systems are also known[26]), suffers from different photo-bleaching of the dyes, light scattering and auto-fluorescence of samples, and detector noise which can influence the intensity ratio.

Luminescent lifetime is a fundamental parameter of the dye, which is independent of instrument variability and dye concentration (except in cases of dye aggregation at higher concentrations), and it informs on dye micro-environment. Luminescence lifetime can be measured in time or phase domains. In time-resolved measurements the dye is excited with a short pulse and its luminescent decay is measured. Mocon's OpTech^{TM} instrument operates based on time-domain principles. Phase-resolved methods measure phase-shift which is related to the analyte concentration. When a luminescent material is illuminated with a sinusoidal light source, the sinusoidal emission will occur after a delay. The shift difference between the excited and emitted waves is referred to as the phase angle or shift (θ)[27]. For O_2 sensitive luminescent dyes, this shift is also O_2 sensitive. A diagrammatic representation of the principle of phase measurement is shown (Fig 1.3).
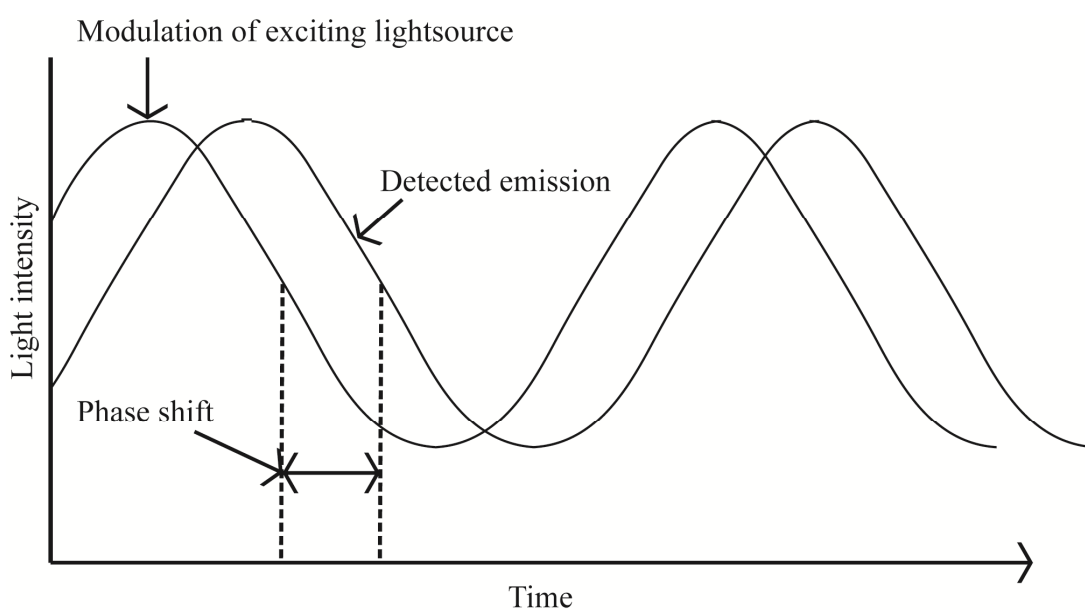
Fig. 1.3 Principle of phase-resolved luminescence lifetime measurement

Phase-based instruments have the advantages of not requiring complex instrumentation and allow the use of low-cost and simple light-sources and

equipment[27-28]. Examples of instruments based on phase-shift reading are the Fibox[TM] produced by PreSens and Firesting[TM] instrument produced by Pyrosciences. If luminescence emission is proportional to the excitation light and the luminescence decay is monoexponential, phase readings can be converted to lifetime values by the use of the following formula:

$$\tau = \frac{\tan(\theta)}{(2\pi\vartheta)}$$
(Eq. 4)

Where τ is lifetime (μs), θ is phase shift (in radians) and ϑ is the modulation frequency of excitation (Hz). The majority of modern O_2 measurement devices are reliant on time-domain and frequency domain measurements.

1.2.1 O_2 sensitive dyes

Luminescent O_2 sensors are created by encapsulation of the dye in a suitable O_2 permeable substrate [17a]. Transition metals complexes and metalloporphyrins [17c, 29] are the most commonly used; due to their relatively long-lived emission (lifetime in the μs range) at room temperature and moderate quenchability by O_2.

Original O_2 sensor investigations looked into the use of polycyclic hydrocarbons (PAHs) as sensing dyes. These fluorescent dyes possess nanosecond lifetime and can be quenched by O_2 in the 0-40 kPa range making them suitable for a variety of biological applications [30]. For example, 1-pyrenebutyric acid [17c] has a longer fluorescent lifetime of 0.2 μs making it suitable for optical O_2 sensing. However, these dyes are not readily compatible with many common polymer matrices, prone to aggregation and possess low sensitivity unless encapsulated in high gas-permeable

matrixes such as silicones. In addition, their UV excitation (300-390 nm range), cause interference by biological matrices.

Organic chromophores such as erythrosine B [31] and boron-dipyrromethene (BODIPY) derivatives [32] have also been proposed, as they phosphoresce at room temperature. However, they exhibit lower wavelength excitation, low brightness and photostability.

Polypyridyl complexes of Ru (II) such as $[Ru(bpy)_3]^{2+}$ and $[Ru(dpp)_3]^{2+}$ have been extensively studied, due to their ease of synthesis and commercial availability[17a, 33]. They exhibit unquenched lifetimes 0.7-5 μs, moderate Stokes shift (the difference in wavelength or frequency between the maxima of the absorption and luminescence bands) and extinction coefficient. Due to poor solubility in hydrophobic matrices, ionic Ru (II) are usually adsorbed on SiO_2 or TiO_2 [34] or paired with lipophilic counter anions (such as dodecyl sulphate) [35]. Ru (II) complexes have moderate quantum yield (usually <0.1), brightness and O_2 quenchability, and high temperature sensitivity which limit their uses in O_2 sensing [36]. An example of a commercial Ru (II) based sensor is the O_2xydot[TM] which is produced by Oxysense Inc, based on $[Ru(dpp)_3](ClO_4)_2$ incorporated into silicone rubber [37].

Some research has gone into Ir^{2+} polypyridine complexes which are soluble in organic polymers. They have strong green phosphorescence with a long lifetime (< 2.0 μs). Tris(2-phenylpyridine) iridium(III) is one complex which shows a relatively long lifetime (1.5 μs) relative to other iridium based compounds. It can be immobilized in different polymer matrices such as poly(styrene-co-trifluoroethylmethacrylate) (TFEM)[38] in order to be applied as an O_2 sensor. However, due to poor molar absorption coefficients (generally <10,000 M^{-1} cm^{-1})
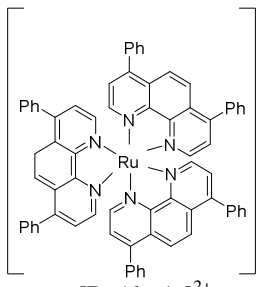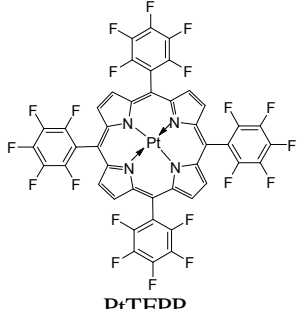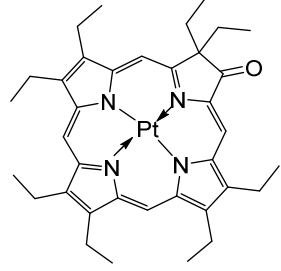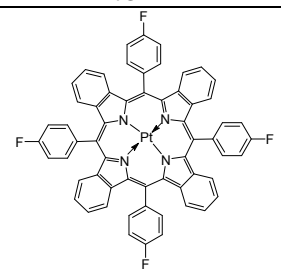
and lifetimes shorter than metalloporphyrins, their use in solid-state O_2 sensors is limited.

The other main candidate dye for luminescent O_2 sensors are Pt(II)-porphyrins and related structures[29]. These complexes show strong phosphorescence at room temperature, a large Stokes shift, and a long emission lifetime (µs) which is moderately quenched by O_2. The central metal ion within the porphyrin influences the properties of the dye with Pd(II)-porphyrins showing 5-10 times longer lifetimes and much higher sensitivity to O_2 is due to the heavier Pd (II) ions having higher spin-orbital coupling[39]. Pd-porphyrins are mostly used for trace O_2 analysis.

Early sensors used Pt(II) octaethylporphyrin (OEP) which has low photo-stability and deteriorated quickly in the polymer matrix [40]. Pt-tetrakis(pentafluorophenyl) porphyrin (PtTFPP) incorporated electron withdrawing perfluorophenyl substituents which improved photo-stability of the dye by reducing electron density on the porphyrin ring [41] is much better in this regard. The major limitation of PtTFPP is the need for excitation at 400 nm in order to achieve high brightness, while excitation at Q bands is weak, which makes it less usable in packaging applications.

Dyes that absorb in the red/near-IR region are more preferred for packaging applications, as they are less susceptible to auto-fluorescence and scattering interferences. In addition, powerful LEDs and laser diodes are available to excite the NIR dyes. A summary of the photophysical properties of commonly used O_2-sensitive dyes is seen on the next page (Table 1.1).

Table 1.1 Summary of photophysical properties of the commonly used O$_2$-sensitive dyes. [42]

Dye	λ_{max}^{Abs}/nm (ε /M^{-1}cm^{-1})	λ_{max}^{Em}/nm	ϕ in solution	τ (μs)	Brightness in PS[a]	Ref.
[Ru(dpp)$_3$]$^{2+}$	463 (2.86 $\times 10^4$)	618	0.366	6.4	10467	36a
PtTFPP	394 (32.3 $\times 10^4$) 504 (2.32 $\times 10^4$) 538 (2.94 $\times 10^4$)	647 710 (shoulder)	0.088	60	92000 5600 7600	43
PtOEPK	398 (8.62 $\times 10^4$) 592 (5.51 $\times 10^4$)	758	0.12[b]	60[b]	19000 12000	44
PtTPTBPF	430 (21.2 $\times 10^4$)), 615 (14.6$\times 10^4$))	773	0.60	50	149000 102000	45

[a] Brightness values were taken from Ref [43b], calculated using, ϕ of Ir(Cs)$_2$(acac) in PS as 1; [b] in micellar sulphite solution

Several porphyrin dyes exist that have red/NIR phosphorescence. Pt (II) complexes of porphyrin ketones[44] and PFPP-lactone[46] have red-shifted and high absorption. Thus, PtOEP-ketone encapsulated in polystyrene shows phosphorescence at 759 nm at room temperature and unquenched lifetime of approximately 61.4 μs. However its brightness is moderate.

Pt(II) benzoporphyrins have absorption and emission in the visible-far-red region (550-700 nm) and are compatible with a variety of different food-safe polymers. Brightness of the dye (defined as: molar extinction coefficient × luminescence quantum yield[42]) is a critical factor as dyes with higher brightness can be incorporated into polymers at lower concentrations, hence reducing aggregation and cost of manufacture.

Tetrabenzoporphyrins (TBPs) have extended π-conjugation by incorporation of benzo ring fused to the core and exhibit red-shifted absorption and emission[47]. By substituting the H-atom of the meso-phenyl ring with a fluorine atom in PtTPTBPF, a red-shift in the phosphorescent emission (λ_{max} approx. 773 nm) and an increase in the brightness, photo-stability and quantum yield was observed[45]. Further substitution of H atoms yielded dyes with reduced quantum yield. The meso-substituted dye is also less likely to aggregate when incorporated into non-polar polymers. When encapsulated in PS (τ_0 = 52.6 µs) and poly(styrene-block-vinylpyrrolidone) nanobeads (τ_0 = 59.6 µs) the dye showed optimal sensitivity towards O_2 in the 0-100 % range.

1.2.2 Polymer matrices

In solid-state O_2 sensors, dyes have to be incorporated into polymer supports or matrices, in order to shield them from quenching interferences and facilitate handling and reuse (Fig. 1.4). Polymer matrices are chosen based on factors such as solubility, retention of the dye (i.e. no leaching or aggregation) and the O_2 permeability (i.e. quenchability) [48]. In addition, the polymer itself should have stable chemical and thermal properties, with minimal change in microstructure over time.

Dye dissolved in polymer
cast as thin film on support

Mechanical support (e.g. Mylar®
film)
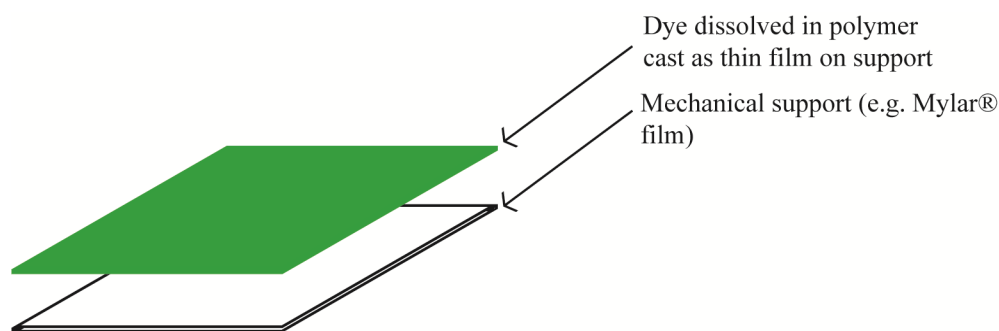
Fig. 1.4 Diagram showing components of traditional solid-state O$_2$ sensors

The sensitivity of the sensor is dependent on the lifetime of the O$_2$-sensitive dye and the O$_2$ permeability of the polymer. Dyes with shorter lifetimes such as $[Ru(dpp)_3]^{2+}$ require polymers with high O$_2$ permeability, such as silicones and fluorinated co-polymers. Dyes with longer lifetimes such as the Pt-porphyrins mentioned above, require polymers with medium to low O$_2$ permeability. As a result, the Pt-porphyrins are generally compatible with many food-grade polymers such as polyolefins (polyethylene (PE) and polypropylene (PP)), polysulfone (PSu), polystyrene (PS) and biodegradable and sustainable polymers such as polylactic acid (PLA) and polyphenylene sulphide (PPS).

Sensors can be tuned to measure specific ranges of O$_2$ depending on the dye/polymer combination selected. The use of dyes with moderately high unquenched lifetime, such as Pt (II)-porphyrins with a moderately O$_2$-permeable polymer matrix, leads to a sensor which can read O$_2$ in the range of 0-21 kPa. Likewise using a dye with long-lived lifetimes, such as Pd (II)-porphyrins with highly O$_2$ permeable polymers, can lead to the production of highly sensitive sensors which measure in the low to trace levels of O$_2$.

Hydrophilic polymers, such as polyurethane and polyacrylamide, show low O$_2$ permeability and are rarely used in solid-state sensors. This is also due to these

polymers swelling in humid conditions, which can shift the O_2 calibrations. However, these polymers can be used for developing biosensors as they show high biocompatibility[49]. Sensor dye microparticles have been incorporated into polyurethane hydrogels for sensing several different analytes [50].

Sol-gel matrices are synthesised through the hydrolysis of silane precursors. These matrices possess desirable properties for O_2 sensing, due to their high optical transparency, good mechanical properties and chemical stability [51]. The porosity and O_2 permeability of sol-gels can be tuned, by varying the fabrication parameters; for example pH, aging time and the ratio of water to precursor [52]. However, there are issues with reproducibility of sensors, sol-gel process complexity, response times and drifts in calibration, due to their tendency to undergo alteration in the network structure (as a result of condensation reactions of the free silanol groups).

Hydrophobic organic polymers, such as polystyrene, are used in O_2 sensors due to their high chemical and mechanical stability, moderate O_2 permeability and ability to form transparent coatings [17a]. In addition to the polymer matrix in which the dye is incorporated, conventional sensors which usually comprises of a thin film coating (to provide fast response) will often need a support material. It is fragile and hard to handle, therefore support materials such as polyester film (e.g. Mylar® [35b]) or microporous supports [53] are needed, to enable easy handling, improved mechanical stability and brightness. The development of covalently conjugated Pt (II) and Pd (II) benzoporphyrins to silicone rubber by Borisov *et al.* [54] has been reported to overcome issues with leaching, migration and aggregation seen in dyes mentioned in the previous section.

Polyolefins are some of the most commonly used polymers in packaging laminates and represent almost half of the total industrial polymers produced in the world [55]. As well as being inexpensive, these polymers exhibit suitable O_2 permeability and good mechanical and chemical properties. However their use in sensors is hindered by limited process-ability and insolubility in commonly used solvents and poor compatibility with common sensor dyes. Some sensors based on PP and PE have been created via solvent crazing [56] and melt-extrusion [56b] which showed promise and general suitability for food packaging, due to their planar nature and thermal stability, lamination and heat sealing options. Discrete sensors have also been produced by spot-crazing on HDPE and PPS films [56a, 57], which exhibited linear Stern-Volmer plots, but also cross-sensitivity to humidity. New sensors which overcome these limitations will be described in later chapters [58].

Some research has gone into producing environmentally friendly and sustainable sensors. Sensors have been fabricated using ethyl cellulose and cellulose acetate matrices. Cellulose derivative polymers possess medium permeability (approx 3-12 cm^3 STP [17c]), however by adding a plasticizer such as tributyl phosphate (TBP) O_2 permeability is increased. A study performed by Mills et $al.$ [59] immobilized Pt(II) and Pd(II) porphyrins in a cellulose acetate and TBP film. However, ethyl cellulose is very hygroscopic leading to limited applications especially in conditions of varying humidities.

Additives can be added to polymers in order to tailor polymer properties such as to improve stability and to tune O_2 permeability of the polymers

Adding plasticizers can improve the efficiency of the O_2 quenching in addition to improving the mechanical properties of the polymer. Plasticizers are often added to

poly(vinyl chloride) polymers to reduce brittleness and facilitate easier handling [17a]. However, the addition of plasticizers can cause issues with leaching which can change sensor function and can also lead to product contamination making sensors produced this way unsuitable for applications in food products.

Fluoropolymers (which have fluoride monomers added) generally have a high O_2 permeability and a negative charge which help hinder photo-oxidation [17c]. O_2 solubility improves 3-10 times on that in parent polymer [17a]. This leads to lower limits of detection and faster response times. Metalloporphyrins have been immobilized in fluoropolymers such as poly(styrene-co-trifluoroethylmethacrylate [41c] to produce working O_2 sensors. In addition, it was shown that increasing the fluorination unit in the polymer increases sensitivity to O_2. Using a combination of fluorination and gas blocking additives, the O_2 permeability of polymers can be adjusted within desired ranges.

However, more complex chemistry results in a more complex sensor structures and expensive fabrication procedures which are not desirable for food packaging. A summary of commonly used sensor materials is on the next page (Table 1.2).

Table 1.2 Summary of commonly used sensor matrices, more detailed tables available in Wang *et al.* review [17a]

Polymer	O_2 permeability	Advantages	Disadvantages	Dyes
Ethyl cellulose	Moderate	Environmentally friendly, Good mechanical strength	Hygroscopic	$Ru(dpp)_3(ClO_4)_2$ [60], Ir (ppy-$NPh_2)_3$ [61], PdEOP [62]
Fluoropolymer	High	Good stability, Tuneable permeability, Limited photo-oxidation	Higher complexity, Added cost	PtOEP [63], PtOEPK [64]
PMMA	Moderate	Low cost, Moderate stability	Background fluorescence in UV range, Requires plasticizer	$Ru(dpp)_3(Ph_4B)_2$ [35a], PtOEP/PdOEP [59]
Polyolefins	Moderate	Low cost, Good stability, Easily available, Good mechanical properties	Poor compatibility with common solvents, Limited process-ability	Fluoranthene [65], PtBP [56a]
Polystyrene	Moderate	Easily manufactured, Low cost, Good stability	Needs support material, Highly hydrophobic leading to slow response in aqueous samples	$Ru(dpp)_3(ClO_4)_2$ [66], $Ir(ppy)_3$ [38], PtOEP [67], PtOEPK [40b]
PVC	Low	Good mechanical properties, Good optical properties	Low O_2 permeability, Needs plasticizers which can leach	Camphorquinone [68], $Ru(dpp)_3(ClO_4)_2$ [60]
Silicone Rubber	High	Good mechanical properties , Good optical properties, High thermal stability, May be steam sterilized	Cannot be easily plasticized, Poor hosts for highly polar dyes, May contain unknown components in precursor material, Final attributes affected by curing procedure	Pyrene [69], $Ru(dpp)_3(laurylsulfate)_2)$ [70], Pd coproporphyrins [71]
Sol-gel	Tuneable	Good mechanical properties, Good optical properties	Poor reproducibility, Process complexity, Change in structure over time (aging)	$Ru(bpy)_3$ [72], PtOEP [73], PtTFPP

1.2.3   Methods of dye encapsulation

Dyes can be incorporated into polymer matrixes in a variety of ways. The most common method involves dissolving the dye and polymer in a suitable solvent, spreading such 'cocktail' onto a suitable substrate (usually a support like Mylar$^{®}$ film or glass slide) as thin film and drying. This method works when the dye and polymer are compatible with the same solvent. Previous efforts at sensor fabrication involve the use of spin-coating (usually on a glass substrate), fabrication of dye solutions in printable ink formats[74], and spotting a dye cocktail on a porous membrane such as filter paper [75].

Some dyes can be covalently linked to the backbone of matrix polymer to form stable sensors which have no leaching and dye migration issues [76]. Dyes with cationic groups such as $[Ru(dpp)_3]^{2+}$ can be adsorbed onto polymeric particles with negatively charged surfaces such as silica. Dyes are increasingly being incorporated into polymer micro and nanoparticles[24, 77] which provide a protective and stable environment for the dye and liquid/dispensable sensor formulation. O_2-sensitive microparticles with tris(4,7-diphenyl-1,10-phenanthroline)ruthenium(II) dichloride ($[Ru(dpp)_3]^{2+}$ absorbed on SiO_2/TiO_2 were also co-extruded into polymer films [56b].

Sensors have also been created by solvent-crazing method [56a, 57] on HDPE and PPS (Fig. 1.5) which allows for previously non-compatible components to be combined. Solvent-crazing of polymers in physically active liquid environments (PALE) allow the incorporation of previously incompatible dyes and polymers. The basic concept of crazing involves the tensile drawing of a polymer film in a suitable solvent which leads to the creation of nanoporous structures in the polymer known as 'crazes'. If an additive is dissolved in the crazing solvent, it can be sucked into and trapped in the crazes once the tensile pressure is released. The crazing is controlled

by the nature of the polymer (crystallinity, chemical structure etc.), PALE, the way the strain is introduced to the polymer (i.e. the tensile strain, applied stress, strain rate and temperature) and the concentration of additive (or dye) in the crazing liquid[78]. In addition to swelling and spot crazing methods, which are generally batch produced, efforts have been made to make sensors on a continuous basis [79].
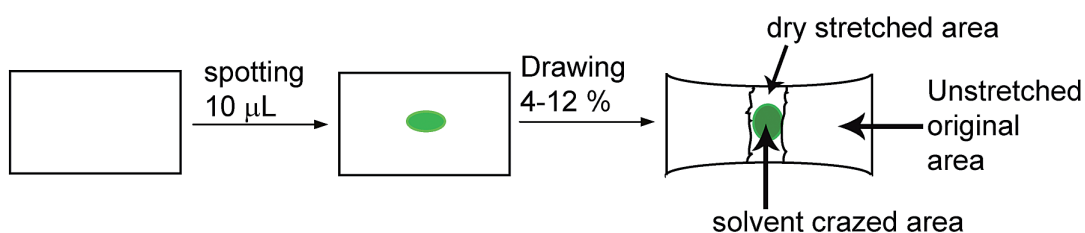
Fig. 1.5 Diagram showing batch spot-crazing system [56a].

Recently, there has been some interest in fabricating sensors in a micro and nano sized fibre format. Fibres are attractive as sensor matrices as they have high sensitivity, fast response times, high porosity and could be easily exposed to analytes [80]. Nanofibres have been fabricated from polystyrene [81], polycaprolactone[82], and more recently, from PE and PP [80]. Although, possessing formidible attributes, production of such fibres consume large amounts of solvent which can increase the production cost. In addition, sensors based on these polymers sometimes have issues wth aggregation within the nanoporous structure, cross-sensitivity to humidity and the fragile nature of the fibres leads to them being quite difficult to handle.

Luminescent dyes can be incorporated into polymer matrices by swelling method. Some polymers, with higher chemical resistance, swell to many times their original size when absorbing a compatible solvent. Additionally, by dissolving compatible dye in the swelling solvent, the dye molecules can diffuse into the polymer. When removed from the swelling solvent, the polymer returns to its original volume

trapping the dye molecules within. The degree of swelling is dependent on the compatibility of the polymer with the solvent and the strength of the solvent.

1.2.4 Preferred Sensor Materials for Food packaging applications

Although there are many O_2 sensing dyes and materials, only a few are actively used in food packaging applications. The main selection criteria are spectral properties, O_2 sensing performance and cost. In addition, the sensor materials have to be compatible with common packaging materials and processes, and are safe to be in packs and in contact with food as laid out by legislation.

For practical applications, the dyes should be compatible with available excitation sources such as LEDs and lasers. The chemical stability and photo-stability of the dyes are also critical factors, as in food packaging the sensors will be exposed to a variety of harsh lighting and chemical conditions. As they will potentially also be in contact with food, the sensors should exhibit low toxicity with no leaching of the dye. Therefore the solvents used to create the sensors should be considered carefully. Furthermore, for large scale food applications the sensors should be reproducible, robust and use minimal components for fabrication [4a].

The sensors should preferably be planar to assist easier integration into food packaging. Integration techniques include free-standing sensor inserts which can placed in containers with the food, adhesive stickers attached to the packaging, printed sensor labels printed on the inside of the packaging label and lamination where the sensor is laminated between the outer barrier packaging and an inner O_2 permeable layer. The main requirements for integration are: the allowance of easy

access of the sensor to the container atmosphere, the interrogating instrument and protection of the sensor from the atmosphere outside of the package.

Additionally, integration processes can often protect the sensor from the food product and *vice versa*. This is often vital as some food components (e.g. meat juices) can affect the sensors characteristics (reduced signals due to discolouration, shift of calibration due to plastification and changing of the availability of O_2 to the sensing dye) and leads to inaccurate readings. From a food safety perspective, the use of a gas permeable film, such as HDPE, laminated on top of the sensor, between the sensor and food product, can prevent migration of the sensor components (dye and polymer matrix) into the food, and product contamination with particles that could be accidentally ingested.

1.2.5   Characterization of sensors

Before implementation, new sensors should undergo detailed characterization. Initial characterization involves plotting the sensors intensity/lifetime readings over a range of O_2 concentrations to obtain a calibration. For applications in food packaging, the sensor should show reproducible calibrations, generally over the range of 0.05-21 kPa O_2. Some food products such as raw MAP meat require sensors measuring up to 100 kPa O_2, while other products require measurement trace O_2 levels (ppm range). The sensors should have no cross-sensitivity to humidity, as humidity is not controlled in many food packages.

Most solid-state sensors show a dependence on temperature and their sensitivity decreases at low temperatures. As many food products are stored in a variety of conditions and transported to various climates abroad, the sensors should exhibit

predictable response over a representative range of temperatures (- 20 °C - + 30 °C). Unfortunately, only a few systematic studies have been performed over such a wide temperature range [83]. The cross-sensitivity of a sensor to temperature is strong, and luminescence measurements must be corrected for temperature fluctuations in food packages.

Additionally, response time is a critical factor. Use of thin film coatings and microporous membranes with high gas permeability, allows for fast (second timescale) response times which are generally desired, especially for in-line monitoring of packaging integrity of large-scale lines. Finally, as mentioned above, photo-stability and long shelf-life stability of the sensors are essential when designing sensors to be applied to food packaging monitoring.

1.2.6 Instrumentation

Currently, several commercial optical O_2 sensors and instruments are available for industrial applications. However, only a few are directly suitable for packaging applications, which demand special requirements, such as operation with detachable, disposable, calibration-free sensors, a broad range of working temperatures, a portable handheld measurement device, high level of validation (i.e. knowledge of cross-sensitivities and interferences) and affordable costs.

Comparison of several most suitable systems is provided on the next page (Table 1.3) [42]:

Table 1.3 Summary of photophysical properties of the commonly used O$_2$-sensitive dyes [42].

Company	Mocon Inc & Luxcel Ltd.	Oxysense	PreSens GmbH
Sensor	OpTech^{TM}-O$_2$ Platinum	O$_2$xydots$^{®}$	Pst3
Dyes	PtTBP	[Ru(dpp)$_3$]Cl$_2$	PtTFPP
Forms	Adhesive stickers(peel able from a card)	Sensor dots applied with silicon glue	Sensor dots applied with silicon glue
Measuring range	0.001- 30 % permeation mode (g) 0.015 %-25 % headspace mode (g) (0.006-10.5 mg/L (l))	0-30 %	0-100 % (g) (0-45 mg/L (l))
Accuracy	± 2 % or ± 150 ppm (whichever is greatest)	5 % of reading	± 0.4 % @ 20.9 % O$_2$ ± 0.05 % @ 0.2 % O$_2$
Detection limit	0.03 % (0.03 kPa)	0.03 % (gas) 15 ppm (liquid)	0.03 % (gas) 15 ppm (liquid)
Compensation	Automatic temperature (contactless IR sensor) and pressure compensation	Integrated temperature and pressure probes	Integrated temperature, and pressure probes
Operating temperature	5-40 °C	0 °C - 70 °C	0-50°C
Response time	< 3 sec (gas) <30 sec (liquid)	< 30 sec	< 6 sec (gas) < 40 sec (liquid)
Price per sensor	$3	$4.30	$33

These systems often require quick re-calibration of sensor (or whole system with instrument) before use to confirm their accuracy. The OpTech^{TM} sensors are calibration-free, but they also have validation "Calcard" (or calibration vial for needle sensors). Oxydots$^{®}$ come with factory calibration however user calibrations may be carried out if deemed necessary. PreSens sensors use a two-point calibration at 0 kPa and 21 kPa before operation. These companies offer customised sensor modification such as sensors for trace O$_2$ analysis (PSt6, PreSens) and individual deployable sensor beads (dOxybead^{TM}, Luxcel-Mocon). (Fig. 1.6)
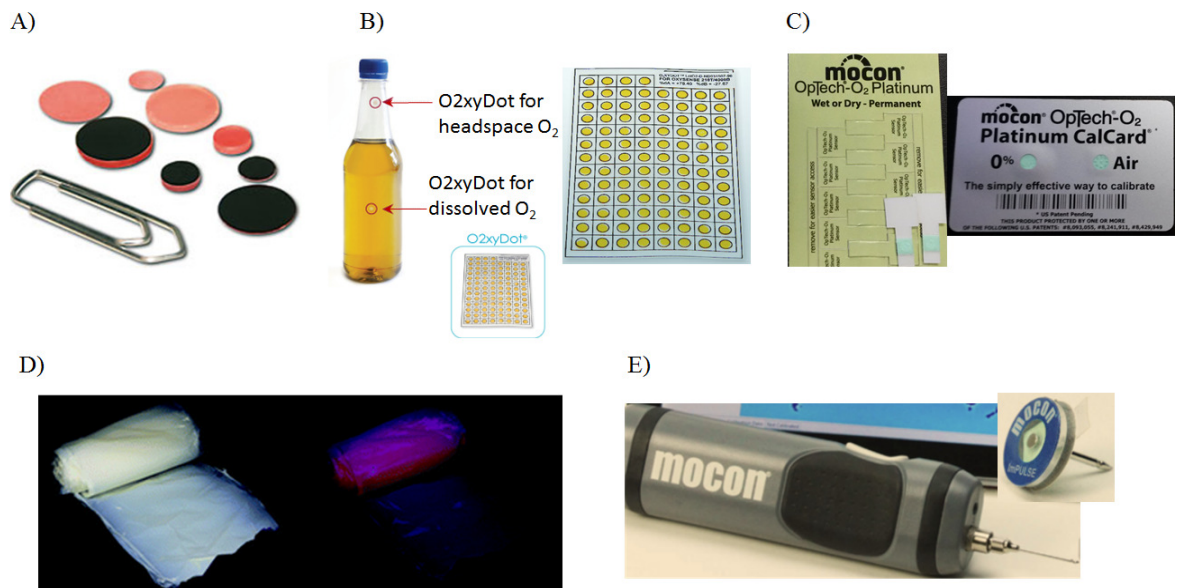
Fig. 1.6 Images of various types of O₂ sensors: A) Presens Sensor spots; B) Oxysense sensor spots glued to the bottle; C) Mocon OpTech™-O₂ Platinum adhesive stickers on a card and CalCard for system validation, D) sheet of extruded sensor film, E) Mocon needle-taken from Banerjee *et al.* [42].

Easy integration of the sensors into food packaging is essential. Oxydot[®] and Presens sensors must be stuck to the packaging using silicone glue. Mocon's OpTech™ sensors come as a self-adhesive sticker, or imPULSE™ probe and a needle sensor for minimally destructive headspace analysis. Although convenient, use of the above sensors is limited by their expense, which in turn limits their inclusion in mass scale manufacturing. The viability of sensors to be used in food packaging are reliant on their production cost which should be less than 1 cent [4a]. As a result, many new studies are carried out to attempt to manufacture new optical sensors, which use less expensive components and can use existing reading instrumentation or newly designed instruments.

1.3   Applications of O_2 sensing in food packaging

Much of the proof of concept work on the use of non-destructive luminescence based O_2 sensing in food packaging was done in the 2000s. Prior to the appearance of advanced commercial O_2 sensor systems; such as Fibox (Presens), O_2 analyser (Oxysense) and Optech[TM] (Mocon), prototype O_2 sensors and instruments [84] were used.

In initial studies, O_2 sensors were used to detect compromised packages so that manufacturers could be aware of failures. MAP protects food products from outside contamination, in addition to inhibiting microbial growth and other degradative processes by tailoring of gases within the packages. Some red meats, such as steaks, require medium levels of O_2 to promote oxygenation of the myoglobin within the meat, which maintains the aesthetically pleasing red colour. Unlike beef, chicken products require lower O_2 levels ($< 1 \% O_2$) in order to maintain quality. Lipid oxygenation can occur in the presence of very low levels of O_2, therefore in products such as cooked meats, O_2 levels must be kept very low in order to prevent quality decline [85].

As O_2 is an important quality indicator, it is therefore a very important analyte to monitor. Levels within packages must be monitored closely, to pick up on any damaged or compromised products where the atmosphere is no longer intact. Packs on manufacturing lines which fail to meet strict O_2 guidelines should be rejected or repackaged if this is a viable alternative before they can leave the factory.

Originally, prototype sensors comprising of phosphorescent PtOEPK dye dissolved in polystyrene and spotted on polymeric membranes or filter paper were used to track O_2 levels in packaged beef and hams [75, 85]. These sensors were also

used to demonstrate the commercial feasibility of such sensors as a means to detect compromised packages. The use of disposable O_2 sensors in individual packs were found to be very useful and informative when placed in direct contact with the food or attached to the lidding material and exposed to package headspace. Reliable optical signals and hence quantitative information about the O_2 levels within the pack were obtained.

In particular, the ham study showcased the great need for continuous monitoring of food packages [85]. Although the products were packaged under anoxic atmosphere, residual O_2 levels in the packs were significant (0.1-1 %) and gradually increased during storage. This can be due to O_2 exchange between O_2 trapped within food products and the package headspace, the permeability of the packaging materials and/or imperfect sealing. Screening of the ham packs exposed multiple failures (1-5 in each batch) which could be missed using the traditional headspace analysis methods, which take packs off the line for analysis on a statistical basis. Prompt detection of these failures can save the company money, as the failed packages can be repackaged without any degradation of the food product if caught in time (Fig. 1.7).
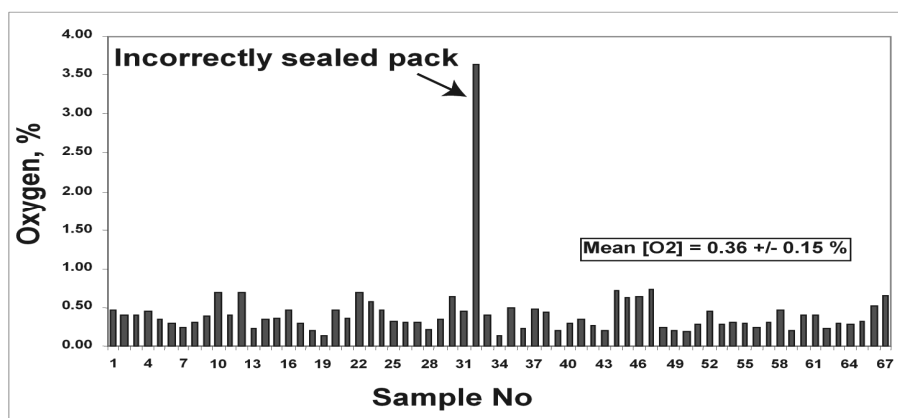

Fig. 1.7 Representative results of screening of a batch of MAP food product with disposable O_2 sensors (adopted from Banerjee *et al.* review[42])

PtOEPK sensors were packaged with cheddar cheese and used as integrity checkers [86]. The study found 3 failures out of 67 packs and yet again demonstrated the need for individual integrity checks in packaging.

PtBP dye based sensors were adhered to green and brown wine bottles to assess the bottles for leaks and track O_2 ingress through the cork [54].

Fresh produce, such as vegetables and salads, are highly perishable and "breathable" i.e. require O_2 to maintain freshness. As these products are alive and respiring, there needs to be minimal time between harvesting, processing and packaging [87]. Perforated lidding was traditionally required for fresh produce to ensure that O_2 levels were sufficient to allow respiration. However this allows air exchange with the food product which encourages microbial growth. Therefore, many of these products are now packaged using MAP[88] which protects the product from outside contamination while ensuring O_2 levels are sufficient. PtOEPK sensors in combination with Mocon's OpTech™ instrument, were shown to provide accurate and comprehensive information on O_2 headspace levels, when placed within commercially packaged bags with fresh salad leaves [88]. In addition, respiration profiles of different types of lettuce were shown to be easily obtained using these sensors.

Lettuce leaves have different rates of respiration subject to the species of the lettuce. It is therefore important to track lettuce respiration as the O_2 levels within the pack must correlate to the leaf with the highest O_2 requirement to maintain freshness for a seven day shelf-life and avoid wilting of any component. The study on lettuce using optical O_2 sensors showed that MAP can be tailored to the type of produce being packaged in order to extend shelf-life.

O$_2$ sensors can also be used to test preservative measures taken on food. PtOEPK sensors were used to track the effects of different ethanol based atmosphere modifiers on MAP breads [89]. Although MA packaged with anoxic atmosphere, the sensors tracked a rise to approximately 14 % O$_2$ as a result of O$_2$ release from the bread products which was introduced during processing. This rise in O$_2$ encouraged the growth of mould on day 12. The use of an ethanol spray reduced the onset of mould to day 13 but left an undesirable aroma and taste on the product. In comparison, the ethanol-emitting LDPE sachet postponed mould growth until day 30 with no noticeable changes in sensory properties of the bread. Therefore, the objective of the study to extend shelf-life was achieved and O$_2$ sensors tracked the O$_2$ content over the period of the study.

Sensory properties such as colour, taste and aroma have a major effect on how the food product is appraised by producers and consumers. Even a slight increase in O$_2$ can have a noticeable effect on these parameters and decrease the quality of the food. Therefore, the monitoring of O$_2$ levels and relating these levels to degradative processes is fundamental in forecasting shelf-life and ensuring quality of food products from factory to fork.

One such study used PtOEPK O$_2$ sensors to correlate O$_2$ levels to lipid oxidation in samples of raw and cooked beef both vacuum-packaged and MA-packaged [75]. It was shown that although oxidation did not occur up to day 35 in vacuum-packed raw and cooked meats, MAP meat had an oxidative stability of 12 days, most likely due to its higher initial O$_2$ levels. The study also concluded that although O$_2$ is needed for lipid oxidation it is not the driving factor as revealed when comparing oxidation levels in MAP cooked meat to vacuum-packed cooked meat. Instead, it was shown that temperature was the driving factor of lipid oxidation as demonstrated by higher

lipid oxidation in cooked meats versus raw meats. This finding indicates measures should be taken to reduce exposure to O_2 between cooking and packaging to limit lipid oxidation.

In the same way, OpTech^{TM} O_2 sensors have been used to measure the depletion of O_2 in raw beef and chicken fillets [90]. Both samples were packaged with a 21 % headspace. The beef and chicken showed a decrease in O_2 levels over a 9 and 10 day span respectively. This confirms that aerobic bacteria which are the most common cause of food spoilage, consume headspace O_2 over time. However, as no sensory data was available in the study, there is no way to ascertain whether the food was deemed spoiled before the O_2 levels were depleted. As chicken is conventionally packaged in 0 % O_2 atmosphere, it would seem likely that this product would be considered spoiled before 10 days due to other degradative processes such as lipid oxidisation.

Studies have also tracked the correlation between the growth of microorganisms on food and O_2 levels. In the cheddar cheese study mentioned previously, PtOEPK sensors were used to trace the O_2 profile of a faulty package of cheese (which is usually packaged in an anoxic environment), showing that as mould grew on the contaminated product the O_2 levels steadily decreased [86]. This is an important factor to consider when monitoring quality and degradative processes within food products, as initial high O_2 concentrations, which would usually indicate a leak, are often depleted to original levels by oxidation and microbial actions within certain windows of time.

Along with influencing some chemical reactions in solid foods, O_2 plays a key role in the quality of liquid products and beverages. Many chemical reactions occur

during the maturation of red wine and the effect of O_2 (either positively or negatively) can impact the final wine characteristics. Therefore, O_2 content in wine products must be quantified and controlled.

Many wine-makers add controlled concentrations of O_2 to wine in order to optimise the maturation of the wine. The influence of different O_2 exposures on the evolution of several volatile sulphur compounds (VSCs) such as H_2S, methyl mercaptan (MeSH) and ethyl mercaptan (EtSH) during Shiraz maturation was investigated by Ugliano et al. [91]. Their aim was to create O_2 procedures to control the evolution of VSCs in the wine. Each bottle was fitted with two PreSens Pst3 sensors; one to measure headspace O_2 and the other to measure dissolved O_2 in the wine. The study findings implied O_2 had a direct effect on the H_2S and MeSH levels, which in turn affected the odour of the wine. By plotting the O_2 levels obtained by the sensors against the concentrations of VSCs, a correlation between lower O_2 levels and higher VSCs was made.

Similar to wine, the flavour and visual appearance of beer are dependent on oxidations during processing and packaging stages [92]. Stability of beer flavour is dependent on low O_2 concentrations. Although, beer should be O_2 free after fermentation, it is most vulnerable to oxidation at this point. Bottles are filled to the top with carbonated beer and capped aim to minimise the O_2 trapped in the bottles. When the foam dissolves, the O_2 levels left in the headspace should be negligible. However, this process is often affected by the different foam structures formed in bottle necks which trap some O_2. High O_2 levels lead to higher levels of carbonyls and development of undesirable tastes during storage. As beer degrades, these carbonyls increase, suggesting that beer would taste best straight after production. O_2 sensors have been used to monitor residual O_2, oxidation and quality of beer over

time. PtOEPK sensors were adhered on the inside of bottles and a phase detector was used to measure the signals from the sensors. The study showed pasteurisation (a technique used to kill microorganisms) caused headspace O_2 to diffuse into the product which was in turn rereleased into the headspace over time. This indicated that O_2 was not utilised in spoilage processes however, sensory analysis performed as part of the study, showed that beers with initial headspace $O_2 > 1$ % were considered unacceptable by the tasting panel. Therefore, O_2 sensors were demonstrated to allow continuous quality monitoring with set quality criteria such as O_2 levels < 1 % O_2.

Ascorbic acid (AA), otherwise known as Vitamin C, is a stabilising antioxidant which can be oxidised and broken down into undesirable by-products. When AA is oxidised over time, it converts into L-dehydroascorbic acid (DHA), which has an antioxidant activity five times lower than AA, [93] which sequentially increases browning in the juice. Additionally, as DHA increases, the biological action of vitamin C is lost. As a result, packaged orange juices are considered to be highly perishable and O_2 sensitive products, resulting in O_2 concentrations being monitored as quality factors during their production and storage. Therefore, residual O_2 and in turn, packaging permeability, is considered to have an effect on the sensory and nutritional quality of the juice. Oxydots® were used in studies by Van Bree *et al.* and Wibowo *et al.* to link O_2 in headspace to the degradation of AA[94]. Both studies found a correlation between higher O_2 levels and rapid, higher DHA formation. This indicates that precautions should be taken to control O_2, during the processing and packaging of orange juice to minimise degradation.

Lastly, the link between storage temperature and O_2 to lipid oxidation in rapeseed oils has been investigated using Oxydots®. Kozak *et al.* [95] monitored the rate of O_2

consumption during storage of rapeseed oil products, with ambient headspace at varying temperatures. The study revealed that higher temperatures increased O_2 consumption and led to higher formation of hydrogen peroxides (a by-product of lipid oxidation). Samples stored with nitrogen headspace showed minor hydroxide peroxide formation. Thus, the optical O_2 measurement technique could be applied to all liquid oil products in order to evaluate optimal storage conditions.

In MAP systems, a gradient of the gas is created between the inner compartment containing the food and external atmosphere (usually air). The permeation of packaging materials, even if they have barrier material properties, can still allow atmospheric O_2 pass into the product. Therefore, having a quantified measurement of packaging gas permeability is very important in the food and packaging industries. Usually, the O_2 permeability of films and other materials are measured on special instruments such as Mocon's Ox-Tran® Model 2/21 system or Oxysense's Oxyperm OTR system. Although very accurate, these systems are limited to planar empty samples, have low sample throughput and are time-consuming. The Oxyperm system has made efforts to combat this by producing an adaption for measuring bottle permeation but is still limited by expense and the need for a trained operator [37].

Introduction of disposable O_2 sensors and non-destructive, contact-less optical measurements can address the shortcomings of the conventional instruments and enable an extended range of gas permeation tests. These sensors can be adhered to almost any surface of an assortment of shaped packs, including whole composite material e.g. trays with sealed lidding, closed bottles, packages filled with liquid or food. In addition, the sensors can be used to measure packaging materials being stressed on the packaging line.

PET carboys, which are used in home winemaking, were evaluated for O_2 permeability using a Mocon OpTech[TM] instrument [96]. The O_2 sensor stickers were adhered to the neck of each carboy and interrogated regularly for the O_2 content in the carboy. The study was dual-purpose by both affirming the suitability of the carboy for use and demonstrating the suitability of the Mocon OpTech[TM] system for measurement of packaging permeability.

A similar study was carried out by Diéval *et al.* using Presens Fibox 3 O_2 meter and PSt6 sensors [97]. Upon adherence of the sensors on glass bottles, bottles with different Normacorc closures were examined for differences in O_2 ingress over 250 days. The bottle necks with closures were also tested on the Mocon Ox-Tran[®] instrument for comparison. The Presens sensors were shown to perform well against the Ox-Tran[®] instrument and provide a simple easy-to-use alternative to traditional O_2 permeability measurement devices. J. Wirth *et al.* [98] and Ugliano *et al.* [99] have both carried out similar studies assessing O_2 transmission rates using Presens sensors.

Although packaging science has advanced significantly in the last few years, the choice of packaging is often a case of trial-and-error which is time-consuming and wasteful. In an interesting study, Van Bree *et al.* carried out a systematic study into the permeation levels of different multilayer packaging compositions [100]. The outcome of the study was the development of simulation software, which could predict the optimum headspace O_2 concentration dependent on packaging configuration and storage conditions. The software was validated using Oxydots[®]. Simulations include the influence of different packing materials, thicknesses, temperatures and headspace on overall O_2 concentration within the pack. This

software has the potential to eliminate some of the package material testing required for new food products.

Dissolved O_2 can also be measured by some optical O_2 sensors. In wines, the concentration of O_2 has a major effect on the wine's final properties. If concentrations are too low, aroma defects such as reduction (dominant smell of egg or rotten vegetables [101]) can occur. In contrast, if O_2 levels are too high, there can be an increase in oxidation and discolouration of the wine [102]. Many of these studies utilize the PreSens sensors as they are non-invasive and can be continuously monitored.

Wine can be discoloured if exposed to excess O_2 e.g. white wine is known to turn brown and red wine an orange-red tone. However, as wines are often required before the colour and texture can be stabilised naturally by aging, controlled oxygenation of the wine is required [103]. This oxygenation usually occurs after fermentation. However, in recent times, the use of rotary fermenters has been recommended to introduce the optimum concentrations of O_2 required for chemical reactions to occur. As these fermenters are closed systems, optical O_2 sensors from Presens were used as they can be used to measure O_2 concentration within the system non-invasively. From the data obtained from the PSt3 and PSt6 sensors, correlations were made between higher O_2 concentrations and lower tannin concentrations; resulting in more stable wine colour and lower astringency. Both astringency and lower tannins increase the desirability of wines to consumers.

Ascorbic acid (AA) is often added to wine in order to reduce oxidative degradation[104]. Along with its antioxidant effects, AA has also been shown to improve wine colour and flavour. Ascorbic acid can degrade both oxidatively and

non-oxidatively. If uncontrolled, the latter can lead to shortened shelf-life as it depletes sulphur dioxide which provides anti-microbial protection to the wine [105]. As data on non-oxidative degradation of AA is sparse, it can be hard to predict optimal O_2 levels in the wine suitable to maintain oxidative degradation (the by-products of which are scavenged by sulphur dioxide). As a solution to this, a study on non-oxidative degradation of AA was carried out by Wallington *et al.* which gathered kinetic data on the process. To ensure anoxic conditions, Presens' sensors were used to measure dissolved O_2 (PSt3) and gaseous O_2 (PSt6). Although, anoxic conditions are difficult to achieve, O_2 concentrations were kept below the limit of detection of the sensors (PSt3 < 50 µg/L) to ensure non-oxidative degradation of the AA would occur. The data showed that lower temperatures inhibited non-oxidative AA degradation. This implies that wines should be stored and transported at lower temperatures to limit non-oxidative degradation of AA.

Although several commercial optical O_2 sensor systems exist, there have been very few validation and benchmark tests performed on these systems against existing instrumental methods. The Mocon OpTech™ system, which has the range of 0-25 % O_2 was compared to the traditional destructive headspace analyser Dansensor™ which has a range of 0-100 % O_2 [87]. The Dansensor™ punctures the package through a septum in order to analyse the atmosphere while the OpTech™ sensor can give readouts via a contactless reader. The study showed closely corresponding values up to 40 % O_2, after which the OpTech™ started to show inaccurate readings. At the same time, OpTech™ showed a better sensitivity in the low O_2 range – 0.03 % as opposed to 0.1 % for the Dansensor™ (which can only give one decimal point readings).

Likewise, very few studies have looked in detail at sensor behaviour and calibration upon its exposure to food products in packs or sensor stability. Likewise the accuracy of O_2 readings in conditions of real life operation with different packaged foods and beverages has rarely been assessed. This data is particularly important when sensors are operating in direct physical contact with food product that may have high fat content (plastification by oil), strong flavours, varying water content or long-term experiments with liquid samples. Package contents could shift sensor calibrations and, if not compensated for, lead to inaccurate readings [106]. A summary of food based O_2 sensor studies is found in Table 1.4 on the next page.

Table 1.4 Summary of sensors used in food based applications.

Product	Analytical Task	Sensor Material	Instrument	Result	Ref
Food					
Beef (Cooked/Raw)	Residual O_2 levels	PtOEPK/PS on filter paper	Phosphorescence phase detector	Lipid oxidation correlated to O_2 levels	75
Beef/Chicken (Raw)	Residual O_2 levels	OpTech[TM] stickers	Mocon OpTech[TM]	O_2 consumption of meat products tracked	90
Bread	Tracking O_2 levels/ product shelf-life	PtOEPK/PS on filter paper	Phosphorescence phase detector	Optimum shelf-life extending treatment discerned	89
Cheese	Integrity testing	PtOEPK/PS on filter paper	Phosphorescence phase detector	Compromised packages detected, O_2 correlated to microbiological growth	86
Lettuce	Monitor O_2 levels	PtOEPK/PS on filter paper	Mocon OpTech[TM]	Respiration profiles of product obtained	88
Ham	Monitor O_2 levels	PtOEPK/PS on filter paper	Phosphorescence phase detector	Compromised packages detected	85
Liquids					
Beer	Headspace O_2 levels	PtOEPK/PS on filter paper	Fluorescence phase detector	Tracked O_2 profile, headspace >1 not palatable	92
Orange juice	Monitor O_2 levels	O_2xydots®	Oxysense® 210T probe	O_2 correlated to AA degradation	94
Rapeseed oil	Monitor O_2 levels	O_2xydots®	Oxysense® 4000B system	Storage temperature correlated to O_2 consumption	95
Wine	Leak detection and O_2 ingress	PtBP/PDMS on PE foil	Pyroscience Firesting[TM]	Proof of concept	54
Wine	Dissolved O_2 levels	Presens PSt3 sensor	Presens Fibox 3	Decreasing O_2 = Increasing VSCs	91
Wine	Tracking O_2 levels	Presens PSt3/PSt6 sensors	Presens Fibox 3	Increasing O_2 = Decreasing tannins	103
Wine	Ensuring anoxic atmosphere	Presens PSt3/PSt6 sensors	Presens Fibox 3	Model for non-oxidative AA in wine obtained	105
Packaging materials					
Normacorc closures	O_2 ingress	PSt6	Presens Fibox 3	Determined most efficient closure	97
Packaging materials	Validation	O_2xydots®	Oxysense® 210T probe	Validated packaging simulation software	100
PET Carboys	O_2 permeability	OpTech[TM]-stickers	Mocon OpTech[TM]	Carboy suitability affirmed	96

1.4 Conclusions

The above outlines the principle of operation, background and current approaches when using solid-state O_2 sensors to monitor quality in food packaging. Disposable O_2 sensors can provide robust, repetitive, fast, non-destructive and reliable readings of dissolved and gaseous O_2 in food products. They have been used in a variety of packaging compositions and have proven to be a useful tool for the monitoring of food quality from production, packaging and transport. By rights given how useful they are, disposable O_2 sensors should be actively used in the food industry for both new product development and maintaining the quality of current products.

Regrettably, this is still not the case. Even though sensor technology has advanced majorly in the past few decades, sensors are still not ideal for food packaging applications. Sensors are still considered as research tools by the food industry rather than a food safety necessity. This is almost completely down to the high cost and complexity of current sensors. Due to low profit margins in the food industry, sensors need to be low-cost and easily incorporated into current packaging materials. Current sensors are still expensive (>$3 a piece), inflexible and are mostly time-consuming to integrate. Before they become viable, several critical factors will have to be addressed. These factors include cost, analytical performance, robustness and ability to be more easily incorporated into current packaging.

In addition, during sensor development, more research needs to go into real-world testing of the sensors. Interactions between the sensor and food product, stability of the sensor in contact with the food, cross-sensitivities and the safety of such sensors need to be studied in depth before they will be deemed suitable for inclusion in food packaging. The sensors in the following chapters have been designed to address these aspects.

2 Chapter 2: Experimental

2.1 Materials

Platinum(II) benzoporphyrin dye (PtBP) was kindly donated by Luxcel Biosciences (Cork, Ireland). Toluene ($\geq$ 99.3 %), tetrahydrofuran (HPLC grade), 2-butanone (analytical grade), ethyl acetate (analytical grade), anisole (analytical grade) and Kolliphor P188 were purchased from Sigma-Aldrich (Ireland). Nitrogen, O_2 and carbon dioxide (CO_2) gases (99.999 % purity) were from Irish Oxygen (Cork, Ireland). All solid chemicals were obtained from Sigma-Aldrich (Ireland).

The non-woven spunbond polypropylene (PP) grafted with acrylic chains (type 700/70, thickness 130 µm $\pm$ 20 µm, fibre size 8-12 µm, mean pore size 17 µm), non-woven wetlaid PP (type 700/30K, thickness 160 µm $\pm$ 20 µm, fibre size 8-12 µm, mean pore size 18 µm) and ungrafted PP (type FS2192i, thickness 80 µm $\pm$ 20 µm, fibre size 8-12 µm, mean pore size 17 µm) were purchased from Freudenberg, UK. High-density polyethylene (HDPE) films (25 µm thick) were from DSC/SABIC (Netherlands), the Fortron® film (blown PPS, 127 µm thick) was from CSHyde (Netherlands) and polypropylene film was obtained from Goodfellow (UK).

Low O_2-permeable trays (polystyrene/ethylene vinyl alcohol (EVOH)/PE, permeation 8-12 cm^3 m^{-2} day^{-1} at STP) sealed with a laminate of orientated polypropylene (OPP) (thickness 20 µm) and co-extruded layer of PE/EVOH/PE were purchased from Cyrovac/WR Grace Europe Inc. (Lausanne, Switzerland).

The meat samples of beef steak and chicken were store-bought. The cheese samples were obtained from a local cheese factory. Beef samples were sourced from a local meat processing factory.

Phosphorescent O_2-sensing probe, Greenlight[TM], was from Luxcel Biosciences (Ireland). Standard 96-well plates (clear polystyrene, flat bottom, with lids, packed sterile) were from Sarstedt (Ireland). Sterile Stomacher bags, Stomacher Lab System Model 400, were from Colworth (UK). 96-well plates were measured by the fluorescent plate reader, FLUOstar Omega (excitation/emission 380/650 nm) controlled by the MARS software.

2.2   Luminescence measurements

For screening and optimization experiments, the phosphorescence intensity and lifetime signals were recorded with a handheld instrument OpTech[TM] (Mocon, Minneapolis, USA) using the sensors held in place in a clear 20 mL polystyrene vial (Sarstedt, Ireland). Each sensor strip/spot was measured five times in different locations and average values and standard deviations (S.D.) were calculated.

Dry and humid gas calibrations of the sensors were carried out by a Firesting[TM] instrument (Pyrosciences GmbH, Germany) which operates with a 1 mm plastic fibre optic probe under standard manufacturer settings. As the probe is brought into contact with the sensor, phase shift readings were measured and converted into lifetime values by using Eq. 4 (pg. 15).

For sensor calibration, O_2/N_2 gas mixtures in varying ratios between 0-100 kPa were produced using a precision gas mixer (LN Industries SA, Switzerland). These gas mixtures were pumped through a flow cell with a glass window through which the O_2 sensors were interrogated by the Firesting[TM] instrument. The flow cell was submerged in a circulating water bath (Julabo) to just below the level of the window keeping the window and probe dry, to equilibrate the gas to the correct temperature.

This water bath was also used to calibrate the sensor at different temperatures in order to observe any cross-sensitivities the sensors had to temperature (Fig. 2.1).
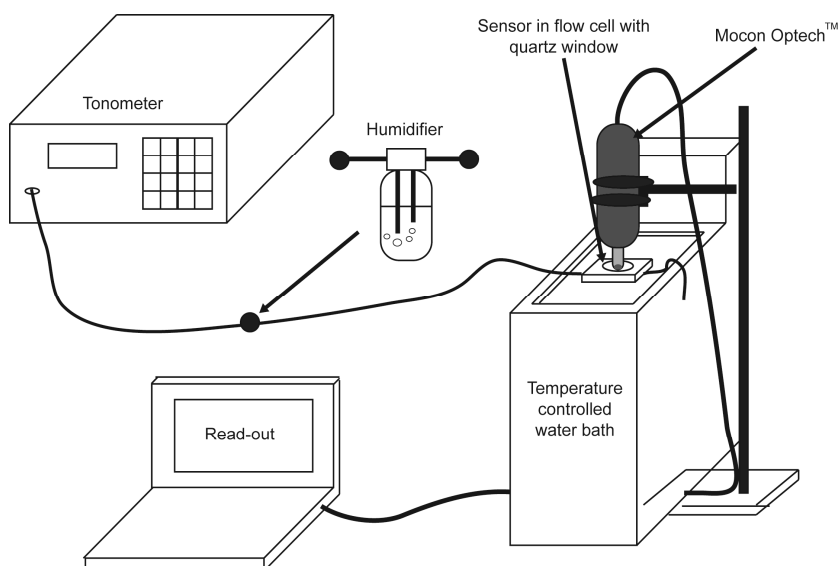

Fig. 2.1 Calibration set-up.

The photostability of the sensors were tested using this set-up over a prolonged period (> 12 h).

Phosphorescence intensity measurements were carried out on a Cary Eclipse fluorescence spectrometer (Varian) equipped with a Peltier temperature control.

2.3 Microscopic Measurements

Wide-field optical imaging was performed on an inverted microscope Axiovert 200 which is equipped with a Plan Neofluar 40 x/1.3 oil immersion objective (Carl Zeiss), pulsed excitation module (590 nm LED), gated CCD camera (LaVision Biotech), excitation 595/40 nm and emission 780/60 nm filter cube, and incubation chamber with O_2 and temperature control (PeCon). In fluorescence and differential interference contrast (DIC) modes the exposure time was 3-30 ms. The

phosphorescence lifetime (PLIM) imaging settings at 21 kPa O_2 were as follows: pulse width 10 µs, repetition time 170 µs, gate time 10 µs, delay time 0-100 µs, 11 images; exposure time 15 ms, no binning. At 1 kPa O_2 the settings were: pulse width 10 µs, repetition time 190 µs, gate time 20 µs, delay time 10-140 µs, 11 images; exposure time 5 ms, no binning.

2.4   Relative air humidity tests

The relative humidity (RH) standards comprised of saturated aqueous solutions of solid salts at 20 °C [107]. The saturated salt solutions prepared represented various humidity levels as stated in the brackets: H_2O (100 %), Na_2HPO_4 (95 %), Na_2SO_4 (93 %), Na_2CO_3 (90 %), $(NH_4)_2SO_4$ (81 %), CH_3COONa (76 %), $CuCl_3$ (68 %), $MgCl_2$ (33 %). 1.5 mL of each standard solution was transferred to a 3 mL glass vial and the sensor sample fixed 1 cm above the solution. The vials were sealed with a PP stopper, covered with tinfoil and left at room temperature for 48 h to equilibrate. The lifetime signal of each sensor was then measured using the OpTech™ instrument.

2.5   Estimation of dye leaching from sensors

The amount of dye encapsulated in each sensor was estimated by extracted the dye from each sensor with toluene. The sensors were submerged in 1 mL toluene in 1.5 mL vials and incubated at 50 °C for 24 h. The absorbance of the supernatant was then obtained by UV/Vis spectrometry (HP/Agilent 8453 General Purpose UV-visible). The absorbance of the supernatant was then compared to a calibration curve, generated by serial dilutions of the PtBP dye stock (0.1 mg/mL in toluene), in order to ascertain the concentration of dye present in the supernatant.

2.6 Food simulant tests

Stock solutions of food simulants were made up of 95 % EtOH, 10 % EtOH, 5 % acetic acid, 3 % lactic acid, 3 % $NaHCO_3$, H_2O, 3 % NaCl and 20 % sucrose [108]. Sensors were placed in HPLC vials and immersed in 2 mL of simulant solution. The vials were sealed and incubated in a shaker at 40 °C over a 21-day period. The vials were assayed periodically on day 7, day 14 and day 21. The sample solutions and PtBP dye standard was assayed by reverse phase HPLC using an Agilent 1100 series system consisting of a quaternary pump, diode array photometric detector, an auto sampler and an Agilent Eclipse XDB-C18 column (150 x 4.6 mm, 5 µm, Agilent). 10 µL of a PtBP dye in tetrahydrofuran (THF) standard (0.02 mg/mL) or the simulant solution was injected into a mobile phase of H_2O/TFA (mobile phase A) and eluted with an ascending stepwise gradient of THF (mobile phase B), using gradient 0-70 % B over 22 mins. A calibration curve of PtBP in THF was prepared and quantified on Agilent 8453 UV-vis spectrometer and the extinction coefficient obtained.

2.7 Packaging Methods

For packaging in MAP containers, sensors were adhered in duplicate to the sealing laminate using scotch tape. The trays were MAP packaged using a VS 100 BS packaging system (Gustav Muller and Co., Bad Homberg, Germany). The gas ratio was set at 55 % O_2 in beef sample trays and 0 % O_2 in the chicken and cheese sample trays. Samples were stored in two orientations: one upright with the product in contact with the headspace and the other inverted with the food product in direct

contact with the sensors. All packages including the blanks were stored in a cold room (4°C) and measured at different time intervals. At the end of the study, sensors were removed from the trays and washed thoroughly with H_2O.

Headspace analysis was performed using the OpTech[TM] Platinum-O_2 system and Dansensor[TM] Checkmate 3 headspace analysis instruments. The Dansensor[TM] covers a range of 0-100 % O_2/CO_2. O_2 concentration is read via a zirconia O_2 sensor and CO_2 readings are read by dual beam infrared. Readings can be taken 3 times before package failure. Sample volume is 6 mL taken over 10 secs. Accuracy is ± 0.01 % O_2 and ± 0.08 % CO_2. Blank containers were filled before and after filling of the food trays and checked for consistency with the Dansensor[TM] device by applying a special septum, piercing the sealing laminate with a needle probe and extracting and analysing headspace gas for O_2 and CO_2 levels. At the end of each study, all packs were tested by the Dansensor[TM] before the sensors were recovered, to assess final gas concentrations.

Dissolved O_2 contents in the beverage study were carried out using dOxybead[TM] sensors comprising 5 mm porous glass beads with PtBP-based O2-sensitive coating were kindly provided by Luxcel Biosciences.

2.8 Microbial Load Measurements

The method used for microbial load tested for the presence of aerobic bacteria. Peptone buffered water (BPW) was made up using peptone (10.0 g), sodium chloride (5.0g), disodium phosphate (3.5 g), monopotassium phosphate (1.5 g) and adjusted to pH 7.2 ± 0.2 using concentrated sodium hydroxide solution. The Greenlight[TM] probe was reconstituted using 1 mL of BPW and diluted up to 10 mL BPW. 10 g of

the meat sample and 90 mL BPW was placed in a stomacher bag which was homogenised for 1 min. 100 µL of reconstituted Greenlight[TM] probe was added to each assay well of the 96-well plate. 100 µL of the homogenated sample was added to each well. 100 µL of pre-warmed mineral oil was used to seal each well. The plate was measured kinetically on the FLUOstar Omega plate reader for 10-12 h at 30 °C. The microbial load (CFU/g) of each sample was calculated using a pre-determined calibration. Pre-set acceptance criteria for microbial load were as follows (Table 2.1):

Table 2.1 Pre-set acceptance criteria for Greenlight[TM] test

CFU/g	Comment
$< 5 \times 10^5$	Satisfactory
$5 \times 10^5 - 5 \times 10^6$	Acceptable
$> 5 \times 10^6$	Unacceptable

3   Chapter 3: Development of new O$_2$ sensors

3.1   Introduction

In recent times, there has been an increase in the use of O$_2$ sensors, based on luminescent quenching, in the fields of biological research [17b], environmental monitoring [30], process control in the chemical industry [109], in the food[42], pharmaceutical industries and in medical and clinical settings. This increased usage can be correlated to the development of stable, robust, disposable, easy-to-use sensors which are not prone to electrical interferences [17a] and can be integrated easily into a number of systems. As a result, luminescent sensors are held as a viable alternative to destructive O$_2$ quantifying methods [30] as they possess a reversible response and can measure O$_2$ in an non-invasive and contactless manner [4a].

The most promising luminescent O$_2$ sensors for use in food packaging are solid-state O$_2$ sensors. These sensors usually consist of O$_2$-sensitive indicator dye encapsulated within an O$_2$-permeable polymer matrix[17a, 110]. The properties of the dye and polymer matrix, such as O$_2$-solubility, permeability and mechanical attributes, influence the final characteristics and operational performance of the sensor unit in particular. In addition, the cross-sensitivity (i.e. to temperature, humidity etc.) and intensity amplitude are influenced by both the materials and methods used in sensor fabrication.

Pd(II)- and Pt(II)-porphyrins and some related structures are common indicator dyes used in solid-state O$_2$ sensors due to being excited in the red region (580-650 nm) and emitting in the near-IR region (700-800 nm). For the encapsulation of such dyes, hydrophobic polymers such as polystyrene, polydimethylsiloxane and

fluorinated polymers, which have a moderate to high O_2 permeability [17a] are often used. O_2 solid-state sensors are usually fabricated as thin films or coatings by solution-based processes, such as a 'cocktail' solution in organic solvent being dried on a support matrix [111], polymerizing or curing liquid precursors [112] or other methods; such as adsorption[113], covalent binding [114], solvent crazing[56a] and polymer swelling [35a].

The thin film nature (which assists O_2 diffusion) of many of these sensors usually requires an additional support material to enhance the mechanical properties of the sensor [53]. Examples of materials commonly used as supports are glass, PMMA and polyester film Mylar[®], microporous membranes. The addition of these materials often lead to higher fabrication costs due to the consumption of more materials, formation of mixed polymer phases and the extra post-processing steps. To ensure cost-viability which is an important factor in food applications, a binary component sensor material and simple fabrication process are desirable.

3.2 Development of spotting methods to produce discrete O_2 sensors

3.2.1 Optimised sensor fabrication

For the optimized sensor fabrication, an emulsion of Kolliphor P188 (17 mg/mL) in 60:40 EtAc/H_2O containing PtBP dye (0.01 mg/mL) was prepared by dissolving the surfactant in 0.4 mL H_2O and the dye in 0.6 mL EtAc and combining the two solutions together. Strips of PP fabric (type 700/70 and 700/30K, 40 mm x 40 mm) were spotted with 20 μL of the solution (Fig. 3.1) and allowed to air dry for 1 h. The sample was then rinsed in H_2O, dried and annealed at 70 °C for 2 h in a dry oven.
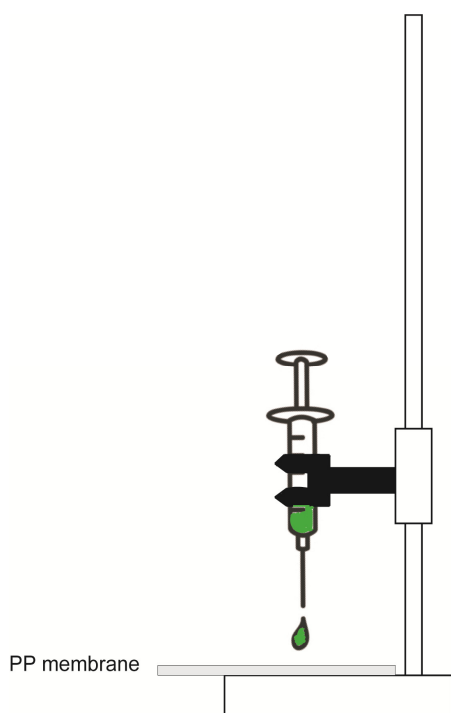
Fig. 3.1 Diagram showing spotting fabrication apparatus.

3.2.2 Selection of optimum fabrication conditions

Non-woven polypropylene (PP) fabric materials have microporous fibre-like structure, large surface area and are compatible with most solvents. Therefore, indicator dyes can be incorporated in such matrices via solvent-mediated methods

[110]. The efficiency of dye incorporation is dependent on several factors; the diffusion of solvent and dye into the polymer, the degree of polymer swelling, the solvent evaporation rate and the drying time. Sensors based on PP grafted with hydrophilic chemical groups for better wettability do not require an additional support layer, as they are mechanically stable and relatively thin (approx. 80 µm). They can also be easily incorporated into food packages due to their planar nature and heat or adhesive sealing capabilities.

In this study, we systematically investigated and optimized discrete sensors produced by the spotting method.

These sensors were fabricated on two new non-woven grafted polyolefin substrates, which were manufactured using two different methods:

> Spunbond materials which comprise continuous pure PP fibres produced by melt extrusion and bonded by pins or the application of heat to produce sheet structures.

> Wetlaid fabrics consisting of a combination of PE and PP fibres and produced by adaption of the wetlaid paper manufacturing technique.

Both fabrics were grafted in a two-step process in which free radicals were created on the surface of the monofibres by UV radiation and were then combined with vinyl monomer units, in order to produce hydrophilic acrylic acid chains [115]. As a result of the modification, both materials have good wettability, wicking characteristics and are stable in organic solvents.

The indicator dye was the near-infrared-emitting PtBP (615 nm excitation/760 nm emission)[30], since it can be measured with OpTech[TM] (Mocon, US) and Firesting[TM] (PyroScience, Germany) instruments available in our lab.

A design of experiment was created, adapting each parameter which influences the final characteristics of the sensors. These parameters included dye concentration, solvent and the amount of surfactant required for miscibility with water. Each parameter was optimised to achieve a sensor with high brightness, robust and stable lifetime signal and high reproducibility between sensors. The initial optimization was carried out on the spunbond material and later adapted to the wetlaid material. The results of the optimization are laid out (Table 3.1, pg 61).

The fabricated sensors were compared to commercial polystyrene-based OpTech[TM] Platinum sensors (Mocon). The differences were ascribed to the difference in O_2 permeability of the materials; as polystyrene has an O_2 permeability approximately two-fold higher than that of PP and PE. This leads to higher dye quenching in the polystyrene-based sensor at 21 kPa.

Initially we tested the effects of solvent on sensor signal. Lifetime and intensity signals were measured from sensor spots produced by applying 0.02 mL aliquots of PtBP dye dissolved in pure THF, toluene, butanone and EtAc onto the spunbond PP material. The EtAc-based sensor spots yielded the most consistent lifetime readings, however intensity signals were below the threshold required for reliable readings on OpTech[TM] instrument. In contrast, toluene-based spots yielded higher intensity signals but showed greater variability in lifetime values most likely due to aggregation of the dye molecules. Sensor spots produced with pure solvent showed too much spread, leading to spots with large diameter (30 mm for EtAc and 26 mm

for toluene). Lifetime signals also showed considerable reductions due to dye aggregation and self-quenching.

In order to reduce spot area and evaporation rate (to allow further penetration of dye into the substrate), we prepared an emulsion of solvent and water stabilised with Kolliphor® P188 surfactant which showed a noticeable thickening effect on the solution at 17 mg/mL. The surfactant allowed for two previous immiscible solutions to mix forming a viscous solution. The solution was prepared by the dissolution of the surfactant in water and the dye in solvent, followed by mixing the two solutions together and vortexing. The optimal water:solvent ratio which achieved stable emulsion formation was 60:40 for EtAc/H_2O and 70:30 for toluene/H_2O. Spotting of 0.02 mL aliquots the sensor surfactant cocktail on the fabrics formed $\approx$ 9 mm diameter spots which exhibited uniform shape and colour.

By trying different concentrations of dye, 0.1 mg/mL was found to be optimal to provide high intensity, stable and reproducible lifetimes and low internal quenching. As the sensors were designed for food applications, the less toxic EtAc solvent (short-term exposure limit = 400 ppm) was chosen for further use.

The use of surfactant provided significant improvement of sensor signals. However it also necessitated the need for a washing step to be added to the fabrication method in order to remove residual surfactant. Final post-processing involved initial rinsing with water to remove water soluble components, followed by annealing at 70 °C to stabilise luminescent signals and lower their variability [58, 106, 116]. This post processing reduced internal quenching effects, stabilised lifetime signals and released the internal stresses within the sensors. The effects of different sequences of post-treatment are shown in Fig. 3.2.
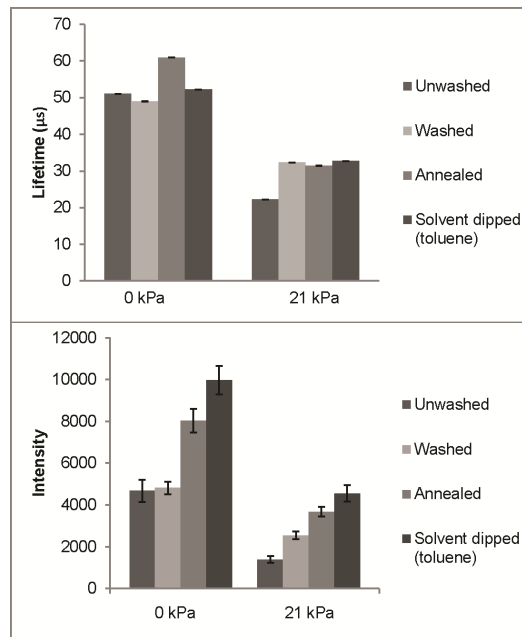
Fig. 3.2 Effect of post-processing sequence on sensor lifetime and intensity signals. Spunbond sensor spotted with 0.02 mL EtAc/H$_2$O/surfactant cocktail.

Table 3.1 Effects of the main process parameters on sensor intensity (I) and lifetime (τ) signals in N_2 (0 kPa O_2) and air (21 kPa O_2). [a] Approximate Ksv calculated using 0 kPa and 21 kPa O_2 lifetime values. [b] After annealing. [c] Initial optimization was performed on spunbond PP membrane. [d] Using EtAc/surfactant, [e] Thin film coating on microporous support.

Parameter	Variation	τ_0 (0 kPa)	τ_{21} (21 kPa)	K_{sv}[a]	I_0 (0 kPa)	I_{21} (21 kPa)
(a) Pure solvent	Ethyl Acetate	43.92 ± 0.02	25.53 ± 0.03	0.03	963.63 ± 37.17	548.22 ± 23.90
	Toluene	41.13 ± 0.04	12.90 ± 0.11	0.10	1999.78 ± 162.04	656.38 ± 82.75
(b) Solvent & surfactant	Ethyl Acetate	51.00 ± 0.03	22.21 ± 0.03	0.06	4680.44 ± 535.83	1391.89 ± 165.80
	Toluene	51.09 ± 0.01	31.87 ± 0.01	0.03	5858.40 ± 1132.23	2787.00 ± 319.08
(c) Dye concentration	0.1 mg/mL	51.00 ± 0.03	22.21 ± 0.03	0.06	4680.44 ± 535.83	1391.89 ± 165.80
	0.2 mg/mL	45.02 ± 0.05	14.27 ±0.04	0.10	10704.40 ± 2136.92	2328.60 ± 431.84
	0.3 mg/mL	47.00± 0.03	14.59 ± 0.03	0.11	10792.20 ± 1636.81	2139.60 ± 286.69
(d) Optimized Sample[b]	**Spunbond[c]**	**49.30 ± 0.29**	**31.27 ± 0.08**	**0.03**	**9982.40 ± 675.94**	**4552.20 ± 397.08**
	Wetlaid[d]	**53.87 ± 0.06**	**27.24 ± 0.09**	**0.05**	**11808.60 ± 348.1893**	**4821.57 ± 185.41**
(e) Reference sensor (OpTech[TM])	**Polystyrene[e]**	**59.80 ± 0.10**	**19.60 ± 0.09**	**0.10**	**25533 ± 2175.39**	**10026 ± 111.55**

3.2.3 Characterisation

Using the above fabrication method, we fabricated sensors based on two separate fabrics; spunbond and wetlaid PP membranes. Detailed characterisation included full O_2 calibrations (0-100 kPa) performed at 10, 20 and 30 °C. These conditions represent the range of storage temperatures and O_2 concentrations that food products habitually experience. The calibrations of the spunbond and wetlaid PP sensors in dry gas at 10 °C are shown in Fig. 3.3.
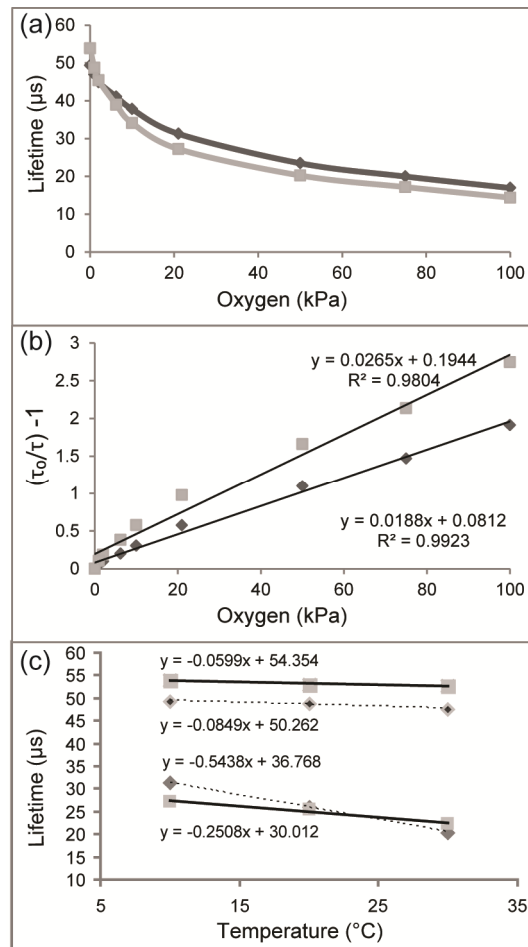
Fig. 3.3 (a) O_2 calibrations in lifetime scale for spunbond (dark grey, ♦) and wetlaid (light grey, ■) PP spotted sensors in dry gas, 10 °C, (b) their Stern-Volmer plots and (c) temperature dependencies.

Going from 0 kPa to 21 kPa O_2, the lifetime reading of the spunbond sensor decreased from 49.30 ± 0.29 μs to 31.27 ± 0.08 μs, whereas the wetlaid sensors exhibited a larger lifetime change – from 58.87 ± 0.06 μs to 27.24 ± 0.09 μs. As indicated by smaller deviation values, the dye was more uniformly dispersed in the wetlaid sensor than the spunbond sensor.

Linearity of the Stern-Volmer plot is important for one or two point calibrations of O_2 sensors. Linearity is connected to the micro heterogeneity of the polymer, uniformity of the dye dispersion within the sensor and the accessibility of the dye molecules to the atmosphere to allow quenching by O_2 molecules [22]. The spunbond PP sensor showed good linearity; however a slight curved trend was seen within the

wetlaid PP plot. This curvature is seen in many sensor calibrations and is thought to be due to the existence of different environments around the dye molecules and/or aggregation of the dye molecules [117]. The K_{SV} (sensitivity) of the wetlaid sensor was 1.4 higher (calculated by ratio of Ksv of wetlaid and spunbond sensor) than the spunbond sensor making it more suitable for measuring in atmospheres with low O_2 concentrations.

The dynamic quenching of the sensor dye by O_2 is also influenced in a complex manner by temperature (T)[56a, 118]:

$$\frac{1}{\tau} = k_f^0 + A_{nr}e^{\frac{-\Delta E_{nr}}{RT}} + A_q^0 e^{\frac{-\Delta E_q}{RT}} \qquad \text{Eq. 5}$$

where k^0f – kinetic constant of the fluorescent decay, A_{nr}- pre-exponential of the non-radiative process, A_q^0 – pre-exponential of the non-radiative and O_2 quenching process, ΔE – activation energies of the non-radiative and quenching process respectively, R- gas constant, and T – absolute temperature. This equation was derived from the relationship between Ksv (Stern-Volmer), τ_0 (lifetime in absence of quenching molecule) , D_{O2} (O_2 diffusion coefficient) and S_{O2} (solubility of O_2 inside membrane) described in detail in the paper by Badocco *et al.*

The studied temperature ranges in this study, showed our sensors obeying a linear dependence from 10 °C to 30 °C. This allows for temperature compensation to be calculated and applied to our sensors using a simple algorithm. Negative slopes indicate that lifetime decreases with an increase of temperature. The temperature coefficient of the Stern-Volmer calculated by: $\frac{\Delta SV}{\Delta T}$ (where ΔSV is the difference the Stern-Volmer constants and ΔT is the difference of temperature) was found to be -

3.20 x 10^{-2} kPa $^{-1}$ C $^{-1}$ and -3.45 x 10^{-2} kPa $^{-1}$ C $^{-1}$ for the spunbond and wetlaid sensors respectively, for the range 10-30 °C.

The variability of O_2 readings between sensors in the same batch was calculated as 3*STD (standard deviation) and were found to be 0.11 kPa and 0.10 kPa at 0 and 21 kPa respectively for the spunbond sensor and 0.22 kPa at both 0 and 21 kPa for the wetlaid sensor. The batch-to-batch variability generated a RSD (relative standard deviation) value of 1.98 % at 21 kPa and 0.47 % at 0 kPa (n = 6). These deviations are expected to improve on up-scaling and automation of the fabrication process.

While the working characteristics of the sensors were good in dry air, a marked cross-sensitivity to humidity was noted upon exposure to humid air. Both sensor sets showed a marked decrease of lifetime signal in humid gas. The effect of humidity on the wetlaid sensor was studied in greater detail by application of a relative humidity study (Fig. 3.4) , as this sensor showed the most prominent sensitivity to relative humidity (RH, %) with a drop of 9 μs at 100 kPa, compared to a drop of 4 μs at 100 kPa observed in the spunbond sensor.
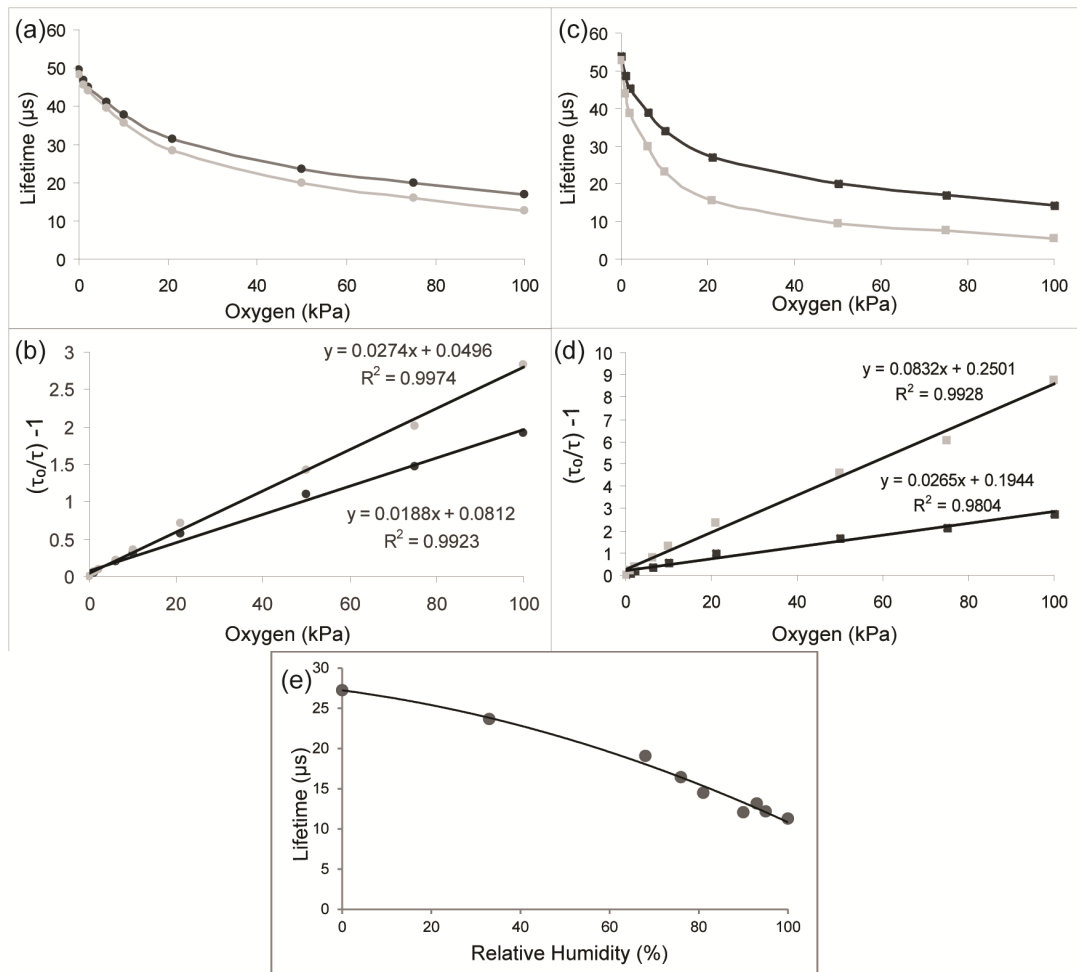
Fig. 3.4 (a) and (c) O_2 calibrations in lifetime scale for spunbond (♦) and wetlaid (■) PP spotted sensors respectively in dry gas (dark grey) and humid gas (light grey), 10 °C, (b) and (d) their respective Stern-Volmer plots and (e) Humidity dependence of lifetime.

At 0 kPa, O_2 upon exposure to humid gas (RH = 100 %) at 10 °C, the lifetime signals of the wetlaid sensors decreased by ≈ 1 μs at 0 kPa (from 53.87 ± 0.01 μs in dry gas to 52.66 ± 0.01 μs in humid gas) and by 9 μs (from 14.38 ± 0.04 μs in dry gas to 5.40 ± 0.03 μs in humid gas) at 100 kPa compared to dry gas (RH=0)(Fig 3.4(c)). Even so, upon being dried, the sensors produced the original calibration which indicates that the humidity effects are fully reversible and do not lead to degradation of the sensor. The Stern-Volmer plots generated in humid gas calibrations are linear, indicating the homogeneity of the sensors has not changed and the K_{S-V} was three times that of the K_{SV} obtained in dry gas (Fig 3.4(d)).

To confirm this effect, the sensors were exposed to different levels of RH (0-100 % range at room temperature, 21 kPa O_2, 48 h). A gradual decrease of sensor lifetime readings with increasing RH was measured (Fig 3.4(e)), which can be fitted to a second polynomial line. As a result of these experiments, we can ascribe the effects of humidity on the sensors to either:

(a) Some of the dye being encapsulated in the hydrophilic grafted layer rather than the hydrophobic bulk PP. When the sensor is exposed to humidity, this hydrophilic layer absorbs the water and swells leading to a change in the micro-environment of the dye and better accessibility of the O_2 molecules to the dye. This increases the quenching efficiency.

(b) Alternatively, some surfactant with solubilised dye may have remained in the polymer material producing a similar effect.

Both spotted sensors showed the same fast and reversible response times (Table 3.2).

Table 3.2 Response and recovery times in humid gas at 10 °C from 21 to 10 kPa O_2

	Humid air @ 10 °C	
	Response (min)	Recovery (min)
Wetlaid spotted PP	4.4	4.9
Spunbond spotted PP	4.4	4.9
OpTech[TM] reference sensor	26.5	28.2

Both sensors showed response times of 4.4 min in humid gas at 100 % response (Fig. 3.5). In contrast, the commercially available polystyrene based sensors showed greater hydrophobicity leading to a much longer response time (6 times) in humid gas (26.5 min). These times included the time required for tonometer and gas cell equilibration (approximately 5-10 seconds).
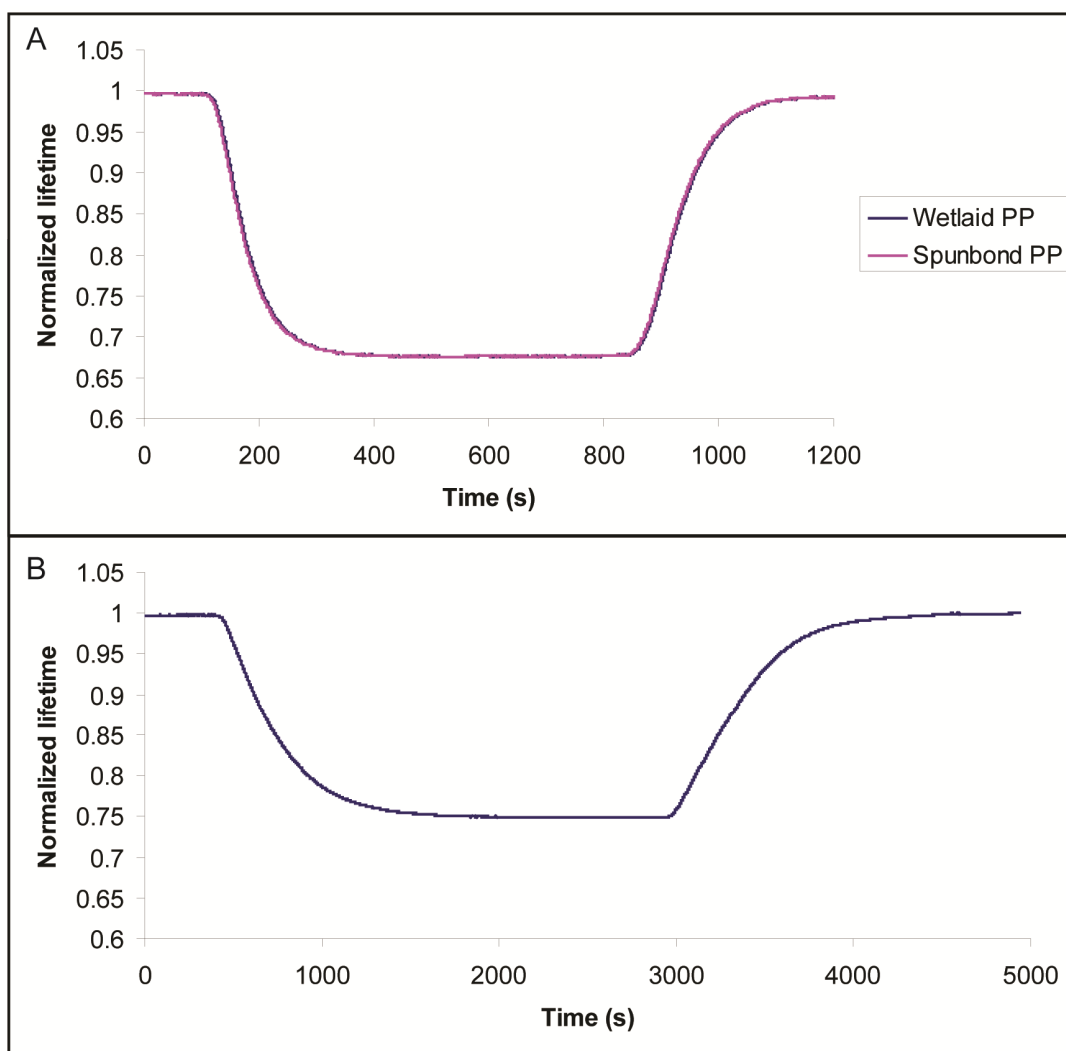
Fig. 3.5 Response and recovery curves of A) Wetlaid and spunbond spotted sensors B) Reference sensor (OpTech[TM]) at 10 °C in humid gas from 21 kPa O_2 to 10 kPa O_2.

The sensors were examined for dye distribution, at 1 kPa and 21 kPa $O_{2,}$, by wide-field microscopy based on gated CCD camera detection phosphorescence lifetime imaging (microsecond FLIM or PLIM) [117].

The bright-field image of the top layer of the sensor membrane is shown in Fig. 3.6 (a). The phosphorescence intensity image shows areas of higher fibre density exhibiting higher intensity signals; this is due to more dye being present in these areas. The lifetime image at 21 kPa O_2 and the corresponding histogram, line profile and surface map show the spread of lifetime values across the selected cross-section

of the sensor [119]. These plots suggest the distribution of dye is quite homogeneous, with a relatively narrow and Gaussian spread of lifetimes (21-23 µs).
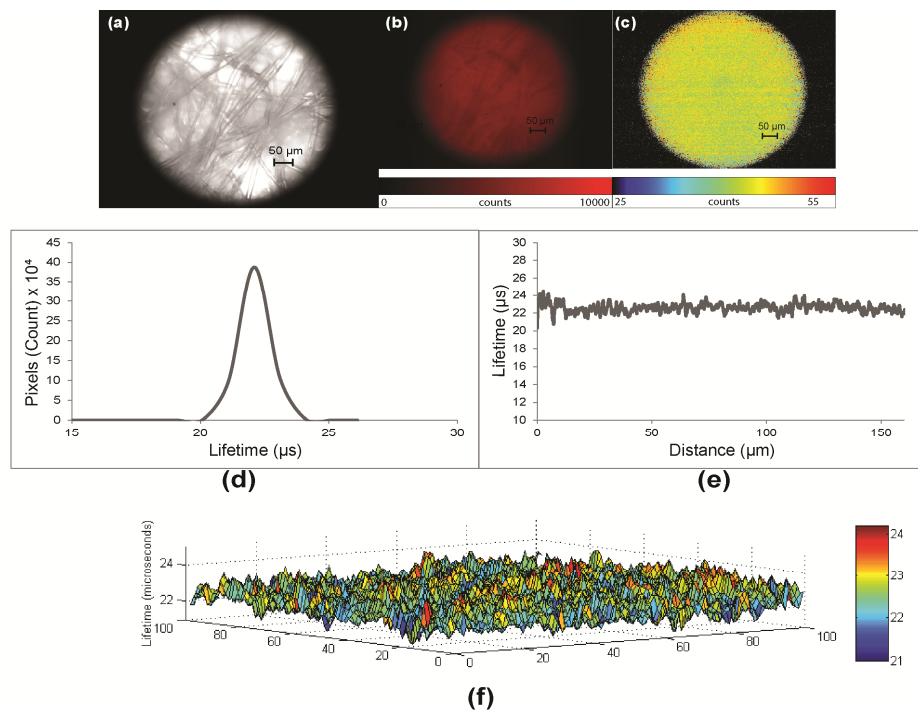
Fig. 3.6 Wide-field microscopy image of dry wetlaid PP spotted sensor : (a,) bright field image (b) phosphorescence intensity image (c) PLIM image (d) histograms (e) line profile (f) 3D surface graph of lifetimes. Sample area analysed: 100 x 100 pixels, 11536.21µm^2. Measured at room temperature, 21 kPa, 40 X magnifications.

3.3　Fabrication of PP sensors by swelling method

3.3.1　Sensor fabrication

The final swelled sensors were fabricated using an impregnation method. A solution of PtBP dye in 70:30 THF/H_2O (0.03 mg/mL) was prepared and 8 mL aliquots were placed in disposable 15 mL plastic vials (Sarstedt). Strips of the PP fabric (24 mm x 12 mm) were cut out from the sheets and inserted into each vial (one strip immersed in each vial). These vials where then capped, sealed with polyfilm, placed in an oven set at 65 °C and incubated for 1 h (Fig 3.7). After this time, the sensor strips were extracted from the vials, rinsed with water to remove any residual dye mixture and allowed to dry in air for 18 h. Subsequently, the sensors were then annealed in a dry oven at 70 °C for 16 h. Optionally, after the initial incubation step, the vials with grafted PP strips (type: 700/70) were opened and incubated in a water bath at 40 °C for 16 h, ensuring the membranes were still submerged the entire time, to allow the solvent to evaporate off.

Fig. 3.7 Diagram showing swelling method. Fabric strip and dye/solvent cocktail are placed in plastic vial and incubated in oven at 65 °C for 1 h.

3.3.2 Selection of optimum fabrication conditions

As above, non-woven polypropylene-based matrices were selected for O_2 sensor fabrication consisting of small PP monofibres bound together in planar sheets [120]. In addition to being flexible, these matrices also possess a large surface area, good mechanical and light-scattering properties and optional surface modifications by grafting the surface of the monofibres.

Simple impregnation by swelling the polymer in a dye-solvent solution can be used to incorporate O_2 sensitive dyes. This approach is commonly used with suspensions of polymeric microparticles [26]. Once the dye is impregnated, no further support is needed, making such sensors binary in nature with only the dye and encapsulation matrix.

With the adaption of this technique, we sought to create solid-state O_2 sensors which were based on non-woven PP substrates and PtBP dye. Unmodified bulk PP material is hydrophobic which limits its wettability and dye compatibility. The spunbond grafted PP provides a hydrophilic and wettable surface. Both features are useful when designing optical O_2 sensors for food packaging applications.

To assist the incorporation of hydrophobic dye molecules into the mostly hydrophobic bulk polymer sheets, we applied a gradient of polarity, where the low polarity solvent was slowly depleted by evaporation from the dye solution (which contains a low water content and the initial polarity of which causes the polymer to swell) [121]. This encouraged the dye molecules to partition favourably out of the increasingly hydrophilic aqueous solution into the hydrophobic bulk polymer. In addition, the increasing polarity of the solution causes the polymer to de-swell and trap the dye molecules. Elevated temperatures (which were below the solvent boiling

point) were used to speed up the diffusion rates and the re-equilibration processes in the system. The dye incorporation process is shown in Fig. 3.8.
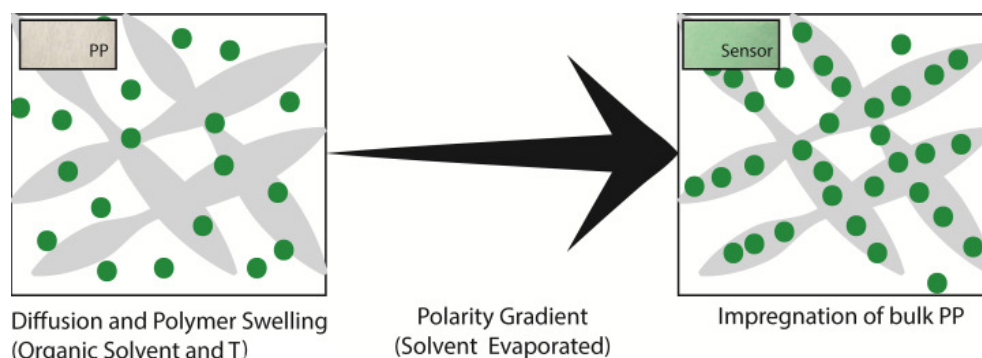
Fig. 3.8 Fabrication process of swelled sensors.

The systematic optimization of the sensors was carried out in a similar fashion to that of the spotting sensors with each parameter optimized. The aim of each optimization was to obtain high intensity, stable lifetime signals and good reproducibility of signal readings between sensors, while keeping usage of fabrication materials to a minimum. The results are collated in Table 3.3 on pg 75.

The penetration of dye into a substrate is largely dependent on the solvent used. To facilitate dye penetration, the solvent must be both compatible with the dye and not degrade the polymer and provide effective swelling. However, as polypropylene is highly chemi-resistant, there are few non-compatible solvents. Therefore, as the dye is hydrophobic, solvents with compatibility with dye and polymer were chosen, such as THF, ethyl acetate, butanone and toluene. Initial tests showed THF produced the highest intensity and lifetime signals in nitrogen. In the other solvents, issues arose with partial aggregation of dye, some evaporation of solvent leading to the dye crashing out of solution and quenching of the dye after impregnation.

It was discovered that using pure solvents with grafted PP yielded inadequate intensity signals. Therefore, the solvent was combined with a higher polarity solvent (water) to aid compatibility. A mix of 70:30 THF:H_2O was deemed the most effective mix, as it gave the highest intensity signals, particularly after the solvent evaporation step. The optimal dye concentration was found to be 0.025 mg mL^{-1}.

Incubation times were varied between 1 h, 2 h and 3 h to assess if longer incubation periods yielded higher intensities. It was found that there was no correlation between longer incubation times and intensity, therefore the fastest time of 1 h was selected. Likewise the incubation temperature was varied as temperature affects rate of dye diffusion into the polymer matrix. The temperatures selected were around the boiling point of THF (66 °C) in the range of 60 °C to 70 °C. A temperature of 65 °C yielded the highest lifetime and intensity signals.

After incubation, the grafted PP sensors were placed in a water bath in a fume hood, in order to allow solvent to evaporate from the dye solution and therefore allow further penetration of the dye into the polymer. Slow evaporation of the solvent at 40 °C increased the concentration of the dye within the polymer and in turn raised its intensity signal by approximately 116 %. Like the previous spotting based sensors, all swelling method sensors were annealed at 70 °C to reduce internal stresses. This increased lifetime signal in nitrogen and air and increased their dye homogeneity (S.D.).

For comparison, swelled PP sensors were prepared based on the non-grafted PP material. Different dye/solvent ratios were tested and a ratio of 50:50 was found to be optimal. The solution became increasingly polar as the THF evaporated during incubation, leading to the dye partitioning out of the less favourable solution into the

more favourable hydrophobic membrane. The concentration of 0.035 mg mL^{-1} yielded a higher lifetime and intensity signal, however the difference was found to be too minor to justify the higher dye usage; therefore a concentration of 0.025 mg mL^{-1} was selected for further fabrications. The already high intensity signals after the incubation step of the ungrafted PP sensor also rendered the solvent evaporation step defunct. This was ascribed to the higher hydrophobicity and/or the different structure of the polymer membranes which lead to higher penetration of the dye.

The dye from each type of sensor (24 mm x 12 mm) was extracted in order to estimate the dye concentration. The dye concentration in the grafted sensor and ungrafted sensor was calculated to be 0.57 µg and 0.39 µg respectively. Batch-to-batch variability was assessed by mean and the relative standard deviation of lifetime readings. The RSD of the grafted PP sensors was found to be 2.90 % at 21 kPa and 0.94 % in 0 kPa, n = 6. In comparison, the RSD of the ungrafted PP sensors were found to be 2.19 % at 21 kPa and 2.16 % at 0 kPa, n = 4. These deviations are expected to reduce upon up-scaling of the process.

Table 3.3 Effects of the main process parameters on sensor intensity (I) and lifetime (τ) signals in N_2 (0 kPa O_2) and air (21 kPa O_2). [a] Approximate Ksv calculated using 0 kPa and 21 kPa O_2 lifetime values. [b] Initial optimization was performed on the grafted PP membrane, [c] Optimized sample: Grafted PP (hydrophilic material), 70:30 THF/H_2O solution, 0.025 mg/ml dye, solvent evaporation dried, annealed. [d] Ungrafted PP (hydrophobic material), 70:30 THF/H_2O solution, 0.025 mg/ml dye, air dried, annealed.

Parameter	Variation	Material	K_{sv}[a]	τ_0	τ_{21}	I_0	I_{21}
a) Solvent	Toluene	Grafted[b]	0.03	48.21 ± 1.07	30.39 ± 0.10	2550 ± 610	1151 ± 255
	THF (100 %)	Grafted	0.02	49.29 ± 0.67	33.78 ± 0.13	5556 ± 485	2709 ± 215
	THF (80 %)	Grafted	0.03	51.03 ± 0.30	33.41 ± 0.06	5805 ± 626	2757 ± 317
	THF (70 %)	Grafted	0.02	50.21 ± 0.52	33.68 ± 0.04	14161 ± 1314	6796 ± 573
b) Dye conc.	0.025 mg/mL	Grafted	0.03	50.77 ± 0.01	29.53 ± 0.02	10752 ±758	4446 ± 272
	0.035 mg/mL	Grafted	0.02	49.54 ± 1.85	32.55 ± 0.24	15778 ± 2316	7340 ±1059
c) Annealing Status	Annealed	Grafted	0.02	50.80 ± 0.34	33.75 ± 0.09	2527 ± 349	1404 ± 221
	Not Annealed	Grafted	0.02	49.20 ± 0.93	32.82 ± 0.16	3767 ± 846	1771 ± 298
d) Drying regime	Solvent evaporation	Grafted	0.03	51.25 ± 0.48	32.25 ± 0.05	5438 ± 696	2274 ± 347
	Air dried	Grafted	0.02	50.80 ± 0.34	33.75 ± 0.09	2527 ± 349	1404 ± 221
e) Optimized Sample		**Grafted**[c]	**0.03**	**50.77 ± 0.01**	**29.53 ± 0.02**	**9896.71 ± 467.50**	**4271.80 ± 239.35**
		Ungrafted[d]	**0.07**	**57.32 ± 0.09**	**22.45 ± 0.07**	**7539.00 ± 276.05**	**3485.86 ± 86.65**

3.3.3 Characterisation

Using the optimized fabrication method, two sensors based on two fabric types; grafted and ungrafted PP membranes, were fabricated. Detailed characterisation included full O_2 calibrations (0-100 kPa) performed at 10, 20 and 30 °C. The calibrations of the grafted and ungrafted PP sensors in dry gas at 10 °C are shown in (Fig. 3.9).
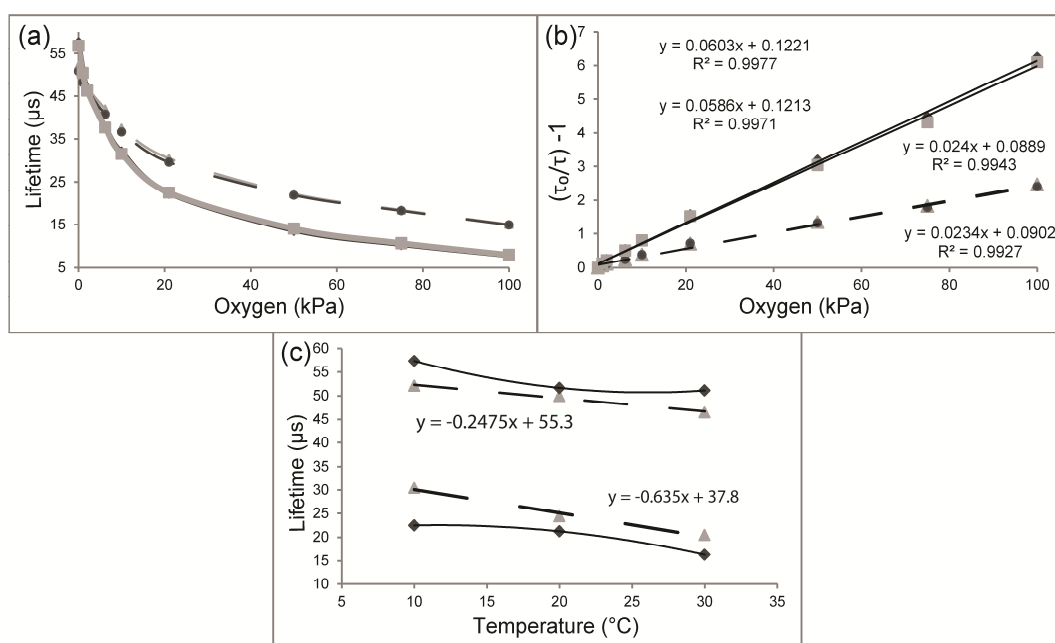
Fig. 3.9 (a) O_2 calibrations of grafted PP (dashed line) sensors in dry gas (▲) and humid gas (●) and ungrafted PP (solid line) in dry gas (♦) and humid gas (■) in lifetime scale. (b) Corresponding Stern-Volmer plots (c) Temperature dependence of grafted (▲) and ungrafted (♦) sensors at 21 kPa and 0 kPa in dry gas.

Going from 0 kPa to 100 kPa O_2, the lifetime reading of the grafted sensor decreased from 50.77 ± 0.01 µs to 14.90 ± 0.01 µs, whereas the ungrafted sensors exhibited a much larger lifetime change – from 57.32 ± 0.09 µs to 7.93 ± 0.01 µs. As indicated by the smaller deviations, the dye was more uniformly dispersed in the grafted sensor.

Stern-Volmer constants indicate the sensitivity of the sensors. Higher Stern-Volmer constants are a reflection of higher sensitivity of the sensor to O_2 [122]. Both sensors exhibit linear behaviour indicating even distribution of the O_2 sensing dye in the polymer support. The ungrafted PP sensor is approximately twice more sensitive than that of the grafted PP sensor. As the bulk polymer (PP) of both sensors is the same, the difference is most likely due to their manufacturer fabrication methods and the thinner nature of the ungrafted PP sensor. The limits of detection for both sensors were 0.09 kPa and 0.27 kPa at 0 and 21 kPa respectively. The grafted PP sensor also demonstrated linear temperature dependence within a narrow T range, indicating that the sensors can be T-compensated. The temperature coefficient of the Stern-Volmer calculated was found to be -3.55 x 10^{-2} kPa $^{-1}$ C $^{-1}$ for the range 10-30 °C. In contrast, the ungrafted PP plots display a polynomial fitted curvature meaning that a more complicated T-compensation will need to be applied.

Quite often, a hydrophobic polymer-based sensor displays poor wettability and formation of microbubbles within sensor materials. As a result hydrophobic sensors may show slow response to O_2 concentration in aqueous samples [53]. Despite this, the ungrafted PP sensors showed fast response times in both dry and humid gas (Table 3.4) unlike the conventional OpTech^{TM} sensors which responded 4-5 times slower in humid gas.

Table 3.4 Response and recovery times in humid gas at 10 °C from 21 to 10 kPa O_2

	Humid gas @ 10 °C	
	Response (min)	Recovery (min)
Grafted swelled PP	4	4.7
Ungrafted swelled PP	7.7	7.9
OpTech^{TM} reference sensor	26.5	28.2

The grafted sensor which is hydrophilic showed a slightly faster response than the ungrafted sensor. Both sensors showed reversible responses, the results are shown in Fig. 3.10.
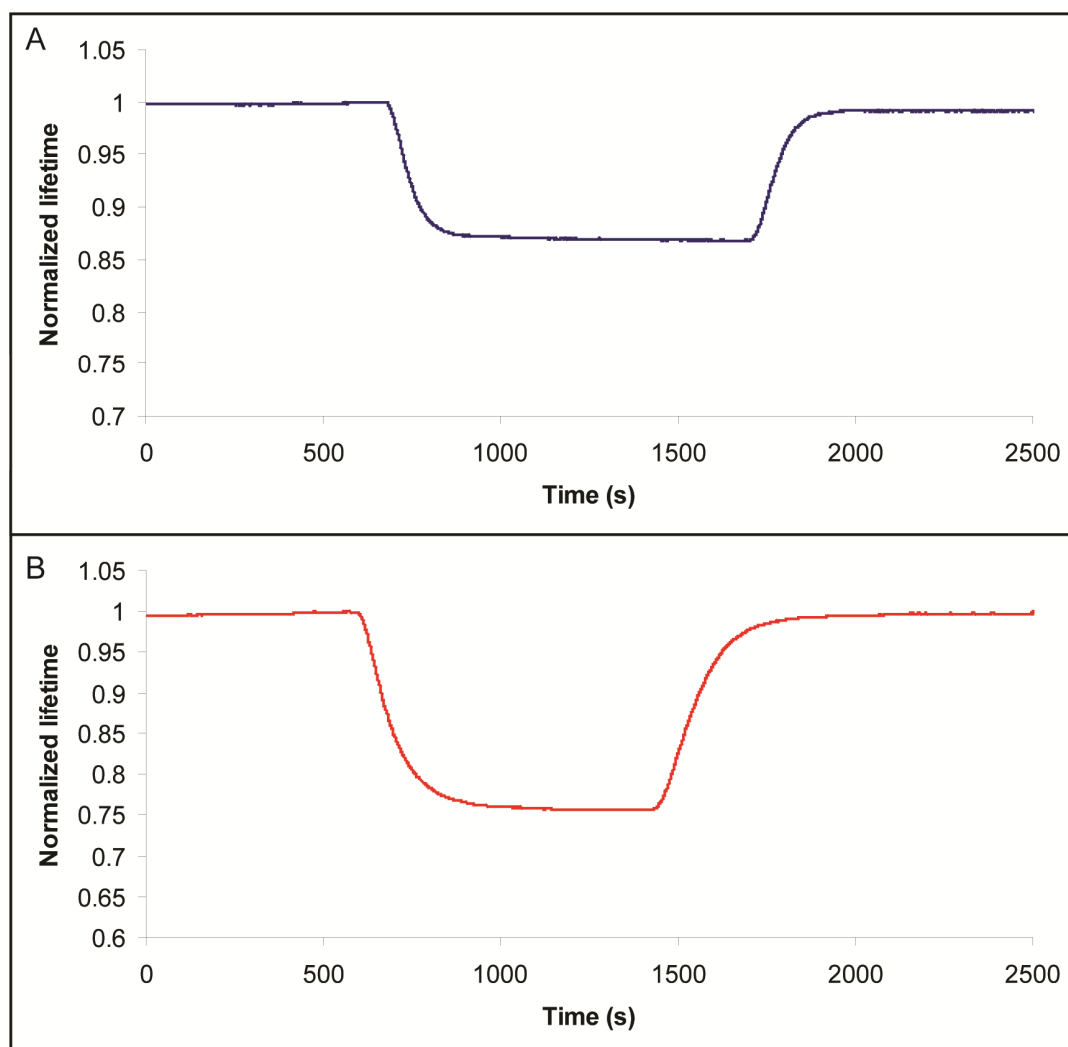
Fig. 3.10 Response and recovery curves of A) Grafted PP sensor B) Ungrafted PP sensor at 10 °C in humid gas from 21 kPa to 10 kPa O₂.

The microstructure and distribution of dye within the sensor were observed under wide-field optical microscopy and FLIM. As the sensing membranes were quite thick (approximately 80 μm thick) and opaque, it was only possible to focus on the top layer of each sensor membrane. As seen in Fig. 3.11, the ungrafted PP exhibits narrower fibres than the grafted PP most likely due to difference in fabrication

method and also to the fact that the grafted PP sensor has a layer of acrylic fibres grafted onto its surface.
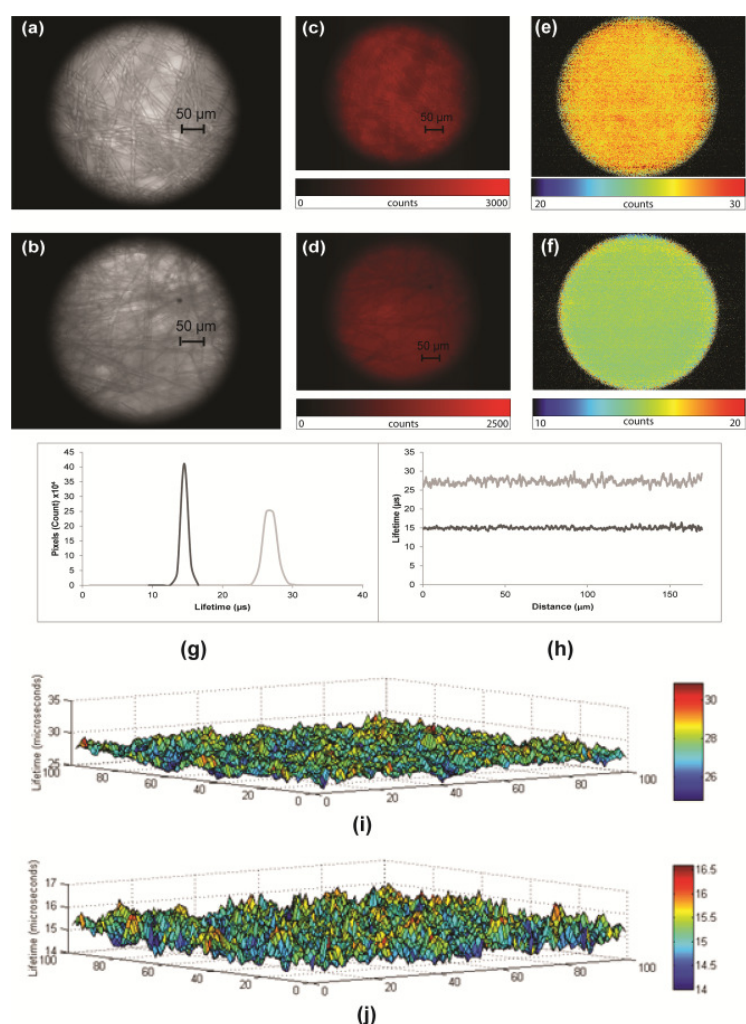
Fig. 3.11 Wide-field microscopy images of grafted and ungrafted PP sensors: (a, b) bright field images of grafted and ungrafted PP; (c, d) phosphorescence intensity images of grafted and ungrafted sensors respectively (e, f) PLIM images grafted and ungrafted sensors , (g) histograms & (h) line profiles of grafted and ungrafted PP (light grey – grafted, dark grey - ungrafted), (i, j) 3D surface graphs of lifetimes of grafted and ungrafted sensors . Sample area analysed: 100 x 100 pixels, 11536.21 μm². Measured at room temperature, 21 kPa, 40 X magnifications.

The phosphorescence images were obtained under 21 kPa and 1 kPa O_2 pressures to demonstrate the effect of quenching on the sensor. The intensity images acquired in air correlate to that seen in the bright-field image. Regions of higher intensity correspond to areas of high fibre density, demonstrating that more dye is entrapped in these regions. The ungrafted PP sensor showed a more even dispersion of dye over the sensor (15.00 ± 0.34 μs) compared to the grafted PP sensor which showed a

wider dispersion (27.25 ± 0.77 µs) at 21 kPa. This is confirmation of the line profiles and histograms generated from the lifetime images, on which the distribution of pixel intensities for selected sections of each sensor can be seen[123]. The 3-D surface graphs generated from intensity data for the same sections show that the spread of lifetimes for both sensors are relatively uniform.

As the distribution of phosphorescence lifetime in air is Gaussian in nature, it can be inferred that the ungrafted PP sensor has uniform distribution of dye and a homogeneous micro-environment. The grafted PP sensor, despite having higher intensity and quenching of dye, shows broader distribution of the lifetime values indicating less uniformity.

3.4   Development of sensors produced by solvent crazing method

3.4.1   Final sensor fabrication

The crazed sensors were produced using a puncture test machine (Mecmesin Multitest-I system, 1000 N load cell, Emperor software controlled). A round-bottomed PP test-tube (Sarstedt, 13 mL) was pierced with a 23 G needle and a cut poly-foam sponge (9 x 9 x 4 mm, 52 mg) was added to the bottom of the tube centred over the pinpricked hole. A 2-butanone dye solution (0.1 mg/mL, 40 µL) was added to the sponge and the puncture test probe was lowered and centred over the sponge before zeroing the instrument (Fig 3.12). The film was then displaced downwardly at a rate of -10 mm/min until a displacement of 16 % (approx. 8 mm) was obtained. After this displacement was achieved, the pressure was released and the solvent was allowed to evaporate off. The residual solvent was wiped off with H_2O. No other post-processing of the sensors was carried out.
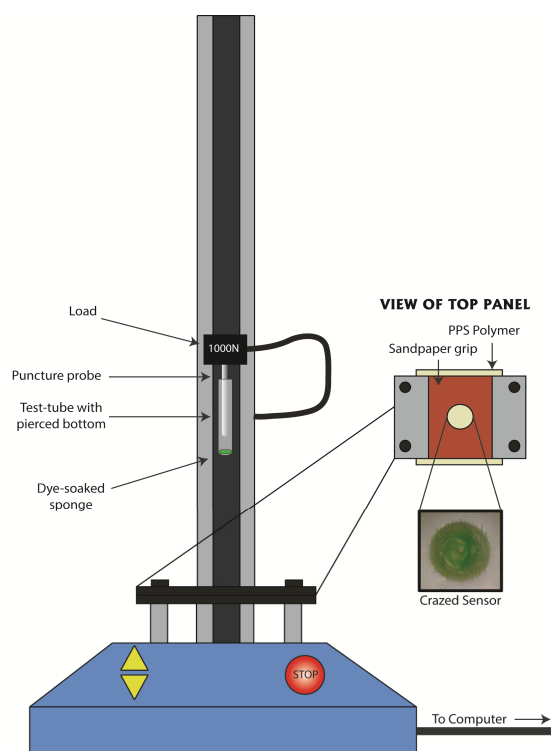
Fig. 3.12 Diagram showing crazing method

3.4.2 Selection of optimum fabrication conditions

Our lab had previously fabricated discrete O_2 sensors based on a solvent-crazing method. In that method, a piece of polymeric film such as HDPE or PPS was clamped in a custom-made device, spotted with PtBP dye solution in 2-butanone and elongated manually with a screw mechanism [57]. Although, the method produced discrete spot sensors with linear Stern-Volmer plots and an O_2 measurement range of 0-100 kPa, there was clear disadvantages. The customized set-up was not commercially available, tended to be reliant on operator skill and could only create one sensor at a time (2-3 min per sensor minimum). As a result, we aimed to modify the crazing method to use commercially available equipment and standardize it so results were no longer dependent on operator bias.

To this end, we adapted the process on an automated puncturing machine in a continuous process with PPS tape. The puncture-test machine is a standard instrument used in food and pharmaceutical packaging and has the potential to be adapted for continuous and automated use. Puncture-test machines (also known as material testers) are used for a wide range of applications within the packaging industry. Different adaptions allow several different types of material testing such as tension and compression testing and force or puncture testing using specialized software (Emperor[TM]). The instrument is suitable for small-scale testing in laboratories or can be programmed for rapid batch-testing in production settings. The latter could be utilized when up-scaling this method.

Initial trials involved testing the different adaptions to the puncture test machine's original probe (aluminium conical pin, upper diameter 13 mm, point diameter 6 mm). The original probe was found to be too sharp to promote controlled and uniform elongation without rupturing the polymer. In addition, there were issues

with feeding the solvent into the cracks formed. A spherical abrasive head (diameter 20 mm) was then attached to the probe and tested. These also proved insufficient as although the material was crazed, the abrasive coating caused scratching on the surface of the polymer material and the bit itself absorbed too much of the dye solution, leading to issues with reproducibility and cleaning.

Ultimately, a two part adaption was designed comprising of a pierced round bottomed polypropylene test tube inserted on the original probe of the puncture test machine and which contained a small poly-foam sponge which was soaked with a set amount of solvent before crazing. The test tube eliminated the previous issues caused by the sharpness of the original probe, while the sponge helped to control the release of the solvent into the crazes in a reproducible and controlled way through the piercing in the polypropylene tube.

After a reliable fabrication system had been selected, we then evaluated its effectiveness on several polymers which had been selected for use based on the previous crazing studies performed in our lab[56a, 57]. The polymers selected were high density polyethylene (HDPE) and polypropylene with toluene as the crazing solvent, and PPS with 2-butanone as crazing solvent. The first tests ascertained maximum and optimal elongation of the polymer before breakage. For reference, 1 % negative displacement was the equivalent of 0.5 mm elongation (395 % of original polymer width). The maximum elongations for PP and HDPE using the puncture test machine were in excess of 10 mm. The PPS showed a maximum elongation of 9 mm due to its more rigid nature. Elongations of 2.5 mm, 5 mm and 10 mm tested for HDPE and PP as they were below the rupture point of the polymer. 2.5 mm and 5 mm showed no crazing, however the phosphorescent signals obtained from the 10 mm elongation crazed sensors were too low (28.0 and 10.9 FU on Cary spectrometer respectively

(Fig 3.13)). This indicated that these sensors would not be reliable when read by commercial instruments such as the OpTech[TM]. In comparison, despite the PPS exhibiting low signals at 2.5 mm elongation, it showed very bright signals (>1000 FU under the same conditions) saturating the instrument at 5 mm and 8 mm elongation.
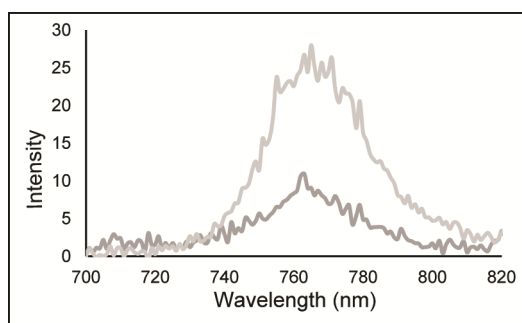
Fig. 3.13 Luminescence intensity spectra of puncture test machine crazed PP (dark grey) and HDPE (light grey) sensors obtained on CARY spectrometer.

Further testing of different elongations confirmed that elongated PPS by 8 mm produced a sensor with the highest intensity and most stable and reproducible lifetime readings. The resultant sensor spots were 9 mm in diameter and less than 0.5 mm thick. The dye concentration added to the sensor was varied from 0.05 mg/mL to 0.4 mg/mL dye in 2-butanone and an optimal concentration of 0.1 mg/mL was selected based on most stable lifetime signal and response to O_2. The amount of dye added to the sponge was determined by testing a range from 20-60 μL solution. 40 μL was deemed the optimum volume to allow the dye into the crazes and also to limit the amount of dye being removed and therefore wasted once pressure was released and the sensor was washed off with water.

3.4.3 Characterisation

The sensors were then subjected for detailed characterisation including O_2 calibrations (0-100 kPa) in dry and humid conditions at 10, 20 and 30 °C (Fig 3.14).

When tested at 10 °C sensors exhibited average lifetime values of 38.23 ± 0.22 μs in air and 48.62 ± 0.34 μs in nitrogen with intensity values of 1251.00 ± 148.49 and 2011.50 ± 273.28, respectively and a K_{SV} of 0.011. For contrast, the sensors produced by the custom hand-drawn method gave lifetime values of 29.64 ± 0.94 μs in air and 44.61 ± 0.26 μs in nitrogen with intensity values five times higher than our sensors and a K_{SV} of 0.015[57]. These differences can be attributed to a lower concentration of dye (0.1 mg/mL vs. 0.04 mg/mL) and a thicker polymer being used (130 μm vs. 75 μm) along with a different micro-environment created in the new crazing process. However, our sensors still show adequate sensitivity for packaging applications covering the range 0-100 kPa O_2, no cross-sensitivity to humidity, good reproducibility (as denoted by RSD) and there is no need for any post-treatment of the sensors.
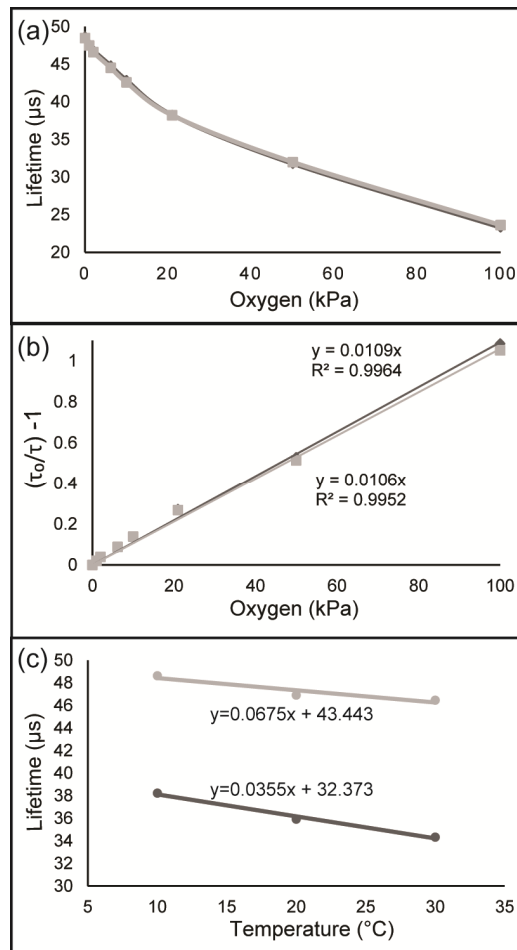
Fig. 3.14 (a) O_2 calibrations of PPS sensors in dry gas (light grey) and humid gas (dark grey) presented in the lifetime scale at 10 °C. (b) Corresponding Stern–Volmer plots. (c) Temperature dependence of PPS sensor at 21 kPa (dark grey) and 0 kPa (light grey) in dry gas.

The RSD of the lifetime signals of the sensors was 3.02 % in air and 1.90 % in nitrogen n = 4. The Stern-Volmer plot is linear, which allows the sensors to be calibrated by simple one point instrument calibrations. Linear temperature dependence was noted, the temperature coefficient of the Stern-Volmer calculated was found to be -1.9 x 10^{-4} kPa $^{-1}$ C $^{-1}$ for the range 10-30 °C.

The response time of the sensors were relatively slow (approximately 8 mins from 21 to 10 kPa O_2) (Table 3.5), however this is still an adequate window to enable the sensors to be used in food packaging.

	Humid air @ 10 °C	
	Response (min)	Recovery (min)
PPS crazed sensor	17.9	19.1
OpTech^{TM} reference sensor	26.5	28.2

In addition, the response and recovery times were faster than those of the commercial Optech^{TM} sensors in humidity (Fig 3.15).
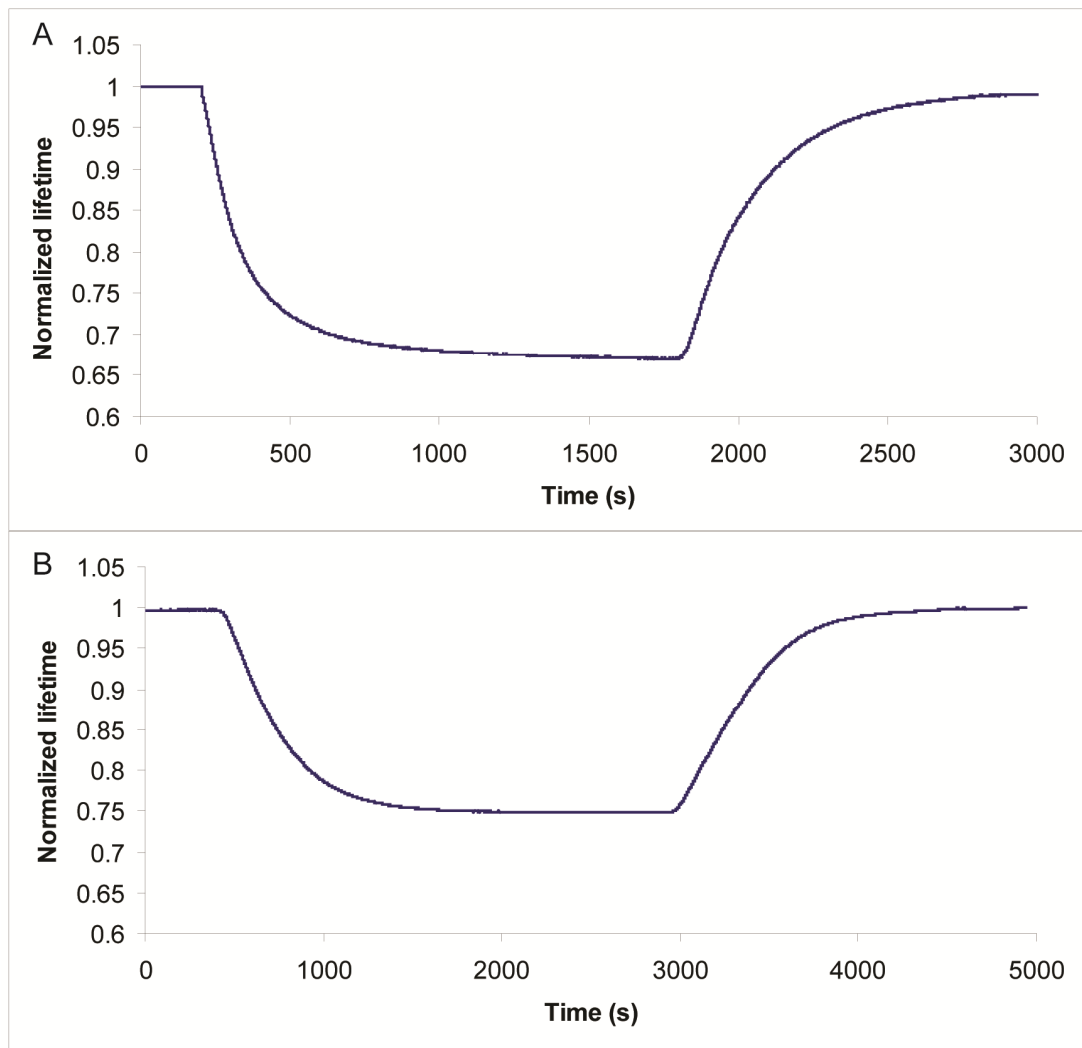
Fig. 3.15 Response and recovery curves of A) Wetlaid and spunbond spotted sensors B) Reference sensor (OpTech^{TM}) at 10 °C in humid gas from 21 kPa O2 to 10 kPa O_2

3.5 Sensor integration tests

A proof of concept study was performed on the PP fabric sensors and the PPS sensors to ascertain whether they could be easily incorporated into food packaging. The PP sensors were initially heat-sealed on the edges of the sensors to the PA/PE packaging materials. Upon calibration of these sensors, no differences in calibration or response time were noted.

The PPS and PP sensors were then laminated with a barrier material on one side. Again no difference in calibration or response time was noted (Fig. 3.16). Upon lamination with a barrier layer on one side and an O_2 permeable layer on the side facing the O_2 atmosphere, a longer response time was noted with no deterioration in lifetime signal. This could be due to the extra layer on the sensors slowing the O_2 permeating into the sensors.
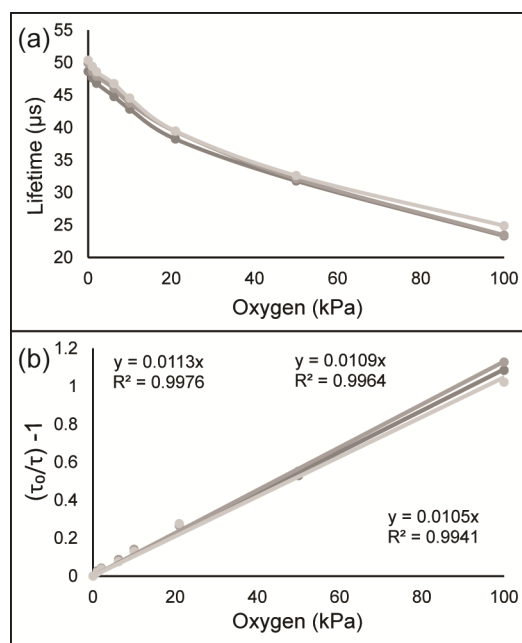
Fig. 3.16 (a) O_2 calibrations of PPS sensors: Laminated sensor facing downwards (light grey), Laminated sensor facing upwards (medium grey) Non-laminated sensor (dark grey) presented in the lifetime scale. (b) Corresponding Stern–Volmer plots, 10 °C, dry gas.

3.6   Long term storage tests

Finally, a long term storage stability study was carried out to assess whether our sensors aged with time. Three units of the swelled sensors (grafted and ungrafted PP) and spotted sensors (spunbond and wetlaid) were fabricated and measured. They were stored in a cupboard in plastic containers at ambient room temperature in ambient atmosphere. Results are found in Table 3.6

Table 3.6 Averaged lifetimes at 21 kPa O_2 and 0 kPa O_2 of sensors over the duration of the study (52 weeks).

	Day 0		Day 14		Day 90		Day 365	
O_2	21 kPa	0 kPa	21 kPa	0 kPa	21 kPa	0 kPa	21 kPa	0 kPa
Grafted PP	21.12	55.45	25.01	56.24	22.85	56.97	24.29	57.06
Ungrafted PP	12.06	56.42	15.21	56.70	13.38	57.21	14.82	56.28
Spunbond spot	27.98	56.19	30.14	56.32	26.36	55.59	27.42	53.89
Wetlaid spot	23.11	54.66	25.61	55.36	23.20	55.60	23.18	55.81

The swelled ungrafted sensors performed well over time with changes of less than 0.5 µs at 0 kPa over 12 months (Fig. 3.17). Small variations in the signals at 21 kPa could be down to differing sites of measurement. The grafted and spotted sensors showed greater deviations of 1-2 µs over twelve months. The grafted sensor showed the lifetime signal increase incrementally over the 12 months from the 1 month time-point while the spotted sensors showed fluctuating lifetimes from two weeks onward culminating in a change in lifetime signal of greater than 2 µs overall at the 12 month time-point.
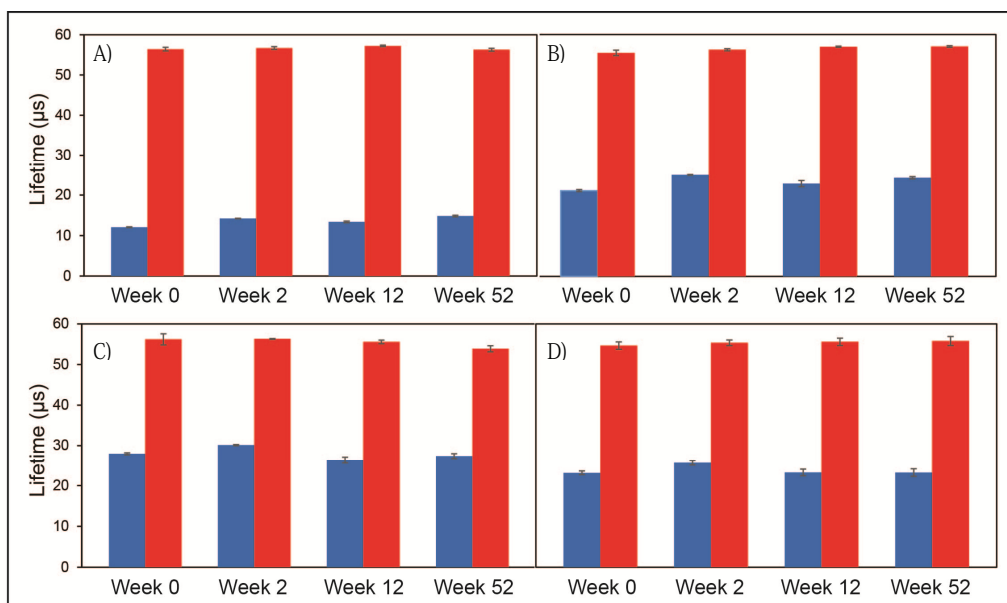
Fig. 3.17 Averaged lifetimes at 21 kPa O$_2$ (blue) and 0 kPa O$_2$ (red) of A) ungrafted sensors, B) grafted sensors, C) spunbond spotted sensors and D) wetlaid spotted sensors over the duration of the study (52 weeks).

3.7   General discussion, conclusions and potential applications
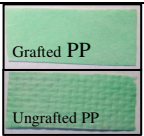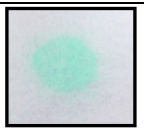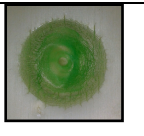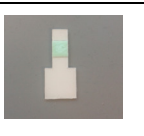
Although possessing good working characteristics in terms of life-time signal and linear calibrations, the high cross-sensitivity of the spotted sensors to humidity restrict their use to aqueous samples (e.g. dissolved O$_2$ measurements) as they are unsuitable in packaging conditions which have variable water vapour content.

Therefore, other fabrication methods were selected in the hopes of creating sensors more suited to food applications. The sensors based on PP fabric material created using a polymer swelling method, show good wettability, high signals and stable calibrations in both dry and humid conditions. The swelled grafted PP sensor showed lower sensitivity which implies it can be applied to the monitoring of higher O$_2$ concentrations (0-100 kPa) whereas the ungrafted PP sensor is better suited for monitoring of low O$_2$ levels (0-21 kPa). Therefore both sensors are suitable for O$_2$ monitoring of food products in packaging.

The PPS sensor created with a new faster method of fabrication show high reproducibility, easy incorporation and create discrete spot sensors which are desirable as no further processing is needed. However, their slow response to O_2 in humidity (Fig. 3.15 pg 87) could cause issues on a fast production line where atmosphere leakages may not be caught in time.

A summary of the main characteristics of each new sensor fabrication versus the commercial sensor is available in Table 3.7.

Table 3.7 Comparison of main characteristics of each sensor

Sensor Type	Swelled	Spotted	Crazed	OpTech[TM]
Homogeneity	High	Medium	Medium	High
Reproducibility	High	Medium	High	High
Response time in water	< 6 mins	< 4 mins	40 mins	> 30 mins
Consumption of materials	High	Low	Low	High
Cross-sensitive to humidity	No	Yes	No	No
Ease of manufacture	Slow	Fast	Fast	Slow
Discrete spots formed	No	Yes	Yes	No
Incorporation into packaging	Heat-sealable	Heat-sealable	Heat-sealable	Sticker added to support
Appearance				

4 Chapter 4: Applications of sensors in packaging

4.1 Introduction

O_2 is an important parameter to monitor in food packaging as a shelf-life limiting factor. Insufficient O_2 control can lead to premature spoiling of food by oxidation, or providing the necessary conditions for the growth of bacteria and other microbes. In addition, oxidation can change the sensory properties of certain foods such as taste, texture and aroma and decrease the nutritional value of food (potato snacks) which can negatively impact the perceptions of the final consumers.

In order to prolong the quality of food products, active packaging methods can be used. MAP, one of the most widely used active packaging methods, involves the tailoring of gas composition inside packages to optimal levels, in order to inhibit microbial growth without affecting the quality of the food product.

Traditional analysis of headspace O_2 entails the removal of packages at random from the product line, inserting a thin needle and withdrawing a precise volume of headspace gas [5]. As well as creating a large amount of wastage, this only provides a time of analysis snapshot of the conditions in the selected packets. This is insufficient to detect all below quality packages with incorrect gas levels, which have been shown to be numerous[124]. Alternatively, an online gas analyser is attached to the feed line from the gas mixer to ensure the correct levels of gas are being fed into the individual packages. Although speedier than headspace analysis, this does not account for faults in packaging materials themselves, such as insufficient sealing or damage to packaging during processing or transport allowing ingress of O_2.

Although successful in many applications, existing commercial sensor systems are not very compatible with large-scale applications such as food packaging due to

their expensive, inflexible and complex natures. To be viable for incorporation in food packaging, sensors should be reproducible, stable and cost less than 1c per cm^2 [4a]. The use of polypropylene (PP) and polyethylene (PE) as matrices for the dye incorporation helps achieve this goal as they possess many desirable qualities for sensor fabrication such as inexpensive cost, good stability and suitable gas permeability.

As outlined in the previous chapter, polypropylene membranes can be used to make robust, stable, low-cost, disposable sensors. In the following studies, we evaluated the stability of these sensors when exposed to various food simulants, meat and cheese products and in modified atmosphere packaging. In addition, we investigated the viability of using O$_2$ sensors in real-life quality control situations, shelf-life extending procedures and in selecting correct packaging.

4.2 Stability testing

The initial screen testing of the sensors in food simulants is designed to assess sensor performance in a variety of food simulants. After exposure to the sensing materials, simulants were tested by HPLC for the presence of PtBP dye which could indicate that the dye is leaching out of the sensors into the simulants. The sample solutions and PtBP dye standard was assayed by reverse phase HPLC. 10 µL of a PtBP dye in tetrahydrofuran (THF) standard (0.02 mg/mL) or the simulant solution was injected into a mobile phase of H$_2$O/TFA (mobile phase A) and eluted with an ascending stepwise gradient of THF (mobile phase B), using gradient 0-70 % B over 22 mins.

HPLC data showed that no leaching occurred for the sensors in the simulants with the exception of the 95 % EtOH control sample (Table 4.1). No leaching of the crazed PPS sensor occurred at all, even in the positive 95 % EtOH control. The leached dye obtained from the swelled ungrafted PP sensor (1.47×10^{-4} mg/mL) was attributed to aggregated dye on the surface of the sensor which was not washed off during the water wash stage.

Table 4.1 Summary of dye leached from sensors in positive control, sensors described in Chapter 3.

Sensor	Concentration dye (μg/mL)	Estimated dye leached out of sensor (%)
Swelled ungrafted PP	0.15	37.69
Swelled grafted PP	2.07	36.33
Spotted spunbond PP	0.49	24.25
Spotted wetlaid PP	0.24	11.95
Crazed PPS	No leaching	No leaching

No notable drift in the lifetime signal of the swelled ungrafted PP sensor was observed in air or nitrogen atmospheres (lifetime signal difference < 0.5 μs in all samples)(Fig. 4.1). The swelled grafted PP and spotted PP (wetlaid and spunbond) sensors show no signal after 7 days immersed in the control (95 % EtOH), this is due to all the dye being leached by the simulant solution.

	Simulant solution
1	95% EtOH
2	10% EtOH
3	5% CH_3COOH
4	3% CH_3CHCO_2H
5	3% $NaHCO_3$
6	H_2O
7	3% NaCl
8	20% Sucrose
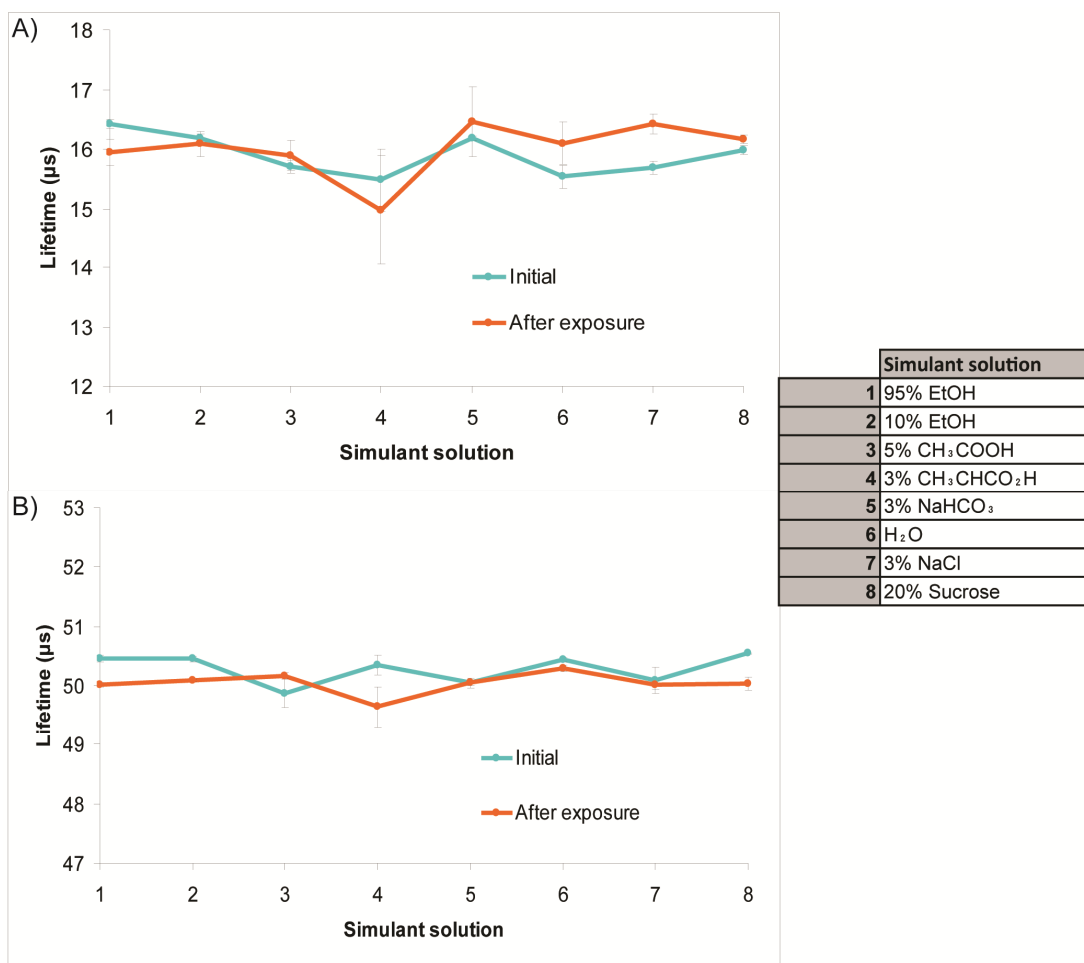
Fig. 4.1 Averaged lifetimes of swelled ungrafted PP sensors at A) 21 kPa O_2 and B) 0 kPa O_2 at day 0 (Blue) at day 21 (Orange)

The grafted sensor showed a rise in lifetime signal at 21 kPa in solutions 2,3,4,7 and 8 but this trend is not seen in the 0 kPa, which signifies a change in O_2 availability to the dye (Fig. 4.2). The degradation caused by solution 2 could be due to the redistribution of the dye by the EtOH. Degradation by the other simulants could be due to the solution sediments blocking or lowering the permeability of the microporous membrane, reducing the availability of O_2 to quench the lifetime signal.

	Simulant solution
1	95% EtOH
2	10% EtOH
3	5% CH_3COOH
4	3% CH_3CHCO_2H
5	3% $NaHCO_3$
6	H_2O
7	3% NaCl
8	20% Sucrose
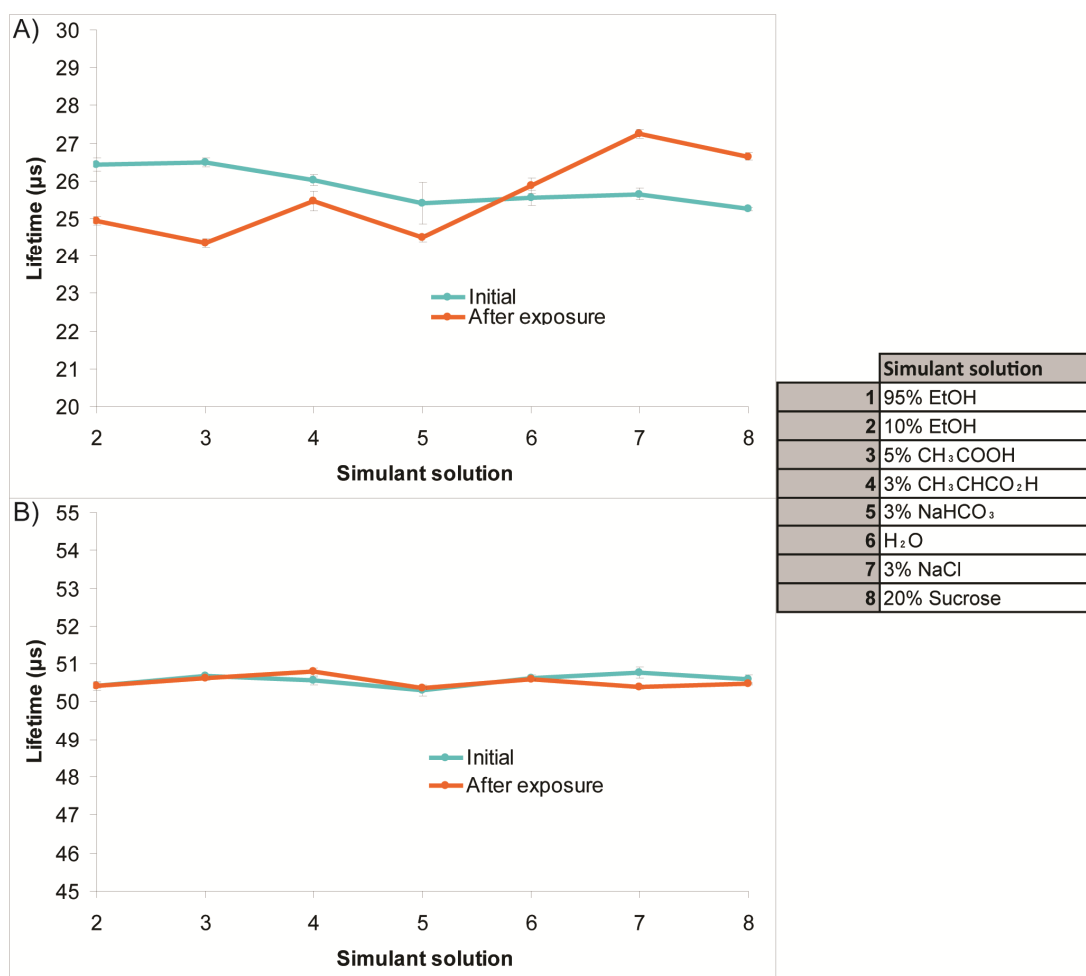
Fig. 4.2 Averaged lifetimes of swelled grafted PP sensors at A) 21 kPa O_2 and B) 0 kPa O_2 at day 0 (Blue) at day 21 (Orange).

In contrast, the crazed PPS sensor HPLC data shows no leaching in any of the sensors, indicating that the dye is firmly embedded in the polymer. Although lifetime data indicates a rise in lifetime signals at 21 kPa and 0 kPa (Fig. 4.3), it is hard to take any relevant information from this, as crazed PPS sensors have been shown to have quite heterogeneous lifetime signals dependent on location of reading.

	Simulant solution
1	95% EtOH
2	10% EtOH
3	5% CH_3COOH
4	3% CH_3CHCO_2H
5	3% $NaHCO_3$
6	H_2O
7	3% NaCl
8	20% Sucrose
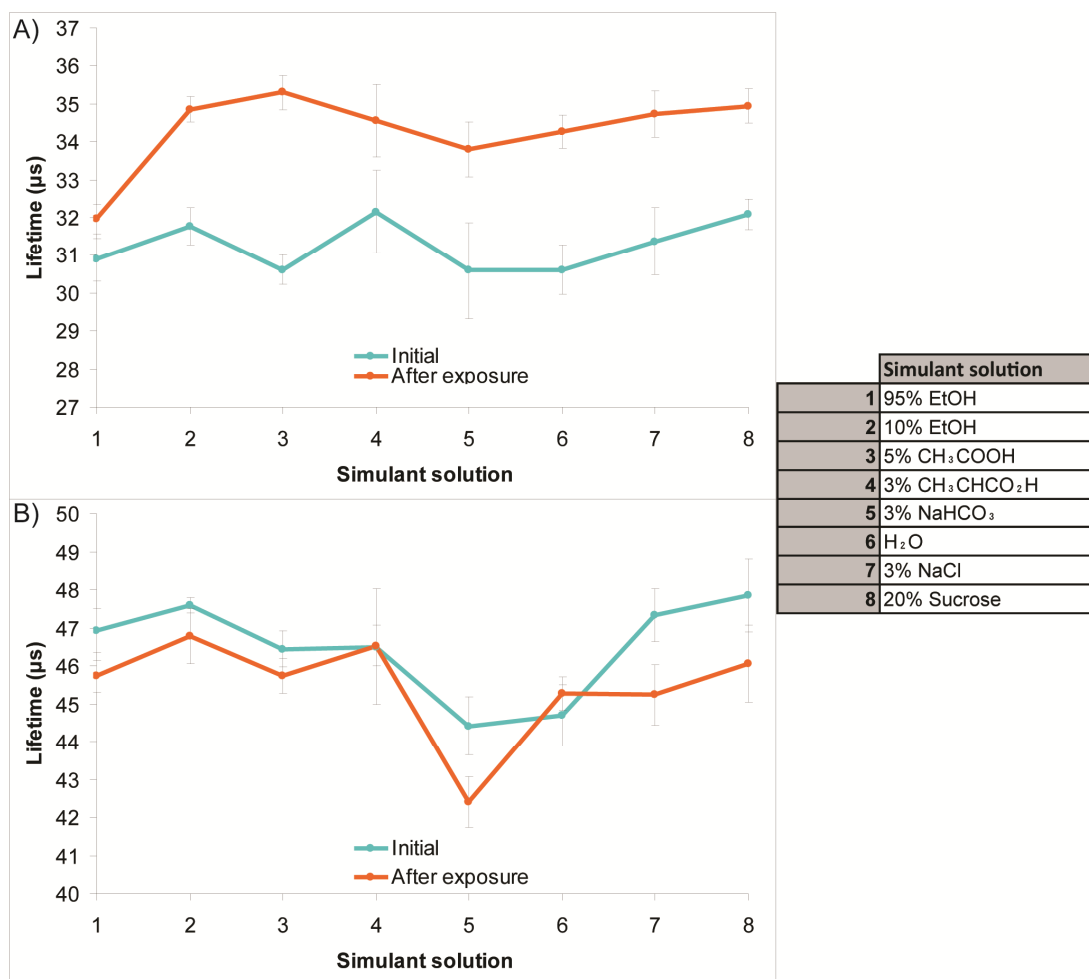
Fig. 4.3 Averaged lifetimes of crazed PPS sensors at A) 21 kPa O2 and B) 0 kPa O2 at day 0 (Blue) at day 21 (Orange).

Like the swelled grafted PP sensors, the spotted spunbond (Fig. 4.4) and wetlaid sensors (Fig. 4.5) show a change in lifetime both in air and nitrogen which can be attributed to the same effect. In addition, it was theorized that liquid could solubilise any residual surfactant retained in the spotted sensors, which could also affect a change in the lifetime signals.
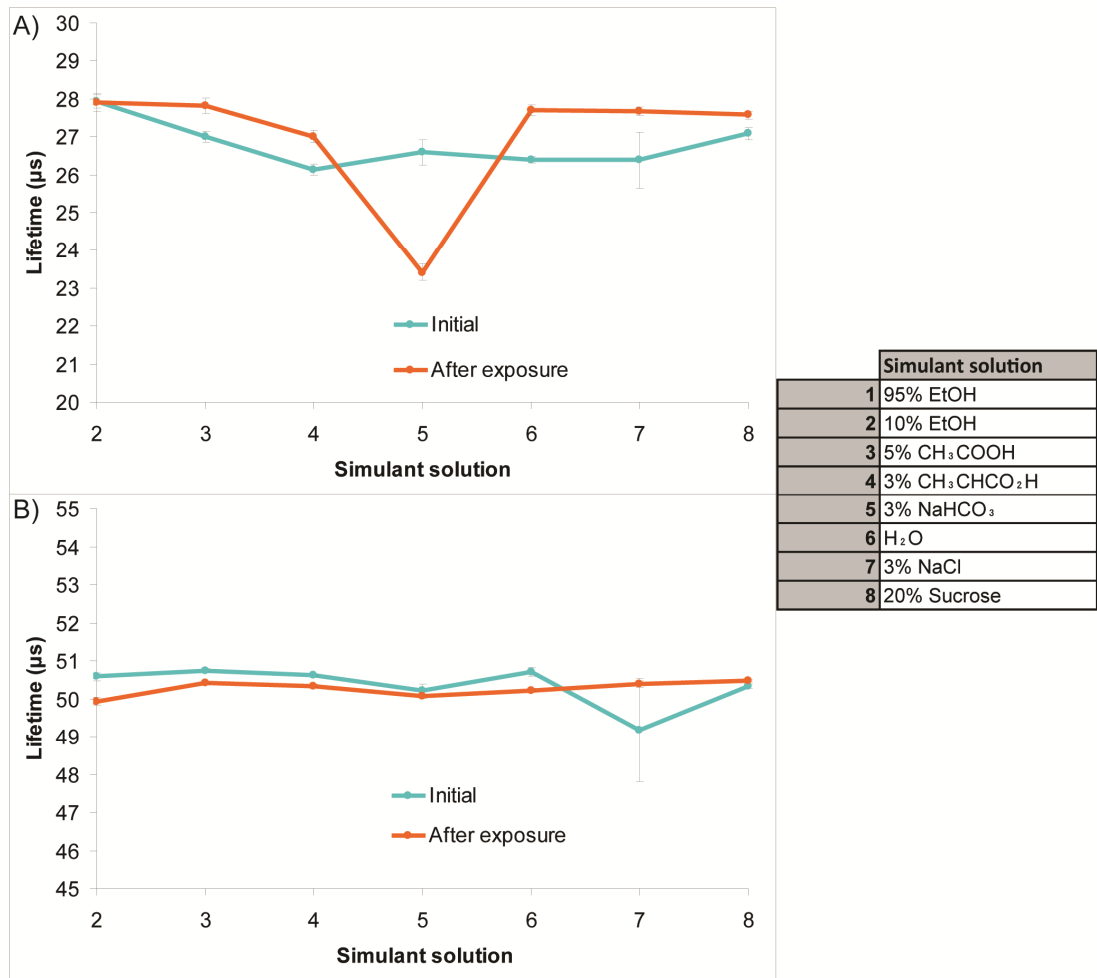
Fig. 4.4 Averaged lifetimes of spunbond sensors at A) 21 kPa O$_2$ and B) 0 kPa O$_2$ at day 0 (Blue) at day 21 (Orange).
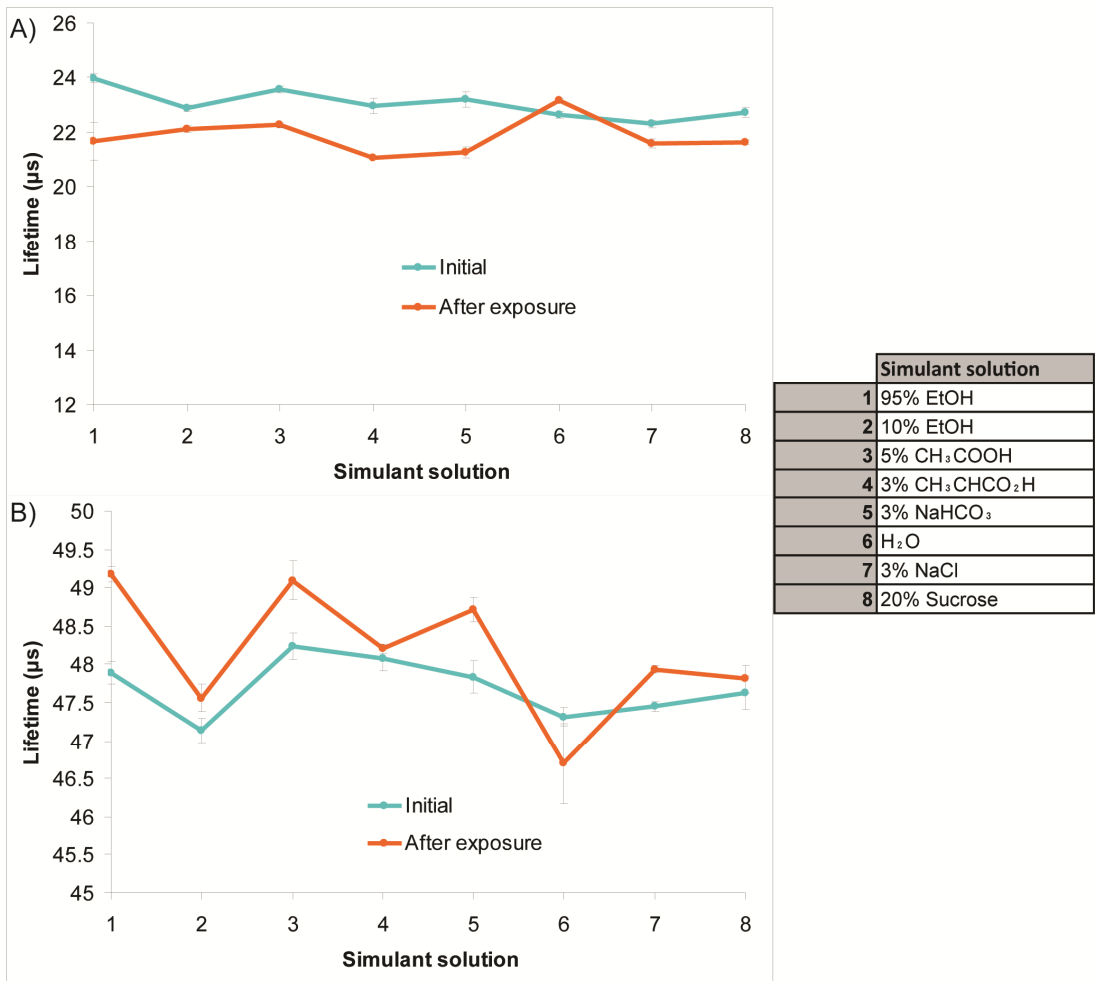
Fig. 4.5 Averaged lifetimes of wetlaid sensors at A) 21 kPa O2 and B) 0 kPa O2 at day 0 (Blue) at day 21 (Orange).

4.3 Stability testing of sensors with packaged food

Based on the results from the simulant studies, the swelled ungrafted PP, swelled grafted PP and crazed PPS sensors were chosen for stability studies involving exposure to meat products and cheese products. The spotted sensors were excluded due to their cross-sensitivity to humidity. Two of each sensor type was attached to the sealing film using scotch tape before the package was sealed (Fig. 4.6).
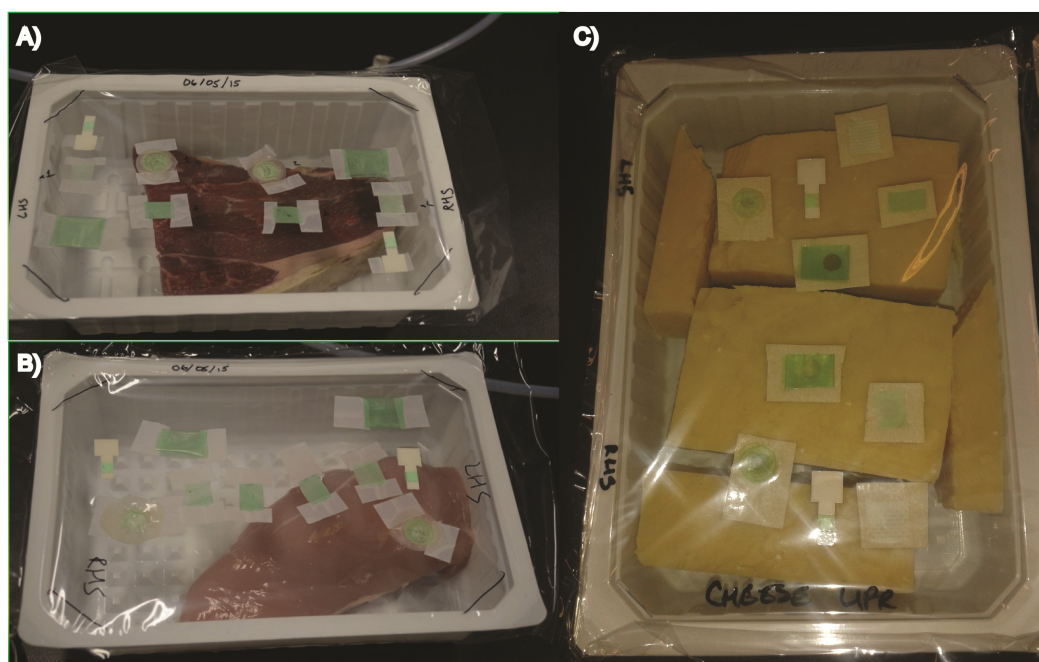
Fig. 4.6 Picture of sensors inserted in A) meat package B) chicken package and C) cheese package.

An OpTech^{TM} Platinum-O_2 sticker was included in each packet as a control. Once sealed, the meat packages were transferred to a 4 °C cold room and one stored upright and the other stored inverted. O_2 levels were measured at day 2, day 5 and day 7 using the OpTech^{TM} handheld instrument. Measurements of O_2 and CO_2 gas content were taken by the Dansensor^{TM} gas analyzer on the first and last days of the study (Table 4.2). Measurements showed that in the packages with chicken, O_2

content reduced by 0.1 %. This could be an indication of O_2 being absorbed by the meat product.

Table 4.2 O_2 and CO_2 concentrations in packages measured by Dansensor[TM] instrument, n=2 for each reading.

Sample	Before storage (%)		After storage for 7 days (%)	
	O_2	CO_2	O_2	CO_2
Blank	55.30 ± 0.00	40.90 ± 0.07	55.40 ± 0.00	40.50 ± 0.07
Beef UPR	55.30 ± 0.00	40.90 ± 0.00	54.30 ± 0.00	41.40 ± 0.07
Beef INV	55.30 ± 0.00	41.20 ± 0.00	54.30 ± 0.00	41.50 ± 0.07
Chix UPR	0.10 ± 0.02	41.00 ± 0.02	0.03 ± 0.07	36.00 ± 0.07
Chix INV	0.09 ± 0.02	41.40 ± 0.00	0.00 ± 0.07	35.80 ± 0.07

The screening of the sample packages (Fig. 4.7) showed the swelled ungrafted PP sensor having the least lifetime deviation (< 0.3 µs (< 0.18 kPa O_2)) over the seven day period in both the chicken packages and the beef package which was stored in an upright position. A higher deviation was observed in the inverted beef package, which could be due to the sensor being soaked in the blood juices from the product throughout the storage period. Likewise, the swelled grafted PP sensor showed small deviations in lifetime signal in chicken packages. However, there were noticeable deviations observed in the beef samples (1.5 µs (1.13 kPa O_2) in the upright sample and 14.3 µs (14.00 kPa O_2) in the inverted sample). The smaller deviation can be attributed to condensation within the packet which gathered around the sensor. The larger deviation was caused by the impregnation of the sensor with blood juices which can limit the O_2 availability of the sensor due to the fatty nature of the juice. The crazed PPS sensor also performed well, with a major deviation of 2.5 µs (9.14 kPa O_2) found in the inverted beef package.
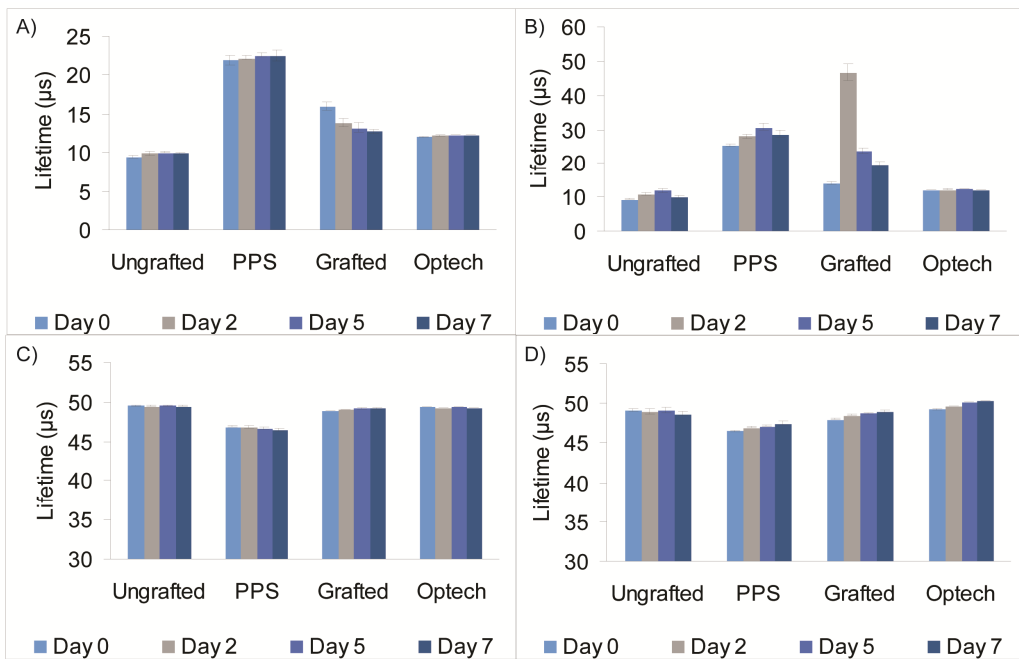
Fig. 4.7 Lifetime values of sensors in packages in A) Upright steak package B) Inverted steak package C) Upright chicken package D) Inverted chicken package.

After removal from the packages, all sensors were washed thoroughly with water to remove any residual meat juices. Characterisation of the sensor, post-incorporation, included a full O_2 calibration (0-100 kPa) performed at 20 °C in dry gas. Calibrations were carried out for each type sensor in each different meat and storage orientation (Fig. 4.8). Sensors stored in the empty package were used as the controls. The swelled ungrafted PP sensors performed well after exposure, with calibrations showing slight deviations (< 0.7 µs) from the calibration of the swelled ungrafted PP sensor in the empty package, however this is within the accepted range for the sensor.
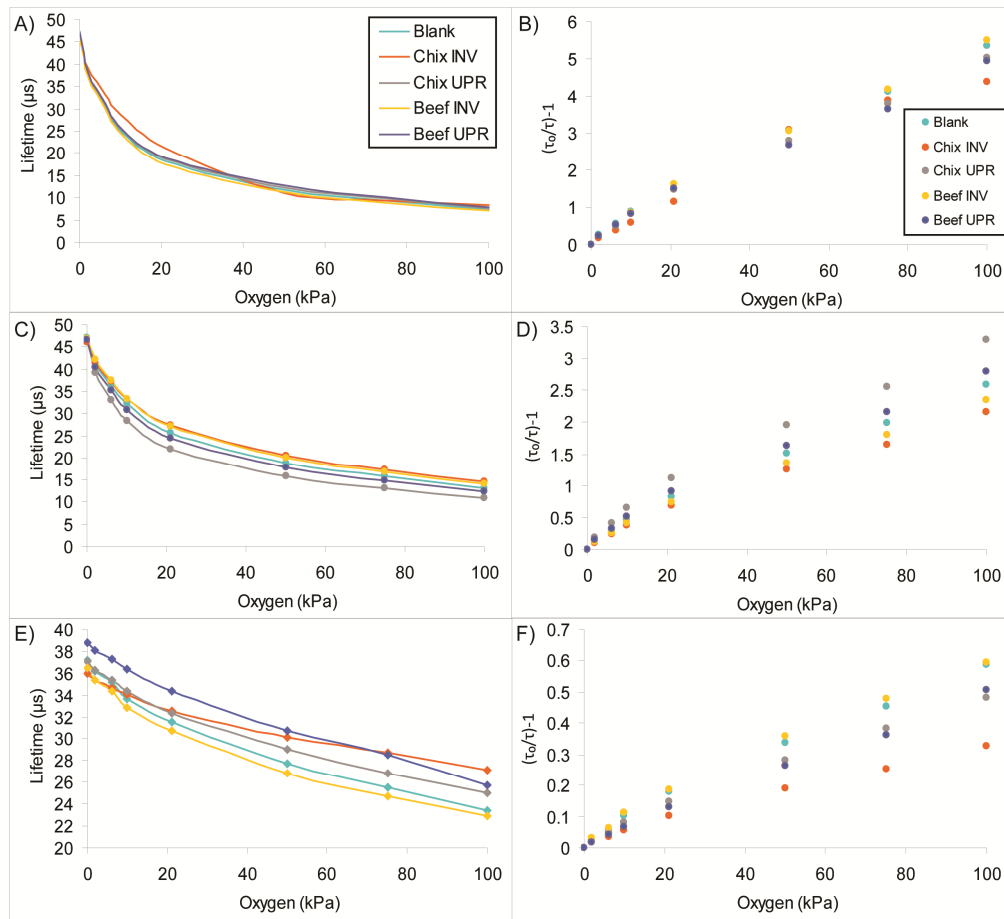
Fig. 4.8 Lifetime calibrations of A) Swelled ungrafted PP sensors C) Swelled grafted PP sensors and E) crazed PPS sensors with corresponding Stern-Volmer plots (B, D and F) post-exposure at 20 °C, 0-100 kPa dry O_2 gas.

As observed previously, during screening of the packages, the swelled ungrafted PP sensor in the inverted chicken package deviated slightly from the original calibration, with differences in lifetime signal of 2.9 µs at 21 kPa and 1.9 µs at 0 kPa. This would suggest that the juices from the chicken product are interfering with the signal and such juices are hard to remove with only water washing. This could be prevented by lamination of the sensor with HDPE to protect it from the juices and prevent soakage.

The swelled grafted PP and crazed PPS sensors showed greater deviation from their original calibrations compared with the ungrafted swelled PP sensor, with deviations of up to 3.7 µs in the swelled grafted PP sensor and crazed PPS sensor.

Like the swelled ungrafted PP sensor, the greatest deviation in the crazed PPS sensor was seen with the sensor that was in direct contact with the chicken. In contrast, the swelled grafted PP sensor showed the least variation in the inverted chicken container indicating that the hydrophilic layer may have facilitated easier washing of the sensor. There was no observed difference in response times seen between any of the exposed and non-exposed sensors.

The sensors are intended for applications where they would be exposed to many different types of food. Therefore cheddar cheese was selected for additional contact testing. The cheese was sliced and divided between two MAP containers with an additional MAP container left empty as a control. As before, the sensors were adhered to the sealing film with tape and sealed in an atmosphere of 32 % CO_2 and 68 % N_2. Blank containers were included in each sealing run. The containers were then stored both upright and inverted in a cold room (3 °C) and tested intermittently over a 32 day time-span. The blank containers were tested using the Dansensor™ gas analyzer at the beginning of the study to confirm atmosphere concentrations of CO_2 and O_2. Upon the end of the study, the Dansensor™ instrument was used to analyze the final gas levels in the packages. The results are outlined in Table 4.3.

Table 4.3 O_2 and CO_2 concentrations in packages measured by Dansensor™ instrument, n=2 for each reading.

Sample	Before storage (%)		After storage for 32 days (%)	
	O_2	CO_2	O_2	CO_2
Blank	0.14 ± 0.00	32.70 ± 0.01	1.22 ± 0.00	28.40 ± 0.00
Cheese UPR	0.09 ± 0.00	32.70 ± 0.00	0.02 ± 0.00	16.70 ± 0.00
Cheese INV	0.10 ± 0.00	32.60 ± 0.00	0.02 ± 0.07	20.10 ± 0.14

Screening showed both the upward and inverted sensors performing well over the time period with a slight upward drift in lifetime signal (0.5 µs) in the commercial OpTech™ sticker over 32 days (Fig. 4.9). This corresponded to upward

drifts in the swelled ungrafted PP and crazed PPS sensors of 0.7 μs and the swelled grafted PP sensor showed the lowest drift of 0.2 μs. The upward drifts in signal indicate a depletion of the already trace level of O_2, possibly due to the cheese absorbing O_2 from the atmosphere. This corresponds to Dansensor[TM] data which indicates that O_2 levels in the containers have decreased by over 0.7 % over the course of the study.
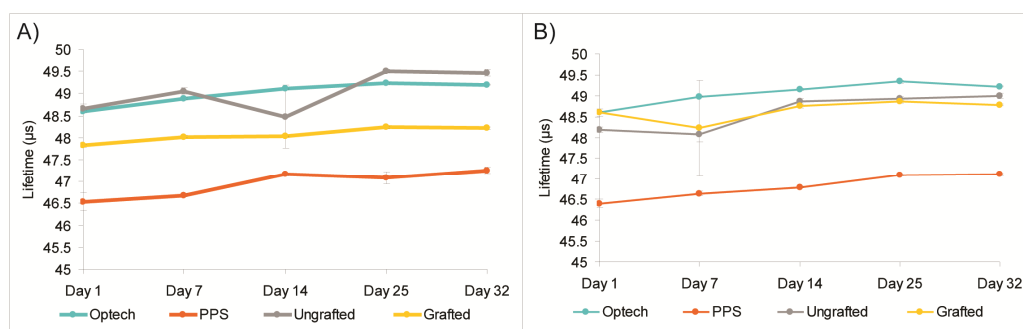
Fig. 4.9 Lifetime values of sensors in packages in A) Upright cheese package B) Inverted cheese package.

The blank container containing sensors used as control was found to have a leak as indicated by lower sensor readings. The OpTech[TM] sensors showed a reading of approx 46 μs instead of the 48-49 μs signals obtained from the cheese containing packages, indicating O_2 ingress had occurred. Upon examining the Dansensor[TM] data, which showed similar O_2 concentrations in all packages, it was assumed that the package containing the sensors had not sealed correctly. This highlights the need of quality testing all packages on-line as the blank package which was sealed on the same run had sealed correctly according to Dansensor[TM] data.

Upon removal from packages on day 32, the sensors were washed with water and dried overnight. Characterisation of the sensor, post-incorporation, included a full O_2 calibration (0-100 kPa) performed at 20 °C in dry gas. Calibrations were carried out for each type sensor in each storage orientation. Sensors stored in the empty package

were used as the controls. As seen with the meat products, swelled ungrafted PP sensors performed well, with calibrations showing slight deviations within the accepted range (< 0.8 µs, 0.34 kPa O_2), from the calibration of the swelled ungrafted PP sensor in the empty package (Fig. 4.10).
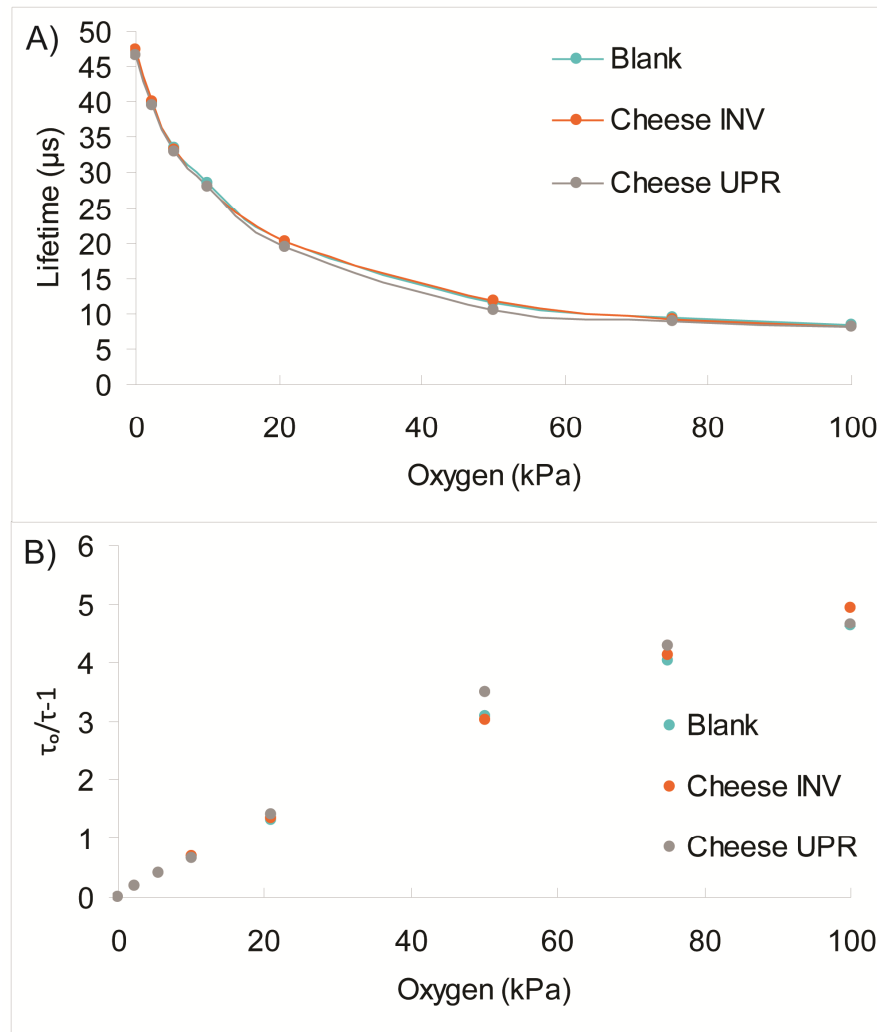
Fig. 4.10 A) Lifetime calibration curves of swelled ungrafted PP sensors B) corresponding Stern-Volmer plot post-exposure at 20 °C, 0-100 kPa dry O_2 gas.

The swelled grafted PP and crazed PPS sensors showed greater deviation from the original calibration (Fig. 4.11), with deviations of up to 1.2 µs (1.03 kPa O_2) in the swelled grafted PP sensor and 1.8 µs (3.00 kPa O_2) crazed PPS sensor. The greatest deviation in the swelled grafted PP sensor was seen with the sensor that was not in direct contact with the cheese product. This difference was attributed to a

slightly different availability of O_2 to the dye within the sensor as the signal only began to deviate as O_2 concentrations increased. In contrast, the crazed PPS sensor showed the greatest deviation in the inverted cheese container indicating that there may be interference from the oily nature of the cheese. As before, there was no observed difference in response times seen between any of the exposed and non-exposed sensors.
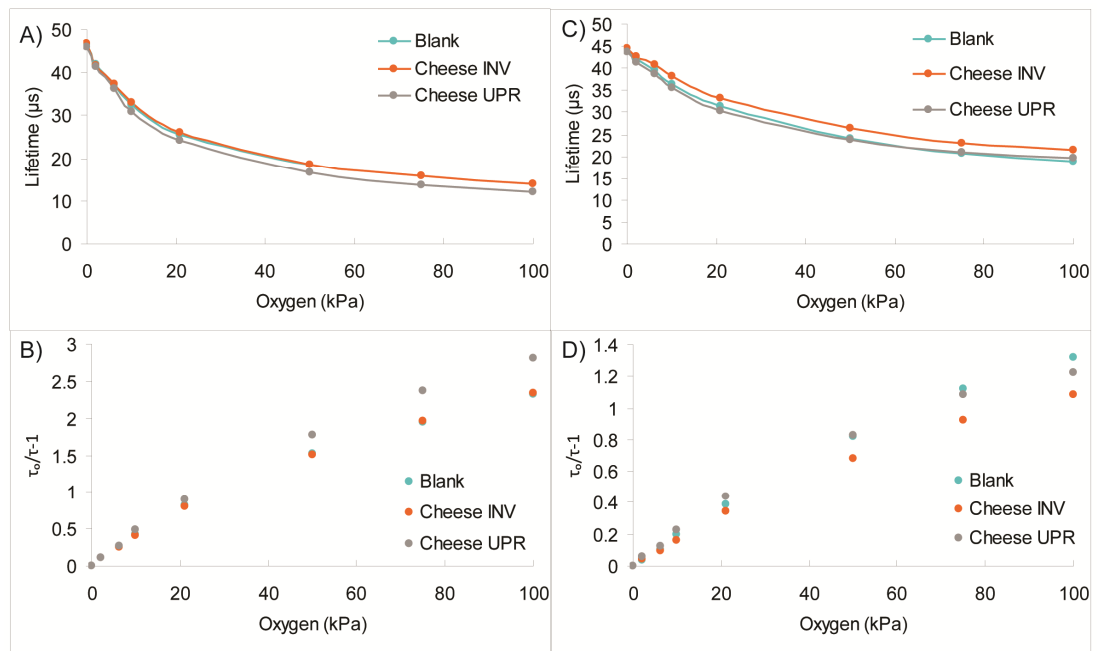
Fig. 4.11 Lifetime calibration curves of A) swelled grafted PP sensors, C) crazed PPS sensor and corresponding Stern-Volmer plots (B & D) post-exposure at 20 °C, 0-100 kPa dry O_2 gas.

4.4 Application of O$_2$ sensors at a meat processing factory

Although, our newly fabricated sensors show good responses when in contact with food products, the signal interference observed in interaction with meat juices require further study and quite possibly lamination to protect the sensors. Therefore, as lamination was not possible in-situ at factory site packaging facilities, commercially proven OpTech^{TM} Platinum-O$_2$ stickers were used to carry out the following proof-of-concept studies.

4.4.1 QC of vacuum packing machines

Three vacuum-packer machines, in a large-scale meat processing factory, were assessed for efficiency using OpTech^{TM} Platinum-O$_2$ stickers. Packaged meat cuts were tested based on aesthetic appearance, O$_2$ content, and shelf-life performance. A total of 26 samples were tested, 10 of which were packaged on an older conventional vacuum packing machine (Code: MVac) and another 10 were packaged on the rotary vacuum packing (Code: Oct). These pieces were created from cow chuck split and divided into 20 pieces. Finally, a shin piece was cut into six pieces and packaged in a new conventional vacuum packing machine (Code: FVac).

The pieces were tested on day 0, day 30, day 60 and day 90 (Table 4.4). Each piece was checked for any off-tones and colour changes. It was noted that both the MVac and Oct samples only showed a slight brown turn in colour from pink-red on day 90 with some off-notes recorded also. In contrast, the FVac samples had turned from an initial pink-red to a pink-white slimy appearance on day 60 to a brown colour on day 90. In addition, the samples had off-notes in smell on day 60 and had a rancid smell indicating it was completely gone off on day 90.

Table 4.4 Aesthetic appearances of samples on Day 0, 30, 60 and 90.

	Sample	Smell	Colour
Day 0	MVac samples	OK	Pink/red
	Oct samples	OK	Pink/red
	FVac samples	OK	Pink/red
Day 30	Oct7	OK	Pink red
	Oct8	OK	Pink red
	Oct9	OK	Pink red
	MVac7	OK	Pink red
	MVac8	OK	Pink red
	MVac9	OK	Pink red
	FVac5	OK	Pink red
Day 60	Oct4	OK	Pink red
	Oct5	OK	Pink red
	Oct6	OK	Pink red
	MVac4	OK	Pink red
	MVac5	OK	Pink red
	MVac6	OK	Pink red
	FVac3	Gone off	Pink/white
	FVac4	Gone off	Pink/white
Day 90	Oct1	Off-tone	red-brown-pink
	Oct2	Off-tone	Pink red
	Oct3	Off-tone	Pink red
	MVac1	Off-tone	red-brown-pink
	MVac2	Off-tone	Pink red
	MVac3	Off-tone	Pink red
	FVac1	Very bad smell	Pink brown
	FVac2	Very bad smell	Pink brown

The packages' O_2 readings were taken before opening and averaged over 3 samples (Table 4.5, Fig. 4.12). All O_2 levels remained below 0.25 % O_2 from day 30 onwards, indicating that no package was leaking or allowing O_2 ingress. The FVac samples showed significantly higher initial O_2 levels on day 0 (approximately 0.3 %). The O_2 levels in all packs declined until day 60 and plateaued on day 90, indicating that some microbial growth and/or lipid oxidation may have occurred in the packs. This would correspond with the off-note scents recorded on day 90 in aesthetic tests.

Table 4.5 Averaged O₂ levels in packs

O₂ (%)	Day 0	Day 30	Day 60	Day 90
MVac	0.50 ± 0.22	0.09 ± 0.02	0.05 ± 0.03	0.07 ± 0.04
Oct	0.65 ± 0.43	0.14 ± 0.03	0.04 ± 0.03	0.06 ± 0.02
FVac	0.94 ± 0.82	0.23 ± 0.41	0.02 ± 0.02	0.05 ± 0.04
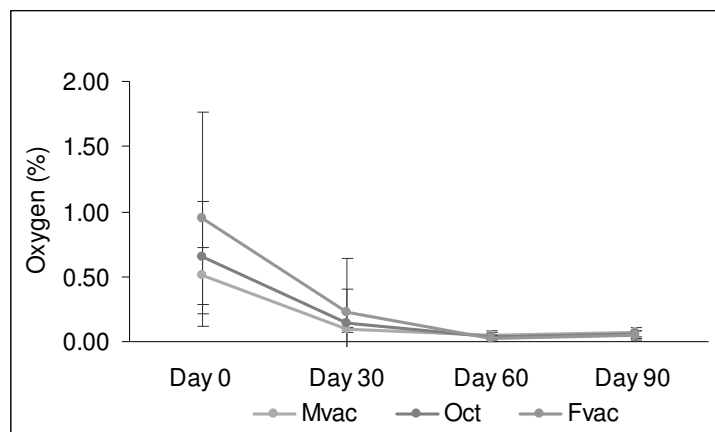
Fig. 4.12 O₂ levels in packs over 90 days.

To confirm whether the O_2 depletion was caused by microbial growth, lipid oxidation or a combination of both, microbial testing via the Greenlight[TM] 96-well plate method was performed (Table 4.6, Fig. 4.13). The microbial levels stayed within the pre-set satisfactory levels over the 90 days for the MVac and Oct samples. However, the FVac showed the highest growth, outside of acceptable limits from day 30. Day 60 and day 90 showed lower growth levels, this could be due to more unfavourable growth conditions i.e. as seen from the O_2 data, causing microbial death.

Table 4.6 CFU values over 90 days.

Log CFU	Day 0	Day 30	Day 60	Day 90
MVac	< 2.0	4.56 ± 0.03	4.71 ± 0.05	4.20 ± 0.83
Oct	< 2.0	4.89 ± 0.04	4.67 ± 0.05	3.43 ± 0.54
FVac	< 2.0	6.84 ± 0.26	6.68 ± 0.26	4.40 ± 1.50
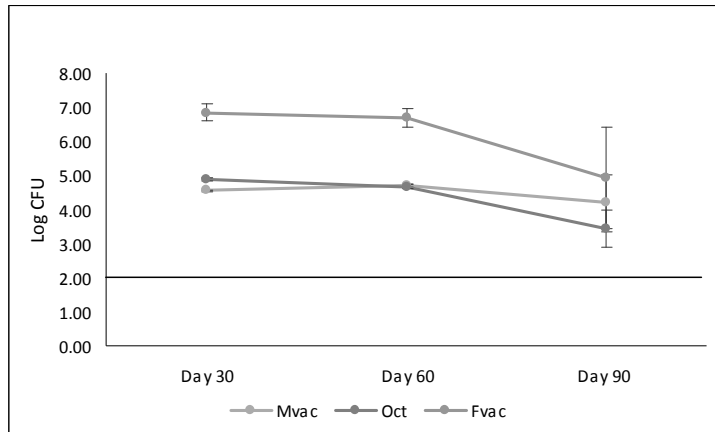
Fig. 4.13 CFU values over 90 days.

The FVac samples yielded the poorest performance over the 90 day study. Unacceptable levels of microbial growth were detected from day 30 and corresponded to the off-notes in smell, which increased in pungency on day 60 and day 90. In addition, there was a notable colour change from red-pink on day 0 to a white/slimy and brown colour from day 30 onwards. These results indicate that a combination of microbial growth and lipid oxidation occurred. Chuck meat has also been tested on the same vacuum packer and withheld acceptable microbial load limits over the same time limit (see Table 2.1), it can be assumed that the different type of meat used (shin meat rather than chuck meat) was the influencing factor on the decline of quality in the meat, rather than the failure of the packaging machine.

4.4.2 Large scale QC testing

O$_2$ sensors can be used to assess efficiency of large scale vacuum packing techniques and quantify quality control parameters for O$_2$ content within these packages. A study on large scale meat containers was performed using OpTech^{TM} Platinum-O$_2$ stickers as the sensors fabricated in Chapter 3 had not been assessed fully for food safety at time of the study. The OpTech^{TM} Platinum-O$_2$ stickers (approx 20 stickers per container) were applied to the packaging materials of three containers before the containers were filled with approximately 300 kg of forequarter meat between layers of dry ice (Fig. 4.14). These containers were allowed to rest for approximately 45 min before sealing.

Fig. 4.14 Orientation of sensors on bin

The containers were then vacuumed (Fig. 4.15) and stored in the cold room warehouse (approximately 1 °C) over 15 days. The stickers which were still accessible were read using the OpTech^{TM} instrument at regular intervals on day 1, day 3, day 7, day 11 and day 15.

Fig. 4.15 Photo demonstrating vacuum pulled on bin.

On day 15, the vacuum was still visibly sufficient in the bins. The sensors were recovered from the packaging and meat samples were taken for microbial content testing.

In bin 1, the O_2 levels remained below 5 % O_2 throughout the 15 day study with the majority of sensors giving readings of less than 2 % (Table 4.7, Fig. 4.16). The initial high O_2 levels seen on day 1 were attributed to the distribution of O_2 and the temperature not being equalized as packaging took place on the factory floor which is a higher temperature than the storage warehouse. O_2 levels stayed relatively stable in the following days, with one sensor showing outlying results of 4.5 % on day 3 which decreased to below 1 % on day 8.

Table 4.7 O$_2$ level readings of each sensor in bin 1 (%).

Location	Day 1	Day 3	Day 8	Day 11	Day 15
Front 1	0.00	0.00	0.11	0.22	0.32
Front 2	1.05	0.25	0.42	0.42	0.75
Front 3	0.45	0.46	0.29	0.33	0.57
Front 4	1.85	0.01	0.13	0.14	0.36
Front 5	0.83	1.63	0.27	0.23	0.16
Front 6	1.13	1.64	0.56	0.81	1.06
Front 7	0.00	4.47	0.97	1.02	0.98
Front 8	2.64	0.03	0.08	1.13	0.00
Front 9	6.80	0.21	0.72	0.12	0.08
Front 10	7.53	1.63	0.25	0.15	0.23
Back 1	1.17	0.00	0.11	0.14	0.43
Back 2	0.00	0.17	0.13	0.07	0.10
Back 3	0.00	0.56	0.19	0.34	0.63
Back 4	0.98	0.05	0.08	0.21	0.29
Back 5	0.06	0.02	0.04	0.14	0.19
Back 6	3.35	0.18	0.07	0.04	0.07
Back 7	2.17	0.65	0.70	0.10	0.12
Back 8	N/A	0.72	0.53	0.59	0.17
Back 9	N/A	0.35	0.07	0.99	0.49
Back 10	N/A	1.02	0.21	0.20	0.11
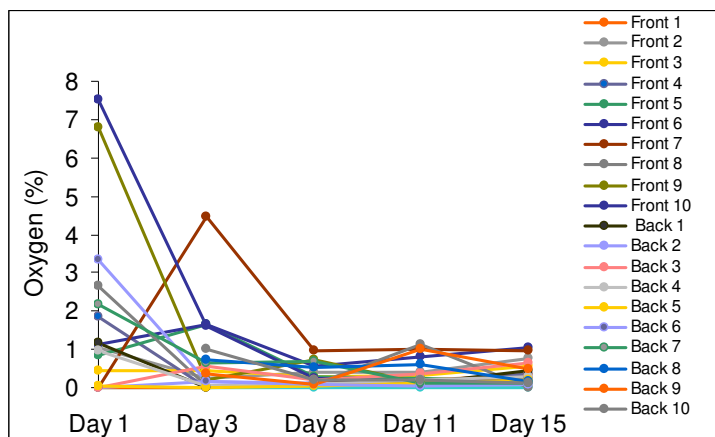
Fig. 4.16 O$_2$ concentration readings obtained from stickers in bin 1.

Likewise, bin 2 showed O$_2$ levels maintained lower than 2 % O$_2$ throughout the study (Table 4.8, Fig. 4.17) . Upon exclusion of day 1 results, the O$_2$ levels remained below 1 % in most cases with the exception of one outlier sensor.

Table 4.8 O$_2$ level readings of each sensor in bin 2 (%).

Location	Day 1	Day 3	Day 8	Day 11	Day 15
Front 1	0.33	0.50	0.00	0.47	0.36
Front 2	0.00	0.41	0.11	0.76	0.79
Front 3	0.45	0.46	0.11	0.15	0.00
Front 4	0.00	0.36	0.14	0.28	0.00
Front 5	0.00	0.27	0.08	0.31	0.00
Front 6	0.23	0.31	0.59	0.00	0.23
Front 7	0.51	0.36	0.13	0.11	0.34
Front 8	3.52	0.42	0.08	0.82	0.32
Front 9	0.63	0.41	0.17	0.30	0.69
Front 10	2.61	0.00	0.17	0.00	0.66
Back 1	1.24	0.38	0.18	0.39	0.43
Back 2	2.23	7.19	3.36	1.65	0.50
Back 3	0.00	0.17	0.00	0.00	0.74
Back 4	0.66	0.49	0.00	0.55	0.43
Back 5	3.32	0.80	0.26	0.50	0.21
Back 6	0.73	1.71	0.08	0.19	0.43
Back 7	2.19	0.30	0.28	0.32	0.25
Back 8	0.00	0.28	0.14	0.19	0.00
Back 9	3.17	N/A	N/A	N/A	N/A
Back 10	3.07	N/A	N/A	N/A	N/A
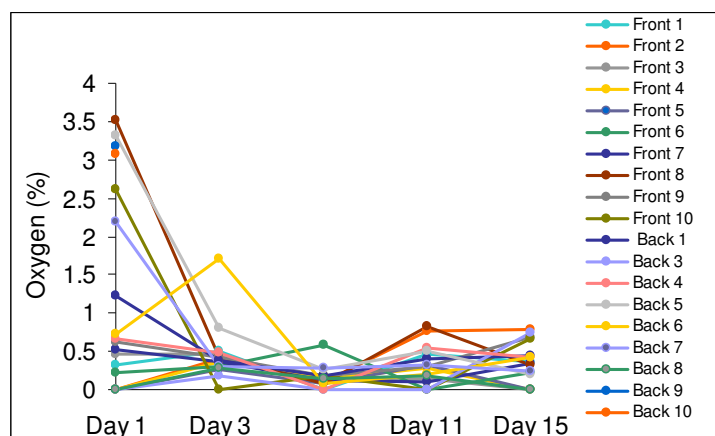
Fig. 4.17 O$_2$ concentration readings obtained from stickers in bin 2.

In contrast, bin 3 showed much lower O$_2$ levels (lower than 1 %) throughout the study (Table 4.9, Fig. 4.18). This could be attributed to the bin being sealed right first time with a good vacuum being pulled during sealing. In comparison, bin 1 and bin 2 did not have a sufficient vacuum pulled on the first attempt and so needed to be opened and resealed. This allowed some of the CO$_2$ atmosphere generated by the dry

ice to escape and be replaced with O_2 atmosphere. From day 3, O_2 levels in bin 3 remained below 0.4 % excepting two sensors which showed a slight increase on day 15. This increase could have been due to the rupture of the packaging or shaking of the bin while being transported from the warehouse to the production floor via forklift. This identified a possible point where product quality could fail. As the O_2 levels throughout the study was consistently low, it showed the importance of packaging large-scale meat packages right first time to maintain quality of meat.

Table 4.9 O_2 level readings of each sensor in bin 3 (%).

Location	Day 1	Day 3	Day 8	Day 11	Day 15
Front 1	0.00	0.28	0.07	0.08	0.20
Front 2	0.14	0.26	0.08	0.13	0.17
Front 3	0.01	0.24	0.01	0.05	0.20
Front 4	0.11	0.13	0.13	0.16	0.84
Front 5	0.00	0.26	0.08	0.19	0.10
Front 6	0.10	0.21	0.11	0.17	0.31
Front 7	0.03	0.19	0.10	0.16	0.22
Front 8	0.43	0.15	0.07	0.17	0.24
Front 9	0.20	0.00	0.05	0.21	0.32
Back 1	0.00	0.27	0.04	0.13	0.19
Back 2	0.00	0.30	0.12	0.12	0.14
Back 3	0.00	0.27	0.09	0.21	0.38
Back 4	0.00	0.28	0.06	0.09	0.80
Back 5	0.00	0.14	0.04	0.04	0.19
Back 6	0.30	0.20	0.10	0.08	0.26
Back 7	0.00	0.34	0.00	0.01	0.02
Back 8	0.00	0.20	0.10	0.00	0.27
Back 9	0.00	0.16	0.00	0.00	0.00
Back 10	0.00	0.28	0.00	0.10	0.14
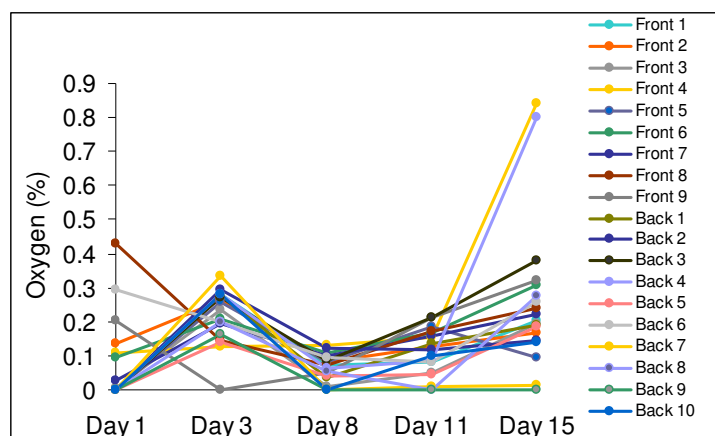
Fig. 4.18 O_2 concentration readings obtained from stickers in bin 3.

The bin O_2 distribution was averaged, to see if any trends in O_2 levels could be observed (Fig 4.19). Day 1 showed increasing O_2 from the bottom to the top of the bins. This could be due to CO_2 generated by the dry ice pushing out the O_2 atmosphere and top section of the bin being more vulnerable to O_2 ingress before sealing. Bin 1 and 2 show greater O_2 concentrations than bin 3 due to their not being sealed properly on the first try. Day 3, 8 and 11 all show the same random redistribution of O_2 concentration throughout each bin. However on day 15, there is a noticeable shift in the distribution, possibly due to the movement of the bins from their storage location in the warehouse.
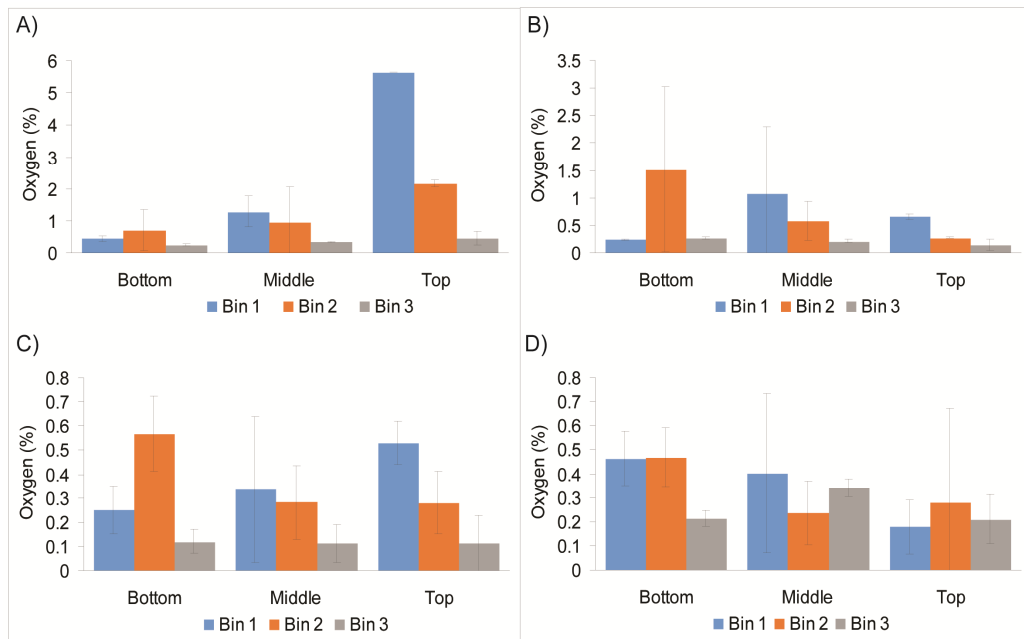
Fig. 4.19 Comparison of top, middle and bottom O_2 concentrations in bin on A) day 1, B) day 3, C) day 11 and D) day 15.

Total Viable Count (TVC) tests were carried out on the bins on day 1 and day 15 to ensure meat quality (Fig. 4.20). The microbial count tests showed no growth of bacteria on day 0 or day 15, therefore it is assumed that no growth, or growth below the limit of detection of the tests (approximately 100 CFU/g), occurred in the bins. A

positive control test was carried out on a piece of meat left out on bench-top for 48 h to ensure the microbial testing was valid.
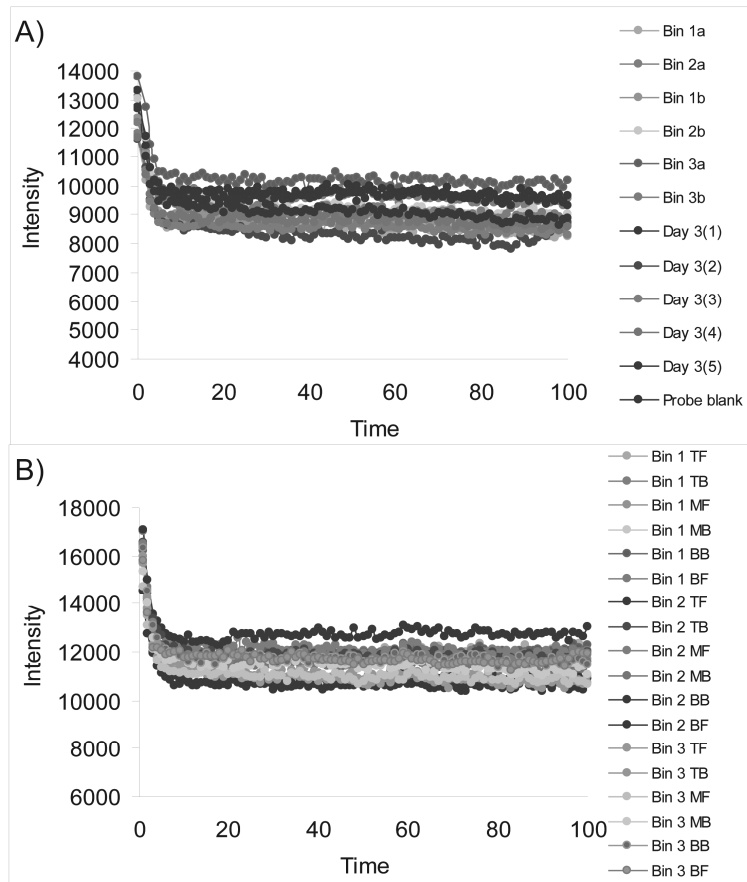
Fig. 4.20 Microbiological results obtain via Greenlight™ 96- well plate test on A) day 0 and B) day 15.

4.4.3 Testing of shelf-life extending treatment

N^α-Lauroyl-*L*-arginine ester monohydrochloride, otherwise known as LAE®, is a derivative of lauric acid, *L*-arginine and ethanol. The molecule has anti-microbial properties and is considered safe for human consumption [125] by the FDA in levels up to 200 ppm and by the EFSA in cooked meats in levels up to 160 ppm. However, studies have shown this compound has anti-microbial effects in µg/mL dosages in the range of 2-128 µg/mL against a wide range of common food-related bacteria, yeasts and moulds[125-126].

The LAE works on the cytoplasmic membranes in order to disrupt metabolic cycles and inhibit their normal cycle. Although, LAE has not been approved yet for use on raw meats in the EU, we carried out a study involving treating cuts of meat to assess its ability to extend shelf-life of the meat. Cuts (small steer pieces (approx 500 g) and large chucks (approx. 7 kg)) were treated with a 100 % concentrated solution of LAE, a 50 % LAE/50 % H_2O diluted solution and compared directly to results obtained from non-LAE-treated samples. Each sample was vacuum-packed with an OpTech^{TM} Platinum-O_2 sticker and stored in a cold room (1 °C) over an 80 day period.

4.4.3.1 Small Chuck Study

Samples were divided into three categories: Non-treated (Code: NT), 100 % concentrate (Code: Conc) and 50/50 % diluted (Code: S5050). 2 samples of each category of the small steer pieces were tested every 10 days for O_2 concentration and microbial levels. The large chucks were stored on-site in the chilled warehouse and tested on day 40 and day 80.

At each time-point, the scent and colour of the samples were assessed on opening (Table 4.10). The non-treated samples began to display some brown off-colours on day 40 along with some off-notes in smell. Although the coated samples turned a brown-red colour from day 40, there were no off-notes in smell noted over the 80 day study.

Table 4.10 Aesthetic appearances of samples every 10 days over an 80-day period.

	Sample	Smell	Colour
Day 10	NT 1	OK	Fresh red
	NT 16	OK	Fresh red
	Conc 8	OK	Pink red
	Conc 16	OK	Pink red
	S5050 8	OK	Off-red/pink
	S5050 16	OK	Off-red/pink
Day 20	NT 2	OK	Fresh red
	NT 15	OK	Red (green/blue sheen)
	Conc 7	OK	Faded pink red (white sheen)
	Conc 15	OK	Pink red
	S5050 6	OK	Pink red
	S5050 15	OK	Pink red
Day 30	NT 3	OK	Pink red
	NT 14	OK	Pink red
	Conc 6	OK	Dark red
	Conc 14	OK	Dark brown red
	S5050 7	OK	Pink red
	S5050 14	OK	Brown red
Day 40	NT 4	OK	Dark red
	NT 13	Off tones noted	Dark red
	Conc 5	OK	Brown red
	Conc 13	OK	Brown red
	S5050 5	OK	Dark red
	S5050 13	OK	Dark red
Day 50	NT 5	Off-tones	Red-pink
	NT 12	Off-tones	Red with brown parts
	Conc 4	OK	Brown-red
	Conc 12	OK	Brown-red with some pink
	S5050 4	OK	Brown-red
	S5050 12	OK	Brown-red
Day 60	NT 6	Off-tones	Whitish sheen on red pink
	NT 9	Off-tones	Red with some brown
	Conc 3	OK	Red brown
	Conc 11	OK	Red brown
	S5050 3	OK	Red brown
	S5050 11	OK	Red brown
Day 70	NT 7	Sour smell	Pink red
	NT 11	Off-tones	Pink red
	Conc 2	OK	Brown-red
	Conc 10	OK	Brown-red
	S5050 2	Slight off-tones	Brown-red

	S5050 10	OK	Brown-red
Day 80	NT 8	Off tones	Pink red
	NT 10	Very slight off-tones	Pink red
	Conc 1	Very slight off-tones	Brown-red
	Conc 9	Very slight off-tones	Brown-red
	S5050 1	OK	Brown-red
	S5050 9	OK	Brown-red

Samples were measured for O_2 content using the OpTech^{TM} instrument before opening and the average obtained between two samples (Fig. 4.21). All O_2 levels remained below 0.2 % O_2 indicating that no leakages occurred over the study. As O_2 concentrations were so consistently low throughout the study, no correlations were seen between microbial load and O_2. However, the inclusion of sensors ensured that the integrity of the packages was maintained. This allowed package rupture to be excluded, when considering causes of outlier results.
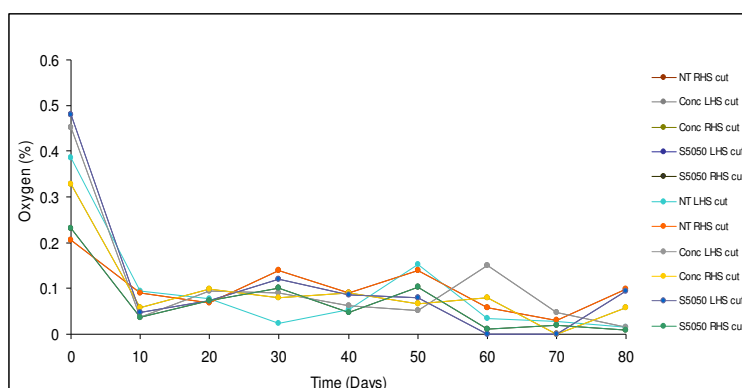
Fig. 4.21 O_2 levels in packs over 80 days.

All samples were analyzed for microbial load, every 10 days, until day 80 (Fig. 4.22). The non-treated samples showed high CFU levels from day 30 onwards. Growth fluctuated from day 20 to day 80 in the non-treated samples. The coated samples showed no microbial growth over the 80 days, with the exception of outliers in a Conc treated piece on day 60 and in a S5050 piece on day 80. These outlying

growth patterns were attributed to either local contamination or the meat samples not being fully coated in LAE before packaging.
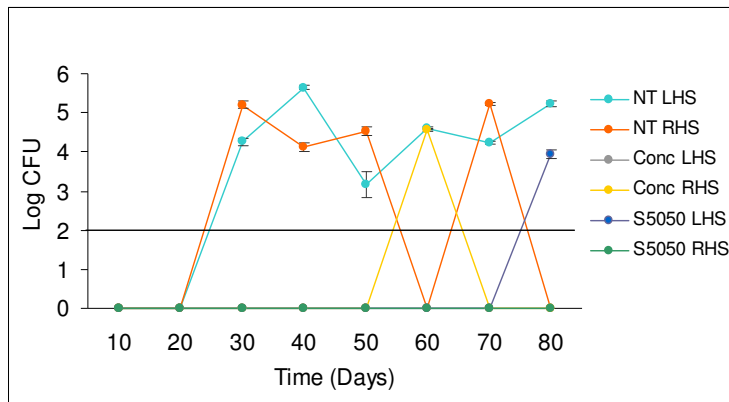
Fig. 4.22 CFU readings in packs over 80 days.

4.4.3.2 Large Chuck Study

The 7 kg chuck samples were analyzed for O2 content on day 40 and day 80 (Table 4.11). O_2 levels were observed to be < 1 % on day 1 and further decreased to < 0.1 % on day 40. A downward trend was observed in the SConc (d80) sample over the 80 days. The NT (d80) sample showed an increase from 0.058 % O_2 to 0.09 % on day 40 indicating a leak. The sample was repackaged into a new vacuum package however there was an additional increase to 0.27 %, indicating that the attempts to save the sample on day 40 were rendered ineffective.

Table 4.11 O_2 levels in chucks over 80 days.

	O_2 (%)		
Chuck code	Day 0	Day 40	Day 80
NT (d40)	0.06	0.07	N/A
NT (d80)	0.06	0.09	0.27
SConc (d40)	0.18	0	N/A
SConc (d80)	0.07	0.06	0.09
S5050 (d40)	0.07	0.05	N/A
S5050 (d80)	0.68	0.06	0.04

The samples were measured for microbial content on day 40 and day 80 (Table 4.12. On day 40, the non-treated sample showed low CFU within satisfactory limits. However on day 80, despite smelling rancid, the non-treated sample showed no CFU growth, perhaps due to large-scale lipid oxidation, rendering conditions unsuitable for bacterial growth or survival. Alternatively, as the Greenlight^{TM} test tests exclusively for aerobic bacteria, this could be an indicator that there are anaerobic bacteria present which could be competing with the aerobic bacteria and causing the decline in aerobic bacteria colonies. This highlights the need for developing low cost O_2 and CO_2 sensors for use as food quality monitors in packaging so that both types of bacteria can be monitored. Both the SConc and S5050 samples showed no growth on day 40. However, the SConc sample showed growth within satisfactory limits on day 80. The S5050 sample showed growth within the acceptable limits on d80 while having no discernable off-notes in smell.

Table 4.12 CFU levels in chucks over 80 days.

Chuck code	Log CFU	CFU	Pass/fail
NT (d40)	3.78	6104.13	Satisfactory
SConc (d40)	N/A	N/A	N/A
S5050 (d40)	N/A	N/A	N/A
NT (d80)	N/A	N/A	N/A
SConc (d80)	4.83	68083.48	Satisfactory
S5050 (d80)	5.74	544644.40	Acceptable/High
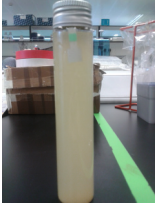
4.4.4 Use of O$_2$ sensors for optimising Beverage closures

Solid-state O$_2$ sensors can be used as a means to assess O$_2$ ingress of packaging materials, in addition to monitoring any in-product processes that can lead to the degradation of the product. A study was performed on the behest of an herbal beverage company, to assess the most efficient storage packaging for a fruit-based beverage.

Initial tests involved three different beverage conformations; vials, jars and bottles. The jars had been assessed by the company previously to maintain a product shelf-life of 6 months. The two new conformations (vials with G-type caps and bottles) had never been tested for O$_2$ ingress or shelf-life.

Five of each conformation were hot-filled with the beverage with two vials hot-filled with water as control (Table 4.13). Two commercial types of sensors were used in this study; OpTech^{TM} Platinum-O$_2$ stickers and dOxybeads, as our previously fabricated sensors had not been assessed for stability in the product matrix. The jar and vial samples contained one Optech^{TM} sticker sensor on the neck and a dOxybead at the base of each jar. The narrow nature of the bottle neck made the secure adherence of the Optech^{TM} sticker difficult, therefore only dOxybeads were used in these conformations. Only Optech^{TM} stickers were used in the water controls.

Table 4.13 Packaging conformations and sensors used in beverage study.

Conformation	OpTech^{TM}- Platinum O$_2$	dOxybead	Image
Jar	Yes	Yes	
Bottle	No	Yes	
Vial	Yes	Yes	

The samples were placed on a shaking table at 250 rpm for 16 days and measured using the OpTech^{TM} instrument at regular intervals.

The water vials, used as controls, showed little deviation in O$_2$ concentration over the 16 day period with standard deviations of less than 0.3 % (Table 4.14, Fig. 4.23). As the water used was sterile, no microbial growth was noted.

Table 4.14 O$_2$ results in water blanks.

	Average O$_2$ (%) concentrations									
Day	1	2	3	4	5	6	7	8	13	16
Blank 1	8.46	8.79	8.96	9.13	9.07	8.80	8.85	9.05	7.85	8.73
Blank 2	7.59	8.39	8.30	8.53	8.80	8.44	8.68	8.69	7.48	8.35
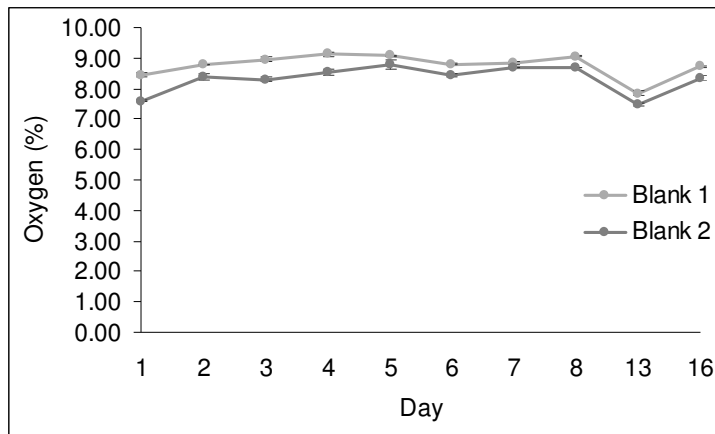
Fig. 4.23 O_2 trends in water blanks.

The jar conformations also showed minor O_2 fluctuations in the 7-10 % range throughout the study (Table 4.15, Fig. 4.24). However, as the jars were previously shown to maintain a good shelf-life, it sets an acceptable range of O_2 fluctuations (approximately 3 %) for both the OpTech[TM] sensors and the dOxybeads.

Table 4.15 O_2 results in jar conformations where A = dOxybead and B = OpTech[TM] sticker.

Average O_2 (%) concentrations										
Day	1	2	3	4	5	6	7	8	13	16
Jar 1A	10.33	10.32	9.35	9.79	9.04	9.06	8.30	8.50	8.44	8.63
Jar 1B	10.18	10.26	9.87	10.12	10.03	9.75	9.65	9.74	7.61	7.10
Jar 2A	11.25	10.13	9.12	9.06	9.93	9.93	9.22	10.22	9.50	9.72
Jar 2B	9.73	9.80	9.21	9.74	9.58	9.03	8.83	9.13	7.29	7.42
Jar 3A	11.19	10.63	9.69	10.02	10.29	9.36	9.33	9.09	9.68	9.74
Jar 3B	9.98	8.37	8.32	9.25	9.36	9.09	8.25	8.83	7.44	6.89
Jar 4A	10.01	8.71	8.95	8.76	8.43	7.96	8.15	8.61	8.34	7.83
Jar 4B	8.10	8.76	8.55	9.37	8.78	8.56	7.66	8.86	6.99	7.15
Jar 5A	9.97	9.07	8.51	8.65	9.03	8.44	8.29	7.58	7.66	7.23
Jar 5B	8.74	9.30	8.95	9.02	8.87	8.69	8.64	8.63	6.67	6.84
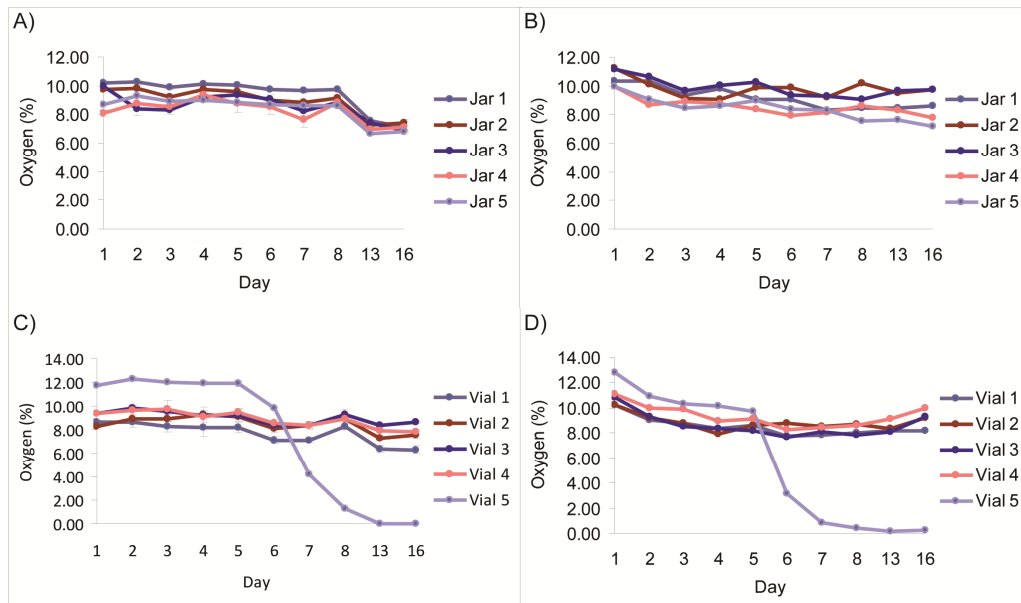
Fig. 4.24 O$_2$ trends in A) jar at baseline B) jar at neckline C) vial at baseline and D) vial at neckline.

The vials and bottle samples showed minor variability of less than 3 % throughout the study excepting Vial 5, which had a cap replaced after initial filling due to a leakage (Table 4.16, Fig. 4.24). As a result, it was deemed that no O$_2$ ingress occurred in either the vials with G-type caps or the bottles. Vial 5 showed a higher initial O$_2$ concentration both at neckline and baseline sensors (12.78 % and 11.72 %) compared to the other bottles (approximately 8-9 % and 10-11 % respectively). In addition, a decrease in O$_2$ from day 5 was observed in Vial 5, indicating the higher O$_2$ levels within the product led to the occurrence of microbial growth, which depleted the O$_2$ within the product.

Table 4.16 O$_2$ results in vial conformations where A= dOxybead and B=OpTech^{TM} sticker.

	Average O$_2$ (%) concentrations									
Day	**1**	**2**	**3**	**4**	**5**	**6**	**7**	**8**	**13**	**16**
Vial 1A	10.24	9.05	8.78	8.37	8.58	7.77	7.82	8.05	8.23	8.20
Vial 1B	8.66	8.61	8.27	8.16	8.19	7.11	7.13	8.26	6.40	6.32
Vial 2A	10.28	9.20	8.82	7.97	8.63	8.76	8.56	8.71	8.40	9.22
Vial 2B	8.23	8.95	8.95	9.26	9.11	8.08	8.40	8.94	7.29	7.53
Vial 3A	10.83	9.31	8.56	8.39	8.22	7.66	8.12	7.88	8.07	9.29
Vial 3B	9.38	9.82	9.56	9.15	9.20	8.33	8.38	9.30	8.32	8.63
Vial 4A	11.11	9.96	9.90	8.92	9.11	8.24	8.44	8.59	9.14	9.98
Vial 4B	9.38	9.62	9.70	9.06	9.42	8.54	8.34	8.91	7.93	7.81
Vial 5A	12.78	10.92	10.29	10.19	9.71	3.19	0.86	0.40	0.15	0.26
Vial 5B	11.72	12.27	12.04	11.94	11.88	9.85	4.21	1.31	0.00	0.00

Bottle 4 also showed a slightly higher initial O$_2$ concentration (approx. 10 %) in comparison to the other bottles (approx. 5.5 - 7.5 %) (Table 4.17, Fig. 4.25). Despite this higher concentration, no microbial growth occurred in the sample with O$_2$ levels remaining stable. This indicates that upon filling, if O$_2$ levels are kept below 11 %, no microbial growth will be encouraged.

Table 4.17 O$_2$ results obtained from dOxybeads in bottle conformations.

	Average O$_2$ (%) concentrations									
Day	**1**	**2**	**3**	**4**	**5**	**6**	**7**	**8**	**13**	**16**
Bottle 1	6.68	6.68	6.70	6.51	6.70	6.98	6.63	6.98	6.35	7.59
Bottle 2	5.71	4.78	6.35	6.10	5.29	6.70	5.85	5.72	5.21	5.14
Bottle 3	7.10	6.99	6.83	7.21	7.85	7.38	6.82	6.46	6.71	6.40
Bottle 4	9.86	9.85	9.82	10.00	10.16	9.84	9.44	9.50	9.19	9.26
Bottle 5	7.35	6.99	6.75	7.12	5.81	5.64	5.77	6.60	6.11	8.77
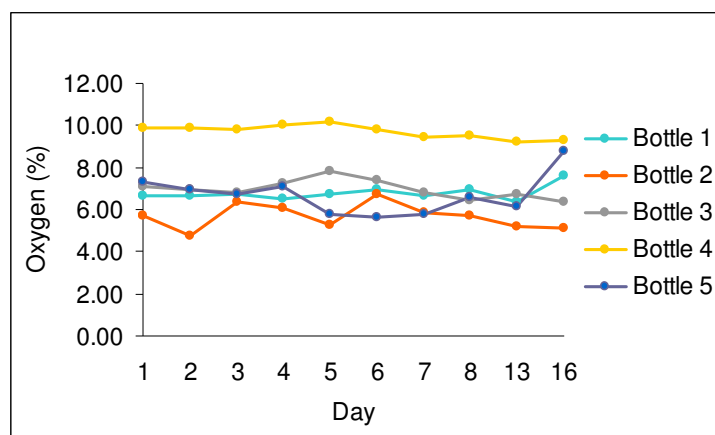
Fig. 4.25 O$_2$ trends in bottle conformations.

Samples of each conformation were analyzed for microbial content and compared to the results of Vial 5 via the Greenlight[TM] 96-well plate method (Fig. 4.26). No microbial growth was noted. This could be due to the growth being beneath the sensitivity of the test ($< 10^2$ CFU) as when the contents of Vial 5 was spread on nutrient agar and incubated at 35 °C for 48 h, some visual growth was seen.
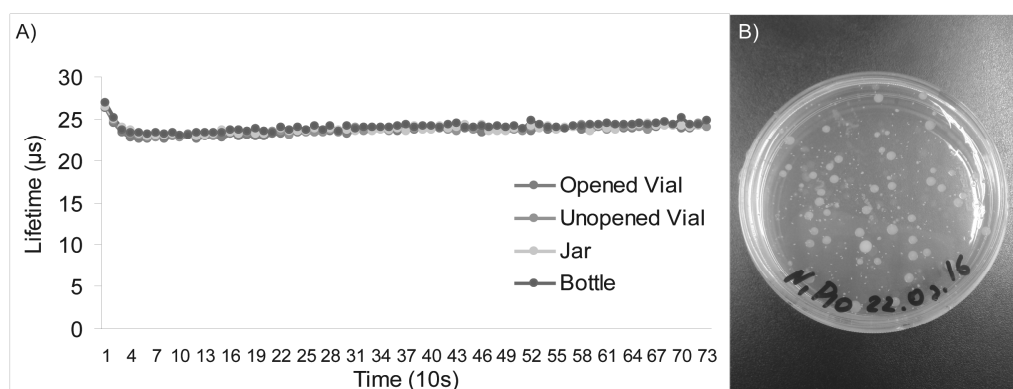
Fig. 4.26 Results of microbiological analysis of samples A) Greenlight[TM] plate method and B) T.V.C. method.

All conformations were shown to provide sufficient protection from O_2 ingress.

After the conformation was selected by the client, there were two different types of vial closures which they wanted to test for O_2 ingress; the G-type closures used in the previous study and a new type of S-type closure. 2 sensors were placed in 20 vials as before at neck level and baseline. 10 vials were capped with closure S-type which the remaining vials capped with G-type closures and all 20 vials were placed on a shaking table at 250 rpm for 7 days (Fig 4.27).

Fig. 4.27 Shaking table with samples.

The majority of the G-type vials showed significant O_2 depletions beginning to occur on day 2 (Table 4.18, Fig. 4.28). On consultation with the client, the closures were found to be recycled which could have led to the high levels of failures (8 out of 10). As the previous study showed that the G-type closures successfully deterred O_2 ingress, this would indicate it is unadvisable to reuse closures when hot-filling beverage containers as torque damage or heat-damage could lead to the caps failing on reuse.

Table 4.18 O_2 readings obtained from G-type capped samples with OpTech[TM] and dOxybead sensors.

Temperature	17°C	17°C	18°C	18°C	19°C
	O_2 reading (%)				
OpTech[TM] Sensors	Day 1	Day 2	Day 3	Day 5	Day 6
G1	0.047	0.057	0.057	0.045	0
G2	4.529	4.527	4.539	4.035	2.677
G3	5.393	5.342	5.328	5.023	3.382
G4	0.004	0.03	0.037	0.043	0
G5	4.665	4.282	0.064	0.034	0
G6	0.046	0.064	0.061	0.032	0
G7	1.278	2.628	0.044	0.031	0
G8	5.891	5.853	4.579	0.024	0
G9	6.38	6.47	5.559	0.041	0
G10	0.452	0.005	0.034	0.034	0
dOxybead Sensors	Day 1	Day 2	Day 3	Day 5	Day 6
G1	0.778	0.783	0.802	0.811	0.727
G2	3.071	2.674	1.87	1.078	1.087
G3	3.977	3.31	2.485	0.939	0.582
G4	0.821	0.807	0.954	0.857	0.724
G5	3.134	0.821	0.792	0.761	0.7
G6	0.775	0.813	0.865	0.776	0.884
G7	1.152	0.681	0.713	0.121	0.62
G8	5.798	3.789	2.892	0.684	0.533
G9	4.831	4.217	3.35	0.758	0.534
G10	0.68	0.694	0.737	0.721	0.514
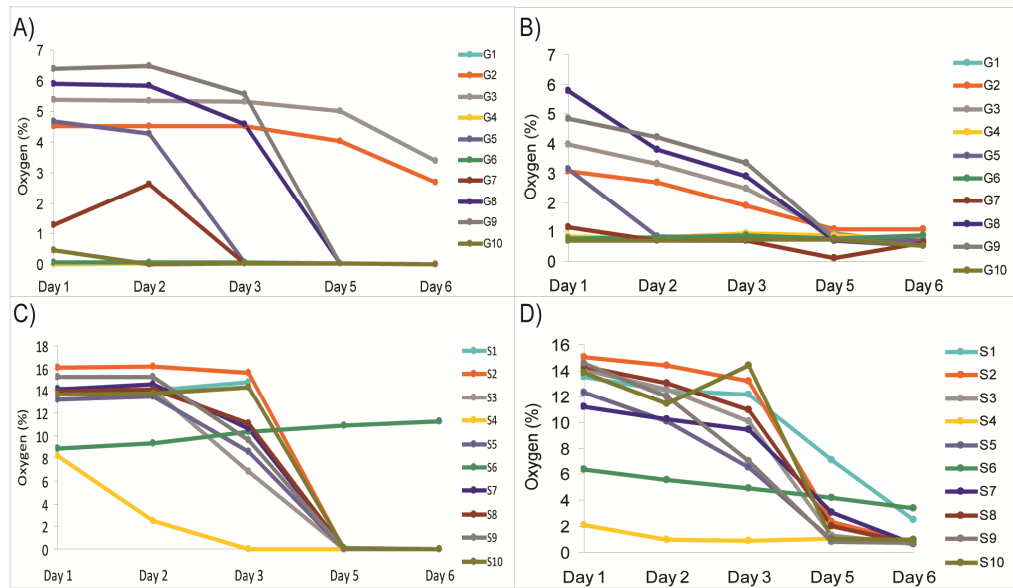
Fig. 4.28 O$_2$ concentrations from A) G-type OpTech^{TM} sensors B) G-type dOxybead sensors C) S-type OptechTM sensors and D) S-type dOxybead sensor

The S-type caps showed 8 out of 10 samples fail, with O$_2$ levels in excess of 12 % on day 1 and a decrease in O$_2$ levels noted from day 2 onwards (Table 4.19, Fig. 4.28). This decrease indicates microbial growth. S6 was the only S-type sample to show sufficiently stable O$_2$ levels, with an initial O$_2$ level on day 1 of approximately 9 %. All other vials, with the exception of S4, had O$_2$ levels in excess of 12 % on day 1. This would indicate that the 9 other vials had failed quite soon after filling and O$_2$ ingress had occurred in the time it took for the vials to reach the laboratory from the production plant. S4 showed lower O$_2$ levels on day 1 (8 %), however due to the sample showing declining O$_2$ levels it could be that microbial growth began from time of filling.

Table 4.19 O$_2$ readings obtained from S-type capped samples with OpTech^{TM} and dOxybead sensors.

Temperature	17°C	17°C	18°C	18°C	19°C
	O$_2$ reading (%)				
OpTech^{TM} Sensors	Day 1	Day 2	Day 3	Day 5	Day 6
S1	14.25	14.01	14.76	0	0
S2	16.03	16.19	15.63	0.001	0
S3	13.76	14.02	6.836	-0.007	0
S4	8.203	2.455	0.028	-0.004	0
S5	13.16	13.5	8.627	0.003	0
S6	8.888	9.351	10.31	10.86	11.28
S7	14.12	14.59	10.64	-0.001	0
S8	13.98	14.13	11.11	0.005	0
S9	15.21	15.23	9.569	-0.008	0
S10	13.69	13.71	14.31	0.049	0
dOxybead Sensors	Day 1	Day 2	Day 3	Day 5	Day 6
S1	13.52	12.5	12.15	7.066	2.481
S2	15.05	14.38	13.21	2.293	0.745
S3	14.06	12.58	10.05	1.276	0.62
S4	2.079	0.931	0.916	1.028	0.977
S5	12.32	10.08	6.488	0.994	0.931
S6	6.375	5.527	4.92	4.142	3.405
S7	11.18	10.19	9.406	3.071	0.656
S8	14.3	13.03	10.97	1.983	0.621
S9	14.57	11.99	7.008	0.819	0.729
S10	13.86	11.44	14.43	1.017	0.963

As a result of this additional study, it was recommended that new non-reused G-type caps be used as closures in future products.

4.5 Conclusions

Several sensors based on PP fabric and PPS were tested for stability both in storage conditions, in food simulants and in real-world conditions in meat and cheese packages (Pg. 93-107) The swelled ungrafted PP sensor exhibited the highest stability out of all the sensors with little change in lifetime signal in all conditions tested. This signifies that this could be a viable alternative for incorporation in food packaging, as previous tests indicate its thin film nature can be easily incorporated into food packaging by heat-sealing or lamination. It can also be produced less expensively than current commercial sensors. The sensors show satisfactory performance after exposure with quasi-linear calibrations and sufficient operation in the 0-50 kPa range.

The new uses of O_2 sensors in real-world food and beverage packaging applications were also demonstrated. These sensors provided non-invasive real-time data and clients were suitably impressed with the high level of information that was available from the use of O_2 sensors. The demonstrations exhibited the usefulness of solid-state O_2 sensors in food packaging, whether it is used to monitor existing food packaging or to choose new conformations.

5   Final Discussion

A number of new solid-state O_2 sensors were developed for application in food packaging. All sensors show good working characteristics with useful lifetime and intensity signals and quasi-linear and linear calibrations.

The polypropylene sensors, fabricated by spotting method[127], possess good working characteristics such as good lifetime signal and linear calibrations (Fig. 3.3 pg 63). The ratio of lifetime signal of 0 kPa to 21 kPa is 1.56 and 2.16 for the spunbond PP and wetlaid PP sensors respectively, signalling that the wetlaid sensor would perform better in a low O_2 atmosphere. This is further enforced by the Stern-Volmer plots which show the wetlaid sensor having higher sensitivity than the spunbond sensor. However, the wetlaid sensor plot shows a curved trend indicating that the O_2 sensitive dye distribution may be somewhat heterogeneous[23]. The spotting method consumes minimal materials and solvent as only 0.02 mL of the dye cocktail was used per spot. Additionally as the resultant spots were approximately 9 mm in diameter, a strip of 10-12 mm wide PP membrane would suffice for on-line production of sensors. The use of EtAc which has a low toxicity makes the sensors suitable for applications in food packaging.

However, noticeable cross-sensitivity to humidity is observed[106]. This sensitivity is attributed to either swelling of the hydrophilic grafted layer in the PP membrane or the inclusion of surfactant in the dye cocktail. This cross-sensitivity could potentially limit the sensors applications, as many food products have variable humidity content. To counter-act this, the spotted sensors would have to be laminated with an O_2 permeable, moisture barrier material such as HDPE before use. This would add to production time and materials cost which must be kept low in order to make O_2

sensors viable in large-scale food packaging purposes. Alternatively, a moisture scavenger could be included in the packs[128], where humidity is not necessary to maintain food quality, though this measure would also increase costs.

Issues with reproducibility are also observed in the spotted sensors but this is expected to be reduced upon up-scaling of the process. Up-scaling of the sensors in theory could be easily managed utilising and adapting current technologies which exist for filling parental products in pharmaceutical plants. The PP membrane could be line-fed as a continuous strip with a dispenser depositing the relevant amount (0.02 mL) of dye cocktail on the membrane in regular intervals via a 90° syringe. The washing and drying steps could be performed on a continuous basis in a similar manner. This up-scaling would have to be tested for viability in a packaging line.

The sensors are easily incorporated by means of heat-sealing. However, as previously mentioned, the sensors would need to be laminated to prevent cross-reaction to humidity. This would slightly lengthen response times, although no change in calibration would occur, making this a valid solution for humidity cross-sensitivity. While there are some minor fluctuations during long-term storage, the sensors are proven stable up to 12 weeks in normal atmospheric conditions. After this time, the sensor signals would no longer be reliable as the sensors show a change in lifetime signal of 2 μs from week 0 to week 52 at 0 kPa O_2.

The low consumption of materials, along with the discrete sensors formed, is ideal for application in food packaging[4a]. Exposure to food simulants shows no leaching of dye out of the sensors. Nonetheless, signal degradation was observed in some simulant solutions most likely due to the porous membrane being clogged with particulates. This further implies that the sensors will have to be protected by

lamination before use. As a result of the cross-sensitivity to humidity, the observed signal degradation in food simulants and no access to lamination within food packaging facilities, these sensors are currently ruled suitable only for aqueous non-acidic samples in the 0-21 % range. The sensors will have to be laminated with moisture barrier materials before exposure to other food products in order to prevent signal degradation. This adds extra cost and complication to the sensor fabrication. In further studies, it would be interesting to test other food-safe surfactants in the dye cocktail to see if the cross-sensitivity could be reduced and to ascertain if the surfactant is the root cause of this sensitivity.

The sensors produced by the swelling method[58] also show excellent working characteristics (Fig. 3.9 pg 76). The ratio of lifetime signal of 0 kPa to 21 kPa is 1.71 and 2.55 for the grafted PP and ungrafted PP sensors respectively, signalling that the ungrafted PP sensor would perform better than the grafted PP sensor in a low O_2 atmosphere. This is further enforced by the Stern-Volmer plots which show the ungrafted PP sensor having higher sensitivity than the grafted PP sensor. The grafted PP sensor has similar sensitivity to the spotted PP sensors, which was expected as both the grafted PP sensor produced by swelling method and the spotted sensors used the same grafted PP materials. In contrast, the ungrafted PP exhibits sensitivity approximately twice that of the grafted PP sensor. This demonstrates the influence sensor matrix has on the O_2 sensitivity of the sensor.

The grafted PP sensor outperforms the ungrafted PP sensor in terms of temperature compensation, as linear T dependence of the grafted PP make compensation simple[118]. The polynomial T dependence of the ungrafted PP makes for more complicated compensation. In comparison to the spotting sensors, swelled

sensors have a more homogenous distribution of dye throughout the sensor, as demonstrated by their linear Stern-Volmer plots.

The swelling method is a batch method, which limits its up-scalability in continuous manner. A high amount of dye per sensor (0.24 mg) is currently used along with high solvent use (5.6 mL THF). It is envisioned upon up-scaling, the ratio of water to solvent may change. In addition, the dye remaining in the cocktail may be recovered by evaporation. However, further tests would have to be carried out on the recovered dye, to ensure that exposure to the solvent or high temperatures has not altered the dye properties. Small to medium up-scaling was envisioned to be performed on a rotary evaporator, which may involve further tailoring of dye concentration, pressure, THF/water ratio, fabrication time and the amount of PP material used. Larger up-scaling would have to be performed in industrial conditions.

Although, THF is considered highly toxic, the solvent is evaporated off and the sensor is washed to remove any residues. Further post-processing of sensors would involve the cutting of sensor materials into spots or squares, as spots only need to be 6 mm in diameter in order to get a reading. These spots can be heat-sealed to current packaging materials with no change in response times or calibration.

Both sensors are suitable for O_2 monitoring in food packaging, the grafted PP for higher O_2 concentrations (0-100 %) and the ungrafted PP sensor for lower O_2 concentrations (0-21 %). The grafted PP sensors are proven stable up to 12 weeks when stored in normal atmospheric conditions while the ungrafted sensors were proven stable in storage up to 12 months (Table 3.6 pg 89). Additionally, the ungrafted PP sensor shows the best performance in the food simulant test with no

significant drift in any solution (< 0.5 μs). The grafted PP shows a significant change in signal in several simulant solutions. In food contact tests, the ungrafted PP sensors show the least signal deviations in the beef, chicken and cheese contact tests (Fig. 4.8 pg 103). However some interference is observed when in direct contact with beef juices, implying that some protection such as lamination will be required in food packaging with blood juices present. The grafted PP sensor shows greater signal deviations than the ungrafted PP sensors in the beef and chicken packages. The grafted PP sensor showed good performance in the cheese package both in screening and calibration with minimal deviation at 0 kPa O_2 which is the most common storage condition for cheese.

The PPS sensors[129] produced by the puncture test machine show differing lifetimes to the custom-drawn PPS sensors[57] and signal intensities five times lower (Fig. 3.14 pg 86). The ratio of lifetime signal of 0 kPa to 21 kPa is 1.27 in the new PPS sensor compared to 1.52 in the previous custom-drawn PPS sensor. However, the K_{SV} values are similar indicating similar sensitivities. Linear temperature compensation can be applied to the PPS sensors. The sensors show adequate signal and sensitivity for food packaging applications.

The batch-to-batch deviations in crazed PPS sensors are expected to decrease on automation and up-scaling of the production technique. The puncture test machine is advertised as being able to perform rapid batch-testing which could be utilised on a packaging production line to quickly and reproducibly created PPS crazed sensors[130]. Alterations to the instrument would involve adding the customized probe and a feed line to allow fast feeding of the solvent/dye cocktail to the sponge adaption. As spots are maximum 12 mm in diameter, the PPS strip would only have to be 25 mm in width to allow sufficient gripping while the crazing was performed. Post processing

would include washing any residual solvent off and the cutting out of the sensor from the bulk material. The PPS sensor was shown to be easily incorporated in current packaging materials by heat-sealing. It is expected that the PPS sensors will have a reliable shelf-life up to 12 months, however these tests will have to be performed in future studies.

The PPS sensors show no dye leaching in the food simulant test, with signal deviations attributed to the heterogeneous nature of the PPS sensors. The PPS sensors perform poorly in the food contact tests, with noticeable deviations in contact with every matrix, indicating they may require protection such as lamination when in contact with food products. This should be investigated further when sensors are up-scaled and signal deviations lowered.

In future work, as previously mentioned sensor production will need to be up-scalable, as currently only small lab bench scale production of the sensors has been carried out. Although initial food simulant testing show promising results, further testing will be needed on the sensors to ensure they are safe and stable for use in food packaging applications. In particular, although no significant leaching was observed, apart in positive control samples, a full toxicity test will need to be carried out on the O_2 sensitive dye to assess safety. Likewise, testing will have to be performed in additional food matrixes, such as seafood and salad, to observe if any more interference in sensor signal occurs. Finally, the viability of heat-sealing the sensors in large scale packaging lines needs to be assessed, along with the viability of laminating sensors on-line for use in red meat packaging. It is hoped upon up-scaling, material consumption per unit will be reduced. In addition, the cost of the sensors will be assessed and is expected to be considerably less expensive than current commercialized O_2 sensors.

As the testing mentioned above was not possible within the timeframe of the project, some proof-of-concept tests were performed using currently available solid-state O_2 sensors (OpTech^{TM} Platinum-O_2 sensors). The sensors were applied in vacuum-packed beef packages both in small packages to test vacuum-machine integrity and a new coating and large packages to test the efficiency of packaging technique. In the small-scale study, the sensors were shown to give accurate non-invasive data of the conditions within the packaging and proved accurate in predicting punctured or ruptured packaging along with indicating microbial growth. The sensors also proved effective in revealing a previously unidentified meat quality issue.

In the large-scale study, the sensors demonstrated the importance of packaging the product right first time especially when an O_2-purging method such as dry ice is used. In addition, the sensors proved useful in identifying O_2 trends within the containers and how different movements can affect the distribution of O_2 within the container (Fig. 4.19 pg 117). If a puncture of the containers had occurred, the sensors would have indicated it, removing the risk of the product reaching the customer in a compromised quality state.

In a different application study, sensors were used to select optimum glass packaging used beverage containers. The data obtained from the sensors allow the O_2 ingress to be tracked in each conformation and the optimum conformations were identified. Afterwards, a study was performed on two different cap types, which identified the optimal cap type, along with demonstrating why caps should not be reused when packaging new product.

In future industrial studies, it would be envisioned that the newly fabricated sensors, in particular the ungrafted PP sensor produced by swelling method, would be used in these application studies. However, for this to happen, the sensors would have to pass rigorous safety tests and their lifetime signals should be reliable in the tested food matrices so as to produce meaningful and trustworthy data. Also, the means to incorporate the sensors by lamination or heat-sealing quickly, securely and easily on the packaging used in such industrial plants is essential.

Appendix

List of tables

List of figures

Thesis Outcomes

Peer reviewed papers:

<u>Kelly CA,</u> Toncelli C, Kerry JP, Papkovsky DB, Phosphorescent O_2 sensors based on polyolefin fabric materials, J. Mater. Chem. C, 2014, 2 (12), 2169-2174.
DOI: 10.1039/C3TC32529F

<u>Kelly CA</u>, Toncelli C, Kerry JP, Papkovsky DB, Discrete O_2 sensors produced by a spotting method on polyolefin fabric substrates, Sensors Actuators B, 2014, 203: 935–940.
DOI: http://dx.doi.org/10.1016/j.snb.2014.06.103

<u>Kelly CA</u>, Toncelli C, Cruz M, Arzhakova OV, Kerry JP, Papkovsky DB, Phosphorescent O_2 sensors integrated in polymeric films by local solvent crazing, Materials & Design, 2015, 77: 110-113.
DOI: http://dx.doi.org/10.1016/j.matdes.2015.03.045

Banerjee S, <u>Kelly CA</u>, Kerry JP, Papkovsky DB, High throughput non-destructive assessment of quality and safety of packaged food products using phosphorescent oxygen sensors (Review), Trends in Food Science & Technology, 2016, 50: 85–102
DOI: http://dx.doi.org/10.1016/j.tifs.2016.01.021

Pankaj SK, <u>Kelly CA</u>, Bueno-Ferrer C, Kerry JP, Papkovsky DB, Bourke P, Cullen PJ, Application of phosphorescent oxygen sensors in in-package dielectric barrier discharge plasma environment, Innov Food Sci Emerg Technol, 2016, 33: 234-239.
DOI: http://dx.doi.org/10.1016/j.ifset.2015.11.005

Conference Abstracts:

Kelly CA, Toncelli C, Papkovsky DP, Phosphorescent Solid-state Oxygen sensors based on microporous polypropylene membrane, Europtrode-2014 (European Conference on Optical Chemical Sensors and Biosensors, Athens, April 13-16, 2014. Poster presented.

Kelly CA, Cruz-Romero M, Kerry JP, Papkovsky DP, Stability assessment of luminescent optical sensors with food packaging application, Europtrode, Graz, Austria, March 20-23, 2016. (Poster presented)

Bibliography

1.   Kerry, J. P., Papkovsky, D.B. , Development and use of non-destructive, continuous assessment, chemical oxygen sensors in packs containing oxygen sensitive foodstuffs. *Res. Adv. Food Sci.* **2002,** *3*, 121–140.

2.   Mohebi, E.; Marquez, L., Intelligent packaging in meat industry: An overview of existing solutions. *J. Food Sci. Technol.* **2015,** *52* (7), 3947-3964.

3.   Yam, K. L.; Takhistov, P. T.; Miltz, J., Intelligent Packaging: Concepts and Applications. *J. Food Sci.* **2005,** *70* (1), R1-R10.

4.   (a) Mills, A., Oxygen indicators and intelligent inks for packaging food. *Chem. Soc. Rev.* **2005,** *34* (12), 1003-1011; (b) Krumhar, K. C.; Karel, M. 1992 Visual indicator system. US Patent 5096813; (c) Ahvenainen, R.; Eilamo, M.; Hurme, E., Detection of improper sealing and quality deterioration of modified-atmosphere-packed pizza by a colour indicator. *Food Control* **1997,** *8* (4), 177-184.

5.   Dansensor http://dansensor.com/products/headspace-analysers (accessed Accessed on 30/06/2015).

6.   Taoukis, P. S.; Labuza, T. P., Applicability of Time-Temperature Indicators as Shelf Life Monitors of Food Products. *J. Food Sci.* **1989,** *54* (4), 783-788.

7.   Vitsab http://vitsab.com/index.php/seafood-tti-labels/ (accessed Accessed on 07/07/2015).

8.   Fresh-Check http://www.fresh-check.com/ (accessed Accessed on 07/07/2015).

9.   3m http://solutions.3m.com (accessed Accessed on 03/07/2015).

10.   Kumari, L.; Narsaiah, K.; Grewal, M. K.; Anurag, R. K., Application of RFID in agri-food sector. *Trends Food Sci. Technol.* **2015,** *43* (2), 144-161.

11.   Smolander, M., Freshness Indicators for Food Packaging. In *Smart Packaging Technologies for Fast Moving Consumer Goods*, John Wiley & Sons, Ltd: 2008; pp 111-127.

12.   Smolander, M.; Hurme, E.; Latva-Kala, K.; Luoma, T.; Alakomi, H. L.; Ahvenainen, R., Myoglobin-based indicators for the evaluation of freshness of unmarinated broiler cuts. *Innovative Food Sci. Emerging Technol.* **2002,** *3* (3), 279-288.

13.   (a) Rokka, M.; Eerola, S.; Smolander, M.; Alakomi, H. L.; Ahvenainen, R., Monitoring of the quality of modified atmosphere packaged broiler chicken cuts

stored in different temperature conditions: B. Biogenic amines as quality-indicating metabolites. *Food Control* **2004,** *15* (8), 601-607; (b) Kaniou, I.; Samouris, G.; Mouratidou, T.; Eleftheriadou, A.; Zantopoulos, N., Determination of biogenic amines in fresh unpacked and vacuum-packed beef during storage at 4°C. *Food Chemistry* **2001,** *74* (4), 515-519.

14.   Randell, K.; Ahvenainen, R.; Latva-Kala, K.; Hurme, E.; Mattila-Sandholm, T.; HyvöNen, L., Modified Atmosphere-packed Marinated Chicken Breast and Rainbow Trout Quality as Affected by Package Leakage. *J. Food Sci.* **1995,** *60* (4), 667-672.

15.   Shu, H.C.; Håkanson, H.; Mattiasson, B., d-Lactic acid in pork as a freshness indicator monitored by immobilized d-lactate dehydrogenase using sequential injection analysis. *Anal. Chim. Acta* **1993,** *283* (2), 727-737.

16.   AgelessEye http://www.mgc.co.jp/eng/products/abc/ageless/eye.html (accessed Accessed on 07/07/2015).

17.   (a) Wang, X.D.; Wolfbeis, O. S., Optical methods for sensing and imaging oxygen: materials, spectroscopies and applications. *Chem. Soc. Rev.* **2014,** *43* (10), 3666-3761; (b) Papkovsky, D. B.; Dmitriev, R. I., Biological detection by optical oxygen sensing. *Chem. Soc. Rev.* **2013,** *42* (22), 8700-8732; (c) Amao, Y., Probes and Polymers for Optical Sensing of Oxygen. *Microchim. Acta* **2003,** *143* (1), 1-12.

18.   Clark, L. C.; Wolf, R.; Granger, D.; Taylor, Z., Continuous Recording of Blood Oxygen Tensions by Polarography. *J. Appl. Physiol.* **1953,** *6* (3), 189-193.

19.   Trettnak, W.; Gruber, W.; Reininger, F.; Klimant, I., Recent progress in optical oxygen sensor instrumentation. *Sens. Actuators, B* **1995,** *29* (1–3), 219-225.

20.   Lakowicz, J. R., *Principles of Fluorescence Spectroscopy*. Third Edition ed.; Springer, USA: 2006.

21.   Di Marco, G.; Lanza, M.; Pieruccini, M.; Campagna, S., A luminescent iridium(III) cyclometallated complex immobilized in a polymeric matrix as a solid-state oxygen sensor. *Advanced Materials* **1996,** *8* (7), 576-580.

22.   Baleizão, C.; Nagl, S.; Schäferling, M.; Berberan-Santos, M. N.; Wolfbeis, O. S., Dual Fluorescence Sensor for Trace Oxygen and Temperature with Unmatched Range and Sensitivity. *Analytical Chemistry* **2008,** *80* (16), 6449-6457.

23.   Demas, J. N.; DeGraff, B. A.; Xu, W., Modeling of Luminescence Quenching-Based Sensors: Comparison of Multisite and Nonlinear Gas Solubility Models. *Anal. Chem.* **1995,** *67* (8), 1377-1380.

24.   Borisov, S. M.; Fischer, R.; Saf, R.; Klimant, I., Exceptional Oxygen Sensing Properties of New Blue Light-Excitable Highly Luminescent Europium(III) and Gadolinium(III) Complexes. *Adv. Funct. Mater.* **2014,** *24* (41), 6548-6560.

25.   (a) Wang, X. D.; Gorris, H. H.; Stolwijk, J. A.; Meier, R. J.; Groegel, D. B. M.; Wegener, J.; Wolfbeis, O. S., Self-referenced RGB colour imaging of intracellular oxygen. *Chem. Sci.* **2011,** *2* (5), 901-906; (b) Kondrashina, A. V.; Dmitriev, R. I.; Borisov, S. M.; Klimant, I.; O'Brien, I.; Nolan, Y. M.; Zhdanov, A. V.; Papkovsky, D. B., A Phosphorescent Nanoparticle-Based Probe for Sensing and Imaging of (Intra)Cellular Oxygen in Multiple Detection Modalities. *Adv. Funct. Mater.* **2012,** *22* (23), 4931-4939.

26.   Wu, C.; Bull, B.; Christensen, K.; McNeill, J., Ratiometric Single-Nanoparticle Oxygen Sensors for Biological Imaging. *Angewandte Chemie International Edition* **2009,** *48* (15), 2741-2745.

27.   Andrzejewski, D.; Klimant, I.; Podbielska, H., Method for lifetime-based chemical sensing using the demodulation of the luminescence signal. *Sensors and Actuators B: Chemical* **2002,** *84* (2–3), 160-166.

28.   (a) McDonagh, C.; Kolle, C.; McEvoy, A. K.; Dowling, D. L.; Cafolla, A. A.; Cullen, S. J.; MacCraith, B. D., Phase fluorometric dissolved oxygen sensor. *Sensors and Actuators B: Chemical* **2001,** *74* (1–3), 124-130; (b) Medina-Rodríguez, S.; de la Torre-Vega, A.; Fernández-Sánchez, J. F.; Fernández-Gutiérrez, A., An open and low-cost optical-fiber measurement system for the optical detection of oxygen using a multifrequency phase-resolved method. *Sensors and Actuators B: Chemical* **2013,** *176*, 1110-1120; (c) Trettnak, W.; Kolle, C.; Reininger, F.; Dolezal, C.; O'Leary, P., Miniaturized luminescence lifetime-based oxygen sensor instrumentation utilizing a phase modulation technique. *Sensors and Actuators B: Chemical* **1996,** *36* (1–3), 506-512.

29.   Amao, Y.; Okura, I., Optical oxygen sensor devices using metalloporphyrins. *J. Porphyrins and Phthalocyanines* **2009,** *13* (11), 1111-1122.

30.   Quaranta, M.; Borisov, S.; Klimant, I., Indicators for optical oxygen sensors. *Bioanal. Rev.* **2012,** *4* (2-4), 115-157.

31.   (a) Gillanders, R. N.; Tedford, M. C.; Crilly, P. J.; Bailey, R. T., A composite sol–gel/fluoropolymer matrix for dissolved oxygen optical sensing. *J. Photochem. Photobiol., A* **2004,** *163* (1–2), 193-199; (b) Lam, S. K.; Chan, M. A.; Lo, D., Characterization of phosphorescence oxygen sensor based on erythrosin B in sol–gel

silica in wide pressure and temperature ranges. *Sens. Actuators, B* **2001,** *73* (2–3), 135-141.

32. (a) Banerjee, S.; Kuznetsova, R. T.; Papkovsky, D. B., Solid-state oxygen sensors based on phosphorescent diiodo-borondipyrromethene dye. *Sens. Actuators, B* **2015,** *212* (0), 229-234; (b) Ermolina, E. G.; Kuznetsova, R. T.; Aksenova, Y. V.; Gadirov, R. M.; Kopylova, T. N.; Antina, E. V.; Berezin, M. B.; Semeikin, A. S., Novel quenchometric oxygen sensing material based on diiodine-substituted boron dipyrromethene dye. *Sens. Actuators, B* **2014,** *197* (0), 206-210.

33. Mills, A.; Graham, A.; O'Rourke, C., A novel, titania sol–gel derived film for luminescence-based oxygen sensing. *Sens. Actuators, B* **2014,** *190* (0), 907-912.

34. (a) Wolfbeis, O.; Leiner, M. P.; Posch, H., A new sensing material for optical oxygen measurement, with the indicator embedded in an aqueous phase. *Microchim. Acta* **1986,** *90* (5-6), 359-366; (b) Chen, X.; Zhong, Z.; Li, Z.; Jiang, Y.; Wang, X.; Wong, K., Characterization of ormosil film for dissolved oxygen-sensing. *Sens. Actuators, B* **2002,** *87* (2), 233-238.

35. (a) Mills, A.; Thomas, M., Fluorescence-based Thin Plastic Film Ion-pair Sensors for Oxygen. *Analyst* **1997,** *122* (1), 63-68; (b) Klimant, I.; Wolfbeis, O. S., Oxygen-Sensitive Luminescent Materials Based on Silicone-Soluble Ruthenium Diimine Complexes. *Anal. Chem.* **1995,** *67* (18), 3160-3166.

36. (a) Alford, P. C.; Cook, M. J.; Lewis, A. P.; McAuliffe, G. S. G.; Skarda, V.; Thomson, A. J.; Glasper, J. L.; Robbins, D. J., Luminescent metal complexes. Part 5. Luminescence properties of ring-substituted 1,10-phenanthroline tris-complexes of ruthenium(II). *J. Chem. Soc., Perkin Trans. 2* **1985,** (5), 705-709; (b) Forster, L. S., Thermal relaxation in excited electronic states of d^3 and d^6 metal complexes. *Coord. Chem. Rev.* **2002,** *227* (1), 59-92.

37. Oxysense http://www.oxysense.com/oxygen-measurement-accessories.html (accessed Accessed on 08/07/2015).

38. Amao, Y.; Ishikawa, Y.; Okura, I., Green luminescent iridium(III) complex immobilized in fluoropolymer film as optical oxygen-sensing material. *Analytica Chimica Acta* **2001,** *445* (2), 177-182.

39. Eastwood, D.; Gouterman, M., Porphyrins: XVIII. Luminescence of (Co), (Ni), Pd, Pt complexes. *J. Mol. Spectrosc.* **1970,** *35* (3), 359-375.

40. (a) Lee, S.K.; Okura, I., Optical Sensor for Oxygen Using a Porphyrin-doped Sol-Gel Glass. *Analyst* **1997,** *122* (1), 81-84; (b) Papkovsky, D. B., New oxygen

sensors and their application to biosensing. *Sens. Actuators, B* **1995,** *29* (1–3), 213-218.

41.   (a) Lee, S.K.; Okura, I., Photostable Optical Oxygen Sensing Material: Platinum Tetrakis(pentafluorophenyl)porphyrin Immobilized in Polystyrene. *Anal. Commun.* **1997,** *34* (6), 185-188; (b) Amao, Y.; Tabuchi, Y.; Yamashita, Y.; Kimura, K., Novel optical oxygen sensing material: metalloporphyrin dispersed in fluorinated poly(aryl ether ketone) films. *Eur. Polym. J.* **2002,** *38* (4), 675-681; (c) Amao, Y.; Miyashita, T.; Okura, I., Platinum tetrakis(pentafluorophenyl)porphyrin immobilized in polytrifluoroethylmethacrylate film as a photostable optical oxygen detection material. *J. Fluorine Chem.* **2001,** *107* (1), 101-106; (d) Puklin, E.; Carlson, B.; Gouin, S.; Costin, C.; Green, E.; Ponomarev, S.; Tanji, H.; Gouterman, M., Ideality of pressure-sensitive paint. I. Platinum tetra(pentafluorophenyl)porphine in fluoroacrylic polymer. *J. Appl. Polym. Sci.* **2000,** *77* (13), 2795-2804.

42.   Banerjee, S.; Kelly, C.; Kerry, J. P.; Papkovsky, D. B., High throughput non-destructive assessment of quality and safety of packaged food products using phosphorescent oxygen sensors. *Trends in Food Science & Technology* **2016,** *50*, 85-102.

43.   (a) Lai, S.W.; Hou, Y. J.; Che, C. M.; Pang, H. L.; Wong, K. Y.; Chang, C. K.; Zhu, N., Electronic Spectroscopy, Photophysical Properties, and Emission Quenching Studies of an Oxidatively Robust Perfluorinated Platinum Porphyrin. *Inorg. Chem.* **2004,** *43* (12), 3724-3732; (b) Borisov, S. M.; Nuss, G.; Klimant, I., Red Light-Excitable Oxygen Sensing Materials Based on Platinum(II) and Palladium(II) Benzoporphyrins. *Anal. Chem.* **2008,** *80* (24), 9435-9442.

44.   Papkovsky, D. B.; Ponomarev, G. V.; Trettnak, W.; O'Leary, P., Phosphorescent Complexes of Porphyrin Ketones: Optical Properties and Application to Oxygen Sensing. *Anal. Chem.* **1995,** *67* (22), 4112-4117.

45.   Borisov, S. M.; Nuss, G.; Haas, W.; Saf, R.; Schmuck, M.; Klimant, I., New NIR-emitting complexes of platinum(II) and palladium(II) with fluorinated benzoporphyrins. *J. Photochem. Photobiol., A* **2009,** *201* (2–3), 128-135.

46.   Khalil, G.; Gouterman, M.; Ching, S.; Costin, C.; Coyle, L.; Gouin, S.; Green, E.; Sadilek, M.; Wan, R.; Yearyean, J.; Zelelow, B., Synthesis and spectroscopic characterization of Ni, Zn, Pd and Pt tetra(pentafluorophenyl)porpholactone with comparisons to Mg, Zn, Y, Pd and Pt

metal complexes of tetra(pentafluorophenyl)porphine. *J. Porphyrins and Phthalocyanines* **2002,** *06* (02), 135-145.

47.   (a) Vinogradov, S. A.; Wilson, D. F., Metallotetrabenzoporphyrins. New phosphorescent probes for oxygen measurements. *J. Chem. Soc., Perkin Trans. 2* **1995,** (1), 103-111; (b) Rogers, J. E.; Nguyen, K. A.; Hufnagle, D. C.; McLean, D. G.; Su, W.; Gossett, K. M.; Burke, A. R.; Vinogradov, S. A.; Pachter, R.; Fleitz, P. A., Observation and Interpretation of Annulated Porphyrins: Studies on the Photophysical Properties of meso-Tetraphenylmetalloporphyrins. *J. Phys. Chem. A* **2003,** *107* (51), 11331-11339.

48.   Korotcenkov, G., *Handbook of Gas Sensor Materials*. Springer, USA: New York, 2014; p 209-222.

49.   (a) Pospiskova, K.; Safarik, I.; Sebela, M.; Kuncova, G., Magnetic particles–based biosensor for biogenic amines using an optical oxygen sensor as a transducer. *Microchim. Acta* **2013,** *180* (3-4), 311-318; (b) Schrenkhammer, P.; Wolfbeis, O. S., Fully reversible optical biosensors for uric acid using oxygen transduction. *Biosens. Bioelectron.* **2008,** *24* (4), 994-999.

50.   Stich, M. I. J.; Schaeferling, M.; Wolfbeis, O. S., Multicolor Fluorescent and Permeation-Selective Microbeads Enable Simultaneous Sensing of pH, Oxygen, and Temperature. *Adv. Mater.* **2009,** *21* (21), 2216-2220.

51.   Jerónimo, P. C. A.; Araújo, A. N.; Conceição B.S.M. Montenegro, M., Optical sensors and biosensors based on sol–gel films. *Talanta* **2007,** *72* (1), 13-27.

52.   McEvoy, A. K.; McDonagh, C.; MacCraith, B. D., Optimisation of Sol-Gel-Derived Silica Films for Optical Oxygen Sensing. *J. Sol-Gel Sci. Technol.* **1997,** *8* (1-3), 1121-1125.

53.   Papkovsky, D. B.; Ovchinnikov, A. N.; Ogurtsov, V. I.; Ponomarev, G. V.; Korpela, T., Biosensors on the basis of luminescent oxygen sensor: the use of microporous light-scattering support materials. *Sens. Actuators, B* **1998,** *51* (1–3), 137-145.

54.   Müller, B. J.; Burger, T.; Borisov, S. M.; Klimant, I., High performance optical trace oxygen sensors based on NIR-emitting benzoporphyrins covalently coupled to silicone matrixes. *Sens. Actuators, B* **2015,** *216* (0), 527-534.

55.   *Plastic Films in Food Packaging: Materials, Technology and Applications*. Elsevier: 2012.

56.   (a) Toncelli, C.; Arzhakova, O. V.; Dolgova, A.; Volynskii, A. L.; Bakeev, N. F.; Kerry, J. P.; Papkovsky, D. B., Oxygen-Sensitive Phosphorescent Nanomaterials Produced from High-Density Polyethylene Films by Local Solvent-Crazing. *Anal. Chem.* **2014,** *86* (3), 1917-1923; (b) Mills, A.; Graham, A., Extruded polymer films pigmented with a heterogeneous ion-pair based lumophore for O_2 sensing. *Analyst* **2013,** *138* (21), 6488-6493.

57.   Toncelli, C.; Arzhakova, O. V.; Dolgova, A.; Volynskii, A. L.; Kerry, J. P.; Papkovsky, D. B., Phosphorescent oxygen sensors produced by spot-crazing of polyphenylenesulfide films. *J. Mater. Chem. C* **2014,** *2* (38), 8035-8041.

58.   Kelly, C. A.; Toncelli, C.; Kerry, J. P.; Papkovsky, D. B., Phosphorescent O_2 sensors based on polyolefin fabric materials. *J. Mater. Chem. C* **2014,** *2* (12), 2169-2174.

59.   Mills, A.; Lepre, A., Controlling the Response Characteristics of Luminescent Porphyrin Plastic Film Sensors for Oxygen. *Analytical Chemistry* **1997,** *69* (22), 4653-4659.

60.   Draxler, S.; Lippitsch, M. E.; Klimant, I.; Kraus, H.; Wolfbeis, O. S., Effects of Polymer Matrixes on the Time-Resolved Luminescence of a Ruthenium Complex Quenched by Oxygen. *J. Phys. Chem.* **1995,** *99* (10), 3162-3167.

61.   Mak, C. S. K.; Pentlehner, D.; Stich, M.; Wolfbeis, O. S.; Chan, W. K.; Yersin, H., Exceptional Oxygen Sensing Capabilities and Triplet State Properties of Ir(ppy-NPh2)3. *Chemistry of Materials* **2009,** *21* (11), 2173-2175.

62.   Douglas, P.; Eaton, K., Response characteristics of thin film oxygen sensors, Pt and Pd octaethylporphyrins in polymer films. *Sens. Actuators, B* **2002,** *82* (2–3), 200-208.

63.   Amao, Y.; Asai, K.; Miyashita, T.; Okura, I., Novel optical oxygen sensing material: platinum porphyrin-fluoropolymer film. *Polymers for Advanced Technologies* **2000,** *11* (8-12), 705-709.

64.   Gillanders, R. N.; Tedford, M. C.; Crilly, P. J.; Bailey, R. T., Thin film dissolved oxygen sensor based on platinum octaethylporphyrin encapsulated in an elastic fluorinated polymer. *Analytica Chimica Acta* **2004,** *502* (1), 1-6.

65.   Bergman, I., Rapid-response Atmospheric Oxygen Monitor based on Fluorescence Quenching. *Nature* **1968,** *218* (5139), 396-396.

66. Hartmann, P.; Leiner, M. J. P.; Lippitsch, M. E., Luminescence Quenching Behavior of an Oxygen Sensor Based on a Ru(II) Complex Dissolved in Polystyrene. *Anal. Chem.* **1995,** *67* (1), 88-93.

67. Klimant, I.; Kühl, M.; Glud, R. N.; Holst, G., Optical measurement of oxygen and temperature in microscale: strategies and biological applications. *Sens. Actuators, B* **1997,** *38* (1–3), 29-37.

68. Charlesworth, J. M., Optical sensing of oxygen using phosphorescence quenching. *Sens. Actuators, B* **1994,** *22* (1), 1-5.

69. Xu, W.; Schmidt, R.; Whaley, M.; Demas, J. N.; DeGraff, B. A.; Karikari, E. K.; Famer, B. A., Oxygen sensors based on luminescence quenching: interactions of pyrene with the polymer supports. *Analytical Chemistry* **1995,** *67* (18), 3172-3180.

70. Amao, Y.; Okura, I., Optical Oxygen Sensing Properties of Tris (4,7[prime]-diphenyl-1,10[prime]-phenanthroline) Ruthenium (II)-Polyacrylic Acid Complex Thin Film. *Polym J* **2000,** *32* (5), 452-455.

71. Gewehr, P. M.; Delpy, D. T., Optical oxygen sensor based on phosphorescence lifetime quenching and employing a polymer immobilised metalloporphyrin probe. *Medical and Biological Engineering and Computing* **1993,** *31* (1), 11-21.

72. Ahmad, M.; Mohammad, N.; Abdullah, J., Sensing material for oxygen gas prepared by doping sol–gel film with tris (2,2-bipyridyl)dichlororuthenium complex. *Journal of Non-Crystalline Solids* **2001,** *290* (1), 86-91.

73. Lee, S. K.; Okura, I., Porphyrin-doped sol-gel glass as a probe for oxygen sensing. *Analytica Chimica Acta* **1997,** *342* (2), 181-188.

74. Lawrie, K.; Mills, A.; Hazafy, D., Simple inkjet-printed, UV-activated oxygen indicator. *Sens. Actuators, B* **2013,** *176*, 1154-1159.

75. Smiddy, M.; Fitzgerald, M.; Kerry, J. P.; Papkovsky, D. B.; O' Sullivan, C. K.; Guilbault, G. G., Use of oxygen sensors to non-destructively measure the oxygen content in modified atmosphere and vacuum packed beef: impact of oxygen content on lipid oxidation. *Meat Sci.* **2002,** *61* (3), 285-290.

76. Koren, K.; Borisov, S. M.; Klimant, I., Stable optical oxygen sensing materials based on click-coupling of fluorinated platinum(II) and palladium(II) porphyrins—A convenient way to eliminate dye migration and leaching. *Sens. Actuators, B* **2012,** *169* (0), 173-181.

77.   Borisov, S. M.; Mayr, T.; Mistlberger, G.; Waich, K.; Koren, K.; Chojnacki, P.; Klimant, I., Precipitation as a simple and versatile method for preparation of optical nanochemosensors. *Talanta* **2009,** *79* (5), 1322-1330.

78.   Rukhlya, E. G.; Litmanovich, E. A.; Dolinnyi, A. I.; Yarysheva, L. M.; Volynskii, A. L.; Bakeev, N. F., Penetration of Poly(ethylene oxide) into the Nanoporous Structure of the Solvent-Crazed Poly(ethylene terephthalate) Films. *Macromolecules* **2011,** *44* (13), 5262-5267.

79.   Gillanders, R. N.; Arzhakova, O. V.; Hempel, A.; Dolgova, A.; Kerry, J. P.; Yarysheva, L. M.; Bakeev, N. F.; Volynskii, A. L.; Papkovsky, D. B., Phosphorescent Oxygen Sensors Based on Nanostructured Polyolefin Substrates. *Anal. Chem.* **2010,** *82* (2), 466-468.

80.   Banerjee, S.; Arzhakova, O. V.; Dolgova, A. A.; Papkovsky, D. B., Phosphorescent oxygen sensors produced from polyolefin fibres by solvent-crazing method. *Sensors and Actuators B: Chemical* **2016,** *230*, 434-441.

81.   Wolf, C.; Tscherner, M.; Köstler, S., Ultra-fast opto-chemical sensors by using electrospun nanofibers as sensing layers. *Sensors and Actuators B: Chemical* **2015,** *209*, 1064-1069.

82.   Ramakrishna, S.; Fujihara, K.; Teo, W. E.; Yong, T.; Ma, Z.; Ramaseshan, R., Electrospun nanofibers: solving global issues. *Materials Today* **2006,** *9* (3), 40-50.

83.   Papkovsky, D. B.; Papkovskaia, N.; Smyth, A.; Kerry, J.; Ogurtsov, V. I., Phosphorescent Sensor Approach for Non-Destructive Measurement of Oxygen in Packaged Foods: Optimisation of Disposable Oxygen Sensors and their Characterization Over a Wide Temperature Range. *Anal. Lett.* **2000,** *33* (9), 1755-1777.

84.   Ogurtsov, V. I.; Papkovsky, D. B., Selection of modulation frequency of excitation for luminescence lifetime-based oxygen sensors. *Sens. Actuators, B* **1998,** *51* (1–3), 377-381.

85.   Papkovsky, D. B.; Smiddy, M. A.; Papkovskaia, N. Y.; Kerry, J. P., Nondestructive Measurement of Oxygen in Modified Atmosphere Packaged Hams Using a Phase-Fluorimetric Sensor System. *J. Food Sci.* **2002,** *67* (8), 3164-3169.

86.   O'Mahony, F. C.; O'Riordan, T. C.; Papkovskaia, N.; Kerry, J. P.; Papkovsky, D. B., Non-destructive assessment of oxygen levels in industrial modified atmosphere packaged cheddar cheese. *Food Control* **2006,** *17* (4), 286-292.

87.   Borchert, N.; Hempel, A.; Walsh, H.; Kerry, J. P.; Papkovsky, D. B., High throughput quality and safety assessment of packaged green produce using two optical oxygen sensor based systems. *Food Control* **2012,** *28* (1), 87-93.

88.   Hempel, A.; Sullivan, M.; Papkovsky, D.; Kerry, J., Assessment and Use of Optical Oxygen Sensors as Tools to Assist in Optimal Product Component Selection for the Development of Packs of Ready-to-Eat Mixed Salads and for the Non-Destructive Monitoring of in-Pack Oxygen Levels Using Chilled Storage. *Foods* **2013,** *2* (2), 213.

89.   Hempel, A. W.; O'Sullivan, M. G.; Papkovsky, D. B.; Kerry, J. P., Use of smart packaging technologies for monitoring and extending the shelf-life quality of modified atmosphere packaged (MAP) bread: application of intelligent oxygen sensors and active ethanol emitters. *Eur Food Res Technol* **2013,** *237* (2), 117-124.

90.   Morsy, M. K., Khalaf, H.H., Sharoba, A.M. and El-Tanahi, H.H., Applicability of Biosensor and Oxygen Sensor for Monitoring Spoilage and Bacterial Contaminants of Packed Minced Beef and Poultry. In *2nd International Conference On Biotechnology Applications In Agriculture (ICBAA)*, Benha University,Moshtohor and Hurghada, Egypt, April 2014.

91.   Ugliano, M.; Dieval, J. B.; Siebert, T. E.; Kwiatkowski, M.; Aagaard, O.; Vidal, S.; Waters, E. J., Oxygen Consumption and Development of Volatile Sulfur Compounds during Bottle Aging of Two Shiraz Wines. Influence of Pre- and Postbottling Controlled Oxygen Exposure. *J. Agric. Food Chem.* **2012,** *60* (35), 8561-8570.

92.   Hempel, A.; O'Sullivan, M. G.; Papkovsky, D. B.; Kerry, J. P., Use of optical oxygen sensors to monitor residual oxygen in pre- and post-pasteurised bottled beer and its effect on sensory attributes and product acceptability during simulated commercial storage. *LWT-Food Sci. Technol.* **2013,** *50* (1), 226-231.

93.   Nkhili, E.; Brat, P., Reexamination of the ORAC assay: effect of metal ions. *Anal. Bioanal. Chem.* **2011,** *400* (5), 1451-1458.

94.   (a) Van Bree, I.; Baetens, J. M.; Samapundo, S.; Devlieghere, F.; Laleman, R.; Vandekinderen, I.; Noseda, B.; Xhaferi, R.; De Baets, B.; De Meulenaer, B., Modelling the degradation kinetics of vitamin C in fruit juice in relation to the initial headspace oxygen concentration. *Food Chem.* **2012,** *134* (1), 207-214; (b) Wibowo, S.; Grauwet, T.; Santiago, J. S.; Tomic, J.; Vervoort, L.; Hendrickx, M.; Van Loey, A., Quality changes of pasteurised orange juice during storage: A kinetic study of

specific parameters and their relation to colour instability. *Food Chem.* **2015,** *187* (0), 140-151.

95.   Kozak, W.; Samotyja, U., The use of oxygen content determination method based on fluorescence quenching for rapeseed oil shelf-life assessment. *Food Control* **2013,** *33* (1), 162-165.

96.   Gibbs, E. L., Oxygen Permeation of BetterBottle® Carboys–Direct Measurement–. **2013**.

97.   Diéval, J. B.; Vidal, S.; Aagaard, O., Measurement of the Oxygen Transmission Rate of Co-extruded Wine Bottle Closures Using a Luminescence-Based Technique. *Packaging Technology and Science* **2011,** *24* (7), 375-385.

98.   Wirth, J.; Caillé, S.; Souquet, J. M.; Samson, A.; Dieval, J. B.; Vidal, S.; Fulcrand, H.; Cheynier, V., Impact of post-bottling oxygen exposure on the sensory characteristics and phenolic composition of Grenache rosé wines. *Food Chem.* **2012,** *132* (4), 1861-1871.

99.   Ugliano, M.; Kwiatkowski, M.; Vidal, S.; Capone, D.; Siebert, T.; Dieval, J. B.; Aagaard, O.; Waters, E. J., Evolution of 3-Mercaptohexanol, Hydrogen Sulfide, and Methyl Mercaptan during Bottle Storage of Sauvignon blanc Wines. Effect of Glutathione, Copper, Oxygen Exposure, and Closure-Derived Oxygen. *J. Agric. Food Chem.* **2011,** *59* (6), 2564-2572.

100.   Van Bree, I.; De Meulenaer, B.; Samapundo, S.; Vermeulen, A.; Ragaert, P.; Maes, K. C.; De Baets, B.; Devlieghere, F., Predicting the headspace oxygen level due to oxygen permeation across multilayer polymer packaging materials: A practical software simulation tool. *Innovative Food Sci. Emerging Technol* **2010,** *11* (3), 511-519.

101.   Mestres, M.; Busto, O.; Guasch, J., Analysis of organic sulfur compounds in wine aroma. *J. Chromatogr. A* **2000,** *881* (1–2), 569-581.

102.   Salmon, J.-M., Interactions between yeast, oxygen and polyphenols during alcoholic fermentations: Practical implications. *LWT-Food Sci. Technol.* **2006,** *39* (9), 959-965.

103.   McRae, J. M.; Day, M. P.; Bindon, K. A.; Kassara, S.; Schmidt, S. A.; Schulkin, A.; Kolouchova, R.; Smith, P. A., Effect of early oxygen exposure on red wine colour and tannins. *Tetrahedron* **2015,** *71* (20), 3131-3137.

104.   Wallington, N.; Clark, A. C.; Prenzler, P. D.; Barril, C.; Scollary, G. R., The decay of ascorbic acid in a model wine system at low oxygen concentration. *Food Chem.* **2013,** *141* (3), 3139-3146.

105.   Bradshaw, M. P.; Barril, C.; Clark, A. C.; Prenzler, P. D.; Scollary, G. R., Ascorbic Acid: A Review of its Chemistry and Reactivity in Relation to a Wine Environment. *Crit. Rev. Food Sci. Nutr.* **2011,** *51* (6), 479-498.

106.   Eaton, K.; Douglas, P., Effect of humidity on the response characteristics of luminescent PtOEP thin film optical oxygen sensors. *Sens. Actuators, B* **2002,** *82* (1), 94-104.

107.   Papkovsky, D. B.; Ponomarev, G. V.; Chernov, S. F.; Ovchinnikov, A. N.; Kurochkin, I. N., Luminescence lifetime-based sensor for relative air humidity. *Sensors and Actuators B: Chemical* **1994,** *22* (1), 57-61.

108.   O'Riordan, T. C.; Voraberger, H.; Kerry, J. P.; Papkovsky, D. B., Study of migration of active components of phosphorescent oxygen sensors for food packaging applications. *Analytica Chimica Acta* **2005,** *530* (1), 135-141.

109.   Hyakutake, T.; Taguchi, H.; Sakaue, H.; Nishide, H., Polypyridylpropyne-Pd and -Pt porphyrin coating for visualization of oxygen pressure. *Polymers for Advanced Technologies* **2008,** *19* (9), 1262-1269.

110.   Borisov, S. M.; Mayr, T.; Klimant, I., Poly(styrene-block-vinylpyrrolidone) Beads as a Versatile Material for Simple Fabrication of Optical Nanosensors. *Analytical Chemistry* **2008,** *80* (3), 573-582.

111.   Koren, K.; Borisov, S. M.; Saf, R.; Klimant, I., Strongly Phosphorescent Iridium(III)–Porphyrins – New Oxygen Indicators with Tuneable Photophysical Properties and Functionalities. *European Journal of Inorganic Chemistry* **2011,** *2011* (10), 1531-1534.

112.   von Bultzingslowen, C.; McEvoy, A. K.; McDonagh, C.; MacCraith, B. D.; Klimant, I.; Krause, C.; Wolfbeis, O. S., Sol-gel based optical carbon dioxide sensor employing dual luminophore referencing for application in food packaging technology. *Analyst* **2002,** *127* (11), 1478-1483.

113.   Kameda, M.; Seki, H.; Makoshi, T.; Amao, Y.; Nakakita, K., A fast-response pressure sensor based on a dye-adsorbed silica nanoparticle film. *Sensors and Actuators B: Chemical* **2012,** *171–172*, 343-349.

114.   Tian, Y.; Shumway, B. R.; Meldrum, D. R., A New Cross-Linkable Oxygen Sensor Covalently Bonded into Poly(2-hydroxyethyl methacrylate)-co-

Polyacrylamide Thin Film for Dissolved Oxygen Sensing. *Chem. Mater.* **2010,** *22* (6), 2069-2078.

115.   Freudenberg, Freudenberg Grafted Products: Technical Manual,. F.N. Limited (Freudenberg Nonwovens Inc.): 2006.

116.   Ding, Z.; Bao, R.; Zhao, B.; Yan, J.; Liu, Z.; Yang, M., Effects of annealing on structure and deformation mechanism of isotactic polypropylene film with row-nucleated lamellar structure. *Journal of Applied Polymer Science* **2013,** *130* (3), 1659-1666.

117.   López-Gejo, J.; Haigh, D.; Orellana, G., Relationship between the Microscopic and Macroscopic World in Optical Oxygen Sensing: A Luminescence Lifetime Microscopy Study. *Langmuir* **2010,** *26* (3), 2144-2150.

118.   Badocco, D.; Mondin, A.; Pastore, P., Determination of thermodynamic parameters from light intensity signals obtained from oxygen optical sensors. *Sens. Actuators, B* **2012,** *163* (1), 165-170.

119.   Becker, W.; Bergmann, A.; Biskup, C., Multispectral fluorescence lifetime imaging by TCSPC. *Microscopy Research and Technique* **2007,** *70* (5), 403-409.

120.   Boukehili, H.; Nguyen-Tri, P., Helium gas barrier and water absorption behavior of bamboo fiber reinforced recycled polypropylene. *Journal of Reinforced Plastics and Composites* **2012,** *31* (23), 1638-1651.

121.   Lee, J. H.; Gomez, I. J.; Sitterle, V. B.; Meredith, J. C., Dye-labeled polystyrene latex microspheres prepared via a combined swelling-diffusion technique. *Journal of Colloid and Interface Science* **2011,** *363* (1), 137-144.

122.   Jin, P.; Guo, Z.; Chu, J.; Tan, J.; Zhang, S.; Zhu, W., Screen-Printed Red Luminescent Copolymer Film Containing Cyclometalated Iridium(III) Complex as a High-Permeability Dissolved-Oxygen Sensor for Fermentation Bioprocess. *Industrial & Engineering Chemistry Research* **2013,** *52* (11), 3980-3987.

123.   Kneas, K. A.; Demas, J. N.; DeGraff, B. A.; Periasamy, A., Fluorescence Microscopy Study of Heterogeneity in Polymer-supported Luminescence-based Oxygen Sensors. *Microscopy and Microanalysis* **2000,** *6* (06), 551-561.

124.   Smiddy, M.; Papkovsky, D.; Kerry, J., Evaluation of oxygen content in commercial modified atmosphere packs (MAP) of processed cooked meats. *Food Res. Int.* **2002,** *35* (6), 571-575.

125.   Lamirsa, LAE[(R)] The best active preservative. Vedeqsa: 2014.

126.   Rodríguez, E.; Seguer, J.; Rocabayera, X.; Manresa, A., Cellular effects of monohydrochloride of l-arginine, Nα-lauroyl ethylester (LAE) on exposure to Salmonella typhimurium and Staphylococcus aureus. *Journal of Applied Microbiology* **2004,** *96* (5), 903-912.

127.   Kelly, C. A.; Toncelli, C.; Kerry, J. P.; Papkovsky, D. B., Discrete O_2 sensors produced by a spotting method on polyolefin fabric substrates. *Sens. Actuators, B* **2014,** *203*, 935-940.

128.   Biji, K. B.; Ravishankar, C. N.; Mohan, C. O.; Srinivasa Gopal, T. K., Smart packaging systems for food applications: a review. *J Food Sci Technol* **2015,** *52* (10), 6125-6135.

129.   Kelly, C. A.; Toncelli, C.; Cruz-Romero, M.; Arzhakova, O. V.; Kerry, J. P.; Papkovsky, D. B., Phosphorescent O_2 sensors integrated in polymeric film materials by local solvent crazing. *Mater. Des.* **2015,** *77* (0), 110-113.

130.   Mecmesin PC Controlled Testers. http://www.mecmesin.com/multitest-5-i-5kn (accessed 10/09/16).